People's Democratic Republic of Algeria

Ministry of Higher Education and Scientific Research

University of Echahid Hamma Lakhdar El-OUED

Faculty of Natural and Life Sciences

Department of Cellular and Molecular Biology

Master's Thesis

END OF STUDIES MEMOIR

Submitted to Obtain the Academic Master's Degre

Speciality: Toxicology

Them

Phytochemical characterization and Antibacterial Efficacy of Two Essential Oils: GC-MS Profiling, In Vitro Antibacterial Testing, and In Silico ADMET, Molecular Docking, and Molecular Dynamics Simulation.

Presented by:

AD Salma, BERCHOU Manal, HANNICHE Hassiba, GHRISSI Nadjla

Jury Members:

President: Dr. GHANIA Ahmed	**M.C.A**	**University of El Oued**
Examiner: Dr. OTMANI Hadjer	**M.C.A**	**University of El Oued**
Supervisor: Mr. BEN AMOR Mohamed Larbi	**M.C.A**	**University of El Oued**
Co-supervisor : Mr. CHAOUA Housseyn	**M.A.B,**	**University of El Oued**

University year: 2024/2025

﴿ بِسْمِ اللَّهِ الرَّحْمَٰنِ الرَّحِيمِ ﴾

﴿ هُوَ الَّذِي بَعَثَ فِي الْأُمِّيِّينَ رَسُولًا مِّنْهُمْ يَتْلُوا عَلَيْهِمْ آيَاتِهِ وَيُزَكِّيهِمْ وَيُعَلِّمُهُمُ الْكِتَابَ وَالْحِكْمَةَ وَإِن كَانُوا مِن قَبْلُ لَفِي ضَلَالٍ مُّبِينٍ ۝٢ ﴾

صَدَقَ اللَّهُ الْعَظِيمُ

سورة الجمعة - الأية (٢)

Acknowledgment

All praise is due to ***Allah***, by whose grace good deeds are completed and efforts bear fruit.

We would like to express our heartfelt gratitude and deep appreciation to our esteemed supervisor, ***Mr. LANEZ Elhafnaoui***, whose continuous guidance and support have been invaluable throughout the preparation of this thesis. His insightful advice, precise observations, and unwavering dedication have been instrumental in guiding us through the scientific journey and overcoming the various challenges encountered.

In addition, we would like to extend our sincere thanks to ***Pr. LANEZ Touhami***, Director of the VTRS Research Laboratory at the University of El Oued, for granting us the privilege of working in his laboratory. His support has played a crucial role in the success of this research, and we are deeply grateful for the opportunity he provided.

Our sincere appreciation also goes to ***Dr. BEN AMOR Mohamed Larbi***, whose invaluable contributions as a co-supervisor significantly enhanced the quality of this work. His readiness to assist and answer our inquiries with kindness and patience was essential in the development of this thesis.

Furthermore, we wish to express our profound gratitude to ***Dr. Aicha ADIAKA***, whose support and guidance throughout the practical and laboratory aspects of this research were indispensable. Her collaboration and dedication have been key to the successful completion of the practical component of this thesis.

To all of you, we offer our highest appreciation and gratitude. We pray that Allah blesses your efforts, makes them a source of reward, and grants you continued success and guidance in all your endeavors.

إهداء

الحمد لله الذي بنعمته تتم الصالحات، وبفضله تتحقق الآمال والطموحات

بحمده وفضله أقدم ثمرة جهدي وتعب سنواتي...

إلى روح والدي الغالي، الذي غاب عن الدنيا وبقي في القلب حيًّا...

رحمك الله وأسكنك فسيح جناته، وجعل هذا العمل نورًا يمتد إليك في دار الخلود.

وإلى والدتي الحبيبة، التي كانت ولا تزال الداعم الأول، والسند الأكبر

أهديكِ كل نجاحي وعرفاني، فأنتِ بعد الله سر هذا الإنجاز.

وإلى ابني الغالي "عبد الله " زينة حياتي ونور دربي

أهديك هذه المذكرة عربون حب وأمل، وأسأل الله أن يجعلك قرة عين، وأن يحقق لك أعظم مما حققته لنفسي.

وإلى إخوتي وأخواتي الأعزاء

رفقاء الدرب، وعنوان المحبة والدعم، من كانوا دومًا الحافز في لحظات الضعف، والفرحة في لحظات الإنجاز...

أهديكم هذه المذكرة تقديرًا وعرفانًا لما قدمتموه من مساندة صادقة ودعوات طيبة، كانت النور الذي أنار طريقي.

وإلى كل من دعمني ولو بكلمة طيبة

أهديكم جزءًا من هذا الإنجاز الذي تحقق بفضل الله ثم بفضل قلوبكم الصافية.

حسيبة

إهداء

"وآخر دعواهم أن الحمد لله رب العالمين" الحمد لله الذي ما تم جهد ولا ختم سعي إلا بفضله وما تخطى العبد عقبات وصعوبات إلا بتوفيقه

أهدي تخرجي

إلى تلك الإنسانة العظيمة التي طالما تمنت أن تقر عينها برؤيتي في يوم كهذا... أمي الحبيبة

إلى من كلل العرق جبينه وعلمني أن النجاح لا يأتي إلا بالصبر والإصرار ... أبي العزيز إلى من يذكرهم القلب قبل أن يكتب القلم، إلى من قاسموني حلو الحياة ومرها تحت سقف واحد أختي وإخوتي

إلى من صعدت أرواحهم في السماء وفارقونا بجسدهم...اجدادي

إلى جميع أقاربي وصديقاتي "قدس، بثينة، شيماء، آمال"

إلى رفيقة الدرب والروح وزميلتي في هذا العمل إلى سندي وأعز شخص على قلبي "سلمى "

إلى كل من أشرف على تعليمي منذ بداية دراستي إلى يومنا هذا.

" فاللهم اجعلها نهاية خير لبداية طريق أعظم".

نجلاء

إهداء

﴿ وَآخِرُ دَعْوَاهُمْ أَنِ الْحَمْدُ لِلَّهِ رَبِّ الْعَالَمِينَ ﴾

الحمد لله الذي لا يتم جهد إلا بفضله وتوفيقه.

إلى من منحتني الحياة، الحضن الدافئ، والمصدر الأول للحب والدعاء...

إلى أمي الحبيبة، التي لا تكف عن دعمي وتشجيعي ومساندتي...

أنتِ سر قوتي ونجاحي، وملهمتي في الصبر والعطاء... لكِ مني كل الحب والدعاء بأن يطيل الله عمرك ويحفظك لي نورًا لا يخبو.

إلى والدي العزيز، من غرس في داخلي الإيمان بالقيم، وكان أول الداعمين...

تحمل تعبي، وساندني في لحظات الضعف...

فيك القوة والحنان، والحكمة والعمل... لك كل الاحترام والامتنان.

إلى إخوتي، من كانوا دومًا نبضي وسندي الذي لا ينكسر.

إلى أختي وابنة عمي عزيزة، التي كانت لي سندًا لا يتكرر...

كنتِ الحافز وقت التعب...

شكرًا لوجودك، لحبك، ولكلماتك التي منحتني طاقة لا توصف.

إلى صديقاتي العزيزات: أمال، قدس، شيماء، بثينة...

وإلى رفيقة الدرب والروح، شريكتي في هذا الإنجاز، وسندي "نجلاء"

يا من كنتم نعم الصحبة والدرب...

لكم مكانة خاصة لا تشبهها صداقة، وشكرًا لكونكم جزءًا من هذا الإنجاز.

إلى أسرتي الصغيرة وعائلتي الكبيرة...

إلى من أحاطوني بدعائهم ومحبتهم، ووقفوا بجانبي...

وإلى كل من أشرف على تعليمي منذ بدايته وحتى اليوم...

أهديكم هذا الإنجاز عربون وفاء وامتنان.

إلى أستاذي الفاضل الأستاذ عانز الحفناوي، خالص الشكر والتقدير.

وأخيرًا... إلى نفسي، التي قاومت وثابرت وصبرت، هذا الإنجاز ثمرة تعبك.

الحمد لله أولًا وآخرًا، ظاهرًا وباطنًا.

سلمى

إهداء

بسم الله الرحمن الرحيم

"يرفع الله الذين آمنوا منكم والذين أوتو العلم درجات"

صدق الله العظيم

لم تكن الرحلة قصيرة ولم يكن الطريق مفروشا بالتسهيلات لكنني مضيت بثبات والقوة والإصرار

***الى من منحني اجمل الألقاب وساندني دون حدود واهداني دروس الحياة بلا مقابل.**

الى من علمني ان الدنيا كفاح سلاحها العلم والمعرفة الى من غرسة في روحي مكارم الاخلاق فكان بعد الله ملاذي وسندي الى فخري واعتزازي " ابي " اطال الله عمره وانار دربه

***واهدي ثمرة جهدي الى من منحتني الحياة وحرصت على تعليمي بصبرها وتضحيتها الى من كان دعائها سر نجاحي * امي * حفظها الله ورعاها**

***والى من هم انس عمري وفرحة حياتي اولادي " ادم ، ليلى ، محمد رائد"**

كما لا يفوتني الشكر والامتنان الى زوجي العزيز.

منال

Abstract

Medicinal plants serve as a prolific source of bioactive compounds with diverse biological activities, positioning them as a pivotal focus in research related to alternative medicine and pharmacology. This study investigates the phytochemical composition and antibacterial potential of essential oils derived from *Cotula cinerea* and *Origanum Majorana L.*, two medicinal plants native to the El Oued region of Algeria and traditionally used in folk remedies for various ailments.

The essential oils exhibited promising antibacterial properties, distinguished by their unique chemical profiles and notable efficacy. Using hydrodistillation, the extraction yield of Origanum Majorana L. oil reached 1.45%, compared to 0.90% for *Cotula cinerea*, with variations influenced by geographical factors such as soil composition and climate. Gas Chromatography-Mass Spectrometry (GC/MS) analysis identified trans-thujone as the predominant compound, accounting for 51.86% of *Cotula cinerea* oil and 33.3% of *Origanum Majorana L.* oil, along with santolina triene (16.4%) in the latter. These results underscore notable chemical differences compared to prior studies conducted in other regions.

In biological assays, *Origanum Majorana L.* oil demonstrated superior antibacterial activity, achieving a 25.6 mm inhibition zone against *S. aureus*, significantly outperforming amoxicillin, which exhibited a mere 0.1 mm zone. Furthermore, IC_{50} values highlighted the oils' potency, with *Origanum Majorana L.* displaying an IC_{50} of 1.5 mg/mL against E. coli, compared to 3.96 mg/mL for amoxicillin.

Computational studies corroborated the experimental findings. Molecular docking revealed that trans-thujone interacts strongly with bacterial protein active sites, particularly binding to HIS299 and ASP197 residues in *E. coli*, with a binding energy of -9.5 kcal/mol, indicating its potential to disrupt bacterial functions. Molecular Dynamics Simulations (MDS) further validated the stability of this interaction over a 100-nanosecond period, characterized by minimal atomic fluctuations (RMSD < 2 Å), reinforcing its candidacy as a potential therapeutic agent.

Regarding pharmacological safety, ADMET predictions indicated low toxicity for the principal compounds (classified under Toxicity Class 5) and favorable blood-brain barrier (BBB) permeability, without susceptibility to P-glycoprotein (P-gp) efflux. Nevertheless, compounds such as cis-Verbenyl acetate demonstrated inhibition of the CYP2C9 enzyme, suggesting the need for further investigation into possible drug interactions.

Keywords: Essential oils, *Cotula cinerea*, *Origanum Majorana L.*, Antibacterial activity, GC/MS analysis, Molecular Docking, Molecular Dynamics Simulations, ADMET properties, trans-thujone compound.

RÉSUMÉ

Les plantes médicinales sont une source riche de composés bioactifs aux activités biologiques variées, ce qui en fait un sujet central de recherche en médecine alternative et en pharmacologie. Cette étude vise à explorer les propriétés phytocinétiques et le potentiel antibactérien des huiles essentielles extraites de *Cotula cinerea* et *Origanum Majorana L*., deux plantes qui poussent dans la région d'El Oued en Algérie et sont traditionnellement utilisées en médecine populaire pour traiter diverses affections.

Les résultats ont révélé un potentiel prometteur pour les huiles essentielles extraites de *Cotula cinerea* et *Origanum Majorana L*. en tant qu'agents antibactériens naturels, caractérisés par leur composition chimique unique et leur efficacité élevée. En utilisant l'hydrodistillation, le rendement d'extraction de l'huile de *Origanum Majorana L*. a atteint 1,45 %, contre 0,90 % pour Cotula cinerea, avec des variations géographiques attribuées à des facteurs tels que le type de sol et le climat. L'analyse par chromatographie en phase gazeuse-spectrométrie de masse (GC/MS) a identifié le trans-thujone comme le composé dominant, représentant 51,86 % de l'huile de *Cotula cinerea* et 33,3 % de l'huile de *Origanum Majorana L*., avec la présence de santolina triene (16,4 % dans ce dernier). Ces résultats soulignent des différences chimiques significatives par rapport aux études antérieures sur ces plantes dans d'autres régions.

Dans les tests biologiques, l'huile de *Origanum Majorana L*. a excellé en activité antibactérienne, montrant une zone d'inhibition de 25,6 mm contre *S. aureus*, surpassant l'amoxicilline qui n'a montré qu'une zone de 0,1 mm contre la même souche. Les mesures de IC_{50} (concentration inhibant la croissance bactérienne à 50 %) ont également souligné la supériorité des huiles, l'huile de *Origanum Majorana L*. ayant un IC_{50} de 1,5 mg/mL contre E. coli, contre 3,96 mg/mL pour l'amoxicilline.

Les études computationnelles ont renforcé ces résultats. Le docking moléculaire a montré que le trans-thujone interagit fortement avec les sites actifs des protéines bactériennes, en particulier avec les résidus HIS299 et ASP197 dans *E. coli*, avec une énergie de liaison de -9,5 kcal/mol, ce qui confirme sa capacité à perturber les fonctions bactériennes. Les simulations de dynamique moléculaire (MDS) ont validé la stabilité de cette interaction sur une période de 100 nanosecondes, avec des fluctuations atomiques limitées (RMSD < 2 Å), renforçant son potentiel en tant que candidat thérapeutique.

En ce qui concerne la sécurité pharmacologique, les prédictions ADMET ont indiqué une faible toxicité pour les principaux composés (classés sous la classe de toxicité 5) et une perméabilité favorable à la barrière hémato-encéphalique (BBB), sans susceptibilité à l'efflux de la protéine P-glycoprotéine (P-gp). Toutefois, des composés comme cis-Verbenyl acetate

ont montré une inhibition de l'enzyme CYP2C9, nécessitant des études supplémentaires sur les interactions médicamenteuses potentielles.

Mots-clés : Huiles essentielles, *Cotula cinerea*, *Origanum Majorana L.*, Activité antibactérienne, Analyse par GC/MS, Docking moléculaire, Simulations de dynamique moléculaire, Propriétés ADMET, Composé trans-thujone.

الملخص

تعد النباتات الطبية مصدرًا غنيًا بالمركبات النشطة بيولوجيًا ذات الفعالية المتنوعة، مما يجعلها محط اهتمام رئيسي في أبحاث الطب البديل والصيدلة. تهدف هذه الدراسة إلى استكشاف الخصائص الكيميائية والنشاط المضاد للبكتيريا للزيوت العطرية المستخلصة من نباتي *شيحية ومردقوش*.، اللذين ينموان في منطقة الوادي بالجزائر، ويستخدمان تقليديًا في الطب الشعبي لعلاج العديد من الأمراض.

أظهرت الزيوت العطرية للنباتين إمكانات واعدة كمضادات طبيعية للبكتيريا، تتميز بتركيبة كيميائية فريدة وفعالية عالية. باستخدام الاستخلاص بالتقطير المائي، بلغ مردود زيت *مردقوش* نحو 1.45% مقارنة بـ 0.90% لزيت *شيحية* ، مع تباين جغرافي ناتج عن عوامل مثل نوعية التربة والمناخ. وقد كشفت تحاليل الكروماتوغرافيا الغازية-مطياف الكتلة (GC/MS)عن سيادة مركب trans-thujone بنسبة 51.86% في زيت *شيحية* و33.3% في زيت *مردقوش* .، إلى جانب مركب santolina triene بنسبة 16.4% في الزيت الأخير. تؤكد هذه النتائج الفروقات الكيميائية الكبيرة مقارنة بالدراسات السابقة على نفس النباتات في مناطق أخرى.

في التجارب العملية، أظهر زيت *مردقوش* تفوقًا في النشاط المضاد للبكتيريا، حيث حقق 25.6 مم في منطقة تثبيط بكتيريا العنقودية الذهبية ، متفوقًا على الأموكسيسيلين الذي أظهر منطقة تثبيط بلغت 0.1 مم فقط ضد نفس السلالة. كما أظهرت قياسات IC_{50} (التركيز المثبط لنمو 50% من البكتيريا) تفوق الزيوت، حيث حقق زيت IC_{50} *مردقوش* قدره 1.5 ملغم/مل ضد البكتيريا الإشريكية ، مقارنة بـ 3.96 ملغم/مل للأموكسيسيلين.

دعم التحليل الحاسوبي هذه النتائج، حيث أظهر الارتباط الجزيئي قدرة مركب trans-thujone على التفاعل بقوة مع المواقع النشطة للبروتينات البكتيرية، خاصة مع بقايا HIS299 و ASP197 في الإشريكية ، بطاقة ارتباط بلغت -9.5 كيلو كالوري/مول، مما يشير إلى قدرته على تعطيل وظائف البكتيريا. كما أكدت محاكاة الديناميكيات الجزيئية (MDS) استقرار هذا الارتباط خلال محاكاة امتدت لـ 100 نانوثانية مع تقلبات ذرية محدودة(RMSD < 2 Å) ، مما يعزز إمكانيته كمركب دوائي محتمل.

أما فيما يتعلق بالسلامة الدوائية، فقد أظهرت تنبؤات ADMET سمية منخفضة للمركبات الرئيسية (مصنفة في فئة السمية 5) ومرورًا جيدًا عبر الحاجز الدموي الدماغي(BBB) ، دون تأثر بآلية طرد الأدوية .(P-gp) ومع ذلك، أظهرت بعض المركبات مثل cis-Verbenyl acetate تثبيطًا لإنزيمCYP2C9 ، مما يستدعي إجراء المزيد من الدراسات حول التداخلات الدوائية المحتملة.

الكلمات المفتاحية: شيحية، مردقوش، زيوت أساسية، النشاط المضاد للبكتيريا، التحليل بواسطة GC/MS، الارتباط الجزيئي، المحاكاة الديناميكية الجزيئية، خصائص ADMET، مركب trans-thujon.

ABBREVIATIONS LIST

%: percentage

ΔG: Binding free energy

A°: Angstrom

A0

Abs: Absorbance

ADMET: Absorption, Distribution, Metabolism, Excretion of drugs and Toxicity

C: Concentration

C°: Degrees Celsius

DMSO: Diméthylsulfoxide

EOs: Essential Oils

EOCc: Essential oils of *Cotula cinerea*

EOOm: Essential oils of *Origanum Majorana L*

g: gramme

GC/MS: Gas Chromatography-Mass Spectrometry

IC50: Concentration causing 50% inhibition of an activity

IFD: Induced Fit docking

Iv: In vitro

K: Constante de liaison

MDS: Molecular Dynamics Simulation

mg: Milligramme

min: Minute

mm: Milimeter

ml: Mililiter

Ms: mass spectrometer

SIB: Swiss Institute of Bioinformatics

Vis: Visible

VTRS: Valorisation and Technology of the Saharian Resources Laboratory

µl: Microlitre

FIGURES LIST

FIRST PART: BIBLIOGRAPHY

CHAPTER ONE: MEDICINAL PLANTS

CHAPTER TWO: ESSENTIAL OILS

CHAPTER THREE: ANTIBACTERIAL ACTIVITY

SECOND PART: EXPERIMENTAL

CHAPTER ONE: MATERIALS AND METHODS

CHAPTER TWO: RESULTS AND DISCUSSION

TABLES LIST

FIRST PART: BIBLIOGRAPHY

CHAPTER ONE: MEDICINAL PLANTS

CHAPTER TWO: ESSENTIAL OILS

SECOND PART: EXPERIMENTAL

CHAPTER ONE: MATERIALS AND METHODS

CHAPTER TWO: RESULTS AND DISCUSSION

Summary

CHAPTER THREE: ANTIBACTERIAL ACTIVITY

SECOND PART: EXPERIMENTAL

CHAPTER ONE: MATERIALS AND METHODS

CHAPTER TWO: RESULTS AND DISCUSSION

GENERAL INTRODUCTION

Introduction

Essential oils are important natural compounds extracted from plant tissues, recognized for their diverse biological activities, particularly their antibacterial properties. Their broad applicability in the food and pharmaceutical industries has fueled growing scientific interest in exploring their potential as safe and effective alternatives to synthetic chemical agents (Özkalp, Özcan, & Sağdıç, 2019). In recent years, the increasing emphasis on natural and sustainable solutions has further highlighted the significance of studying medicinal plants and their bioactive components.

Numerous studies have demonstrated the efficacy of essential oils in inhibiting the growth of a wide range of microorganisms, including foodborne pathogens, thereby underscoring their role in food preservation and infection control (Özkalp et al., 2019). This antimicrobial effect is closely related to their rich and complex chemical compositions, which include terpenes, phenolics, and other biologically active molecules.

Algeria, endowed with rich plant biodiversity, possesses a long-standing tradition of utilizing medicinal plants for the treatment of various ailments. In Algerian folk medicine, numerous plant species have been employed for their therapeutic properties across generations (Khacheba, Derridj, Meddah, & Allali, 2017). Among these, *Cotula cinerea* and *Origanum Majorana L.* are particularly notable for their traditional uses and natural occurrence in the El Oued region, located in southeastern Algeria.

Bacteria, as single-celled microorganisms, inhabit diverse environments and, while most are harmless or beneficial, some pathogenic strains can cause serious diseases such as gastrointestinal infections, pneumonia, and meningitis. Given the escalating problem of antibiotic resistance, the search for new natural antimicrobial agents has become more urgent than ever (Madigan et al., 2018).

In this context, the present study aims to investigate the phytochemical and antibacterial potential of *Cotula cinerea* and *Origanum Majorana L.*. The essential oils from these plants were extracted using hydrodistillation and subsequently analyzed for their chemical composition using gas chromatography–mass spectrometry (GC/MS). The antibacterial activities were evaluated both *in vitro* and *in silico* against selected reference bacterial strains, namely:

- *Escherichia coli* (ATCC 25922)
- *Klebsiella pneumoniae* (ATCC 13883)
- *Staphylococcus aureus* (ATCC 25923)

Through this study, we seek to contribute to the growing body of knowledge on the biological potential of local medicinal plants and to support ongoing efforts to find natural alternatives to conventional antibiotics, particularly in addressing the global challenge of antibiotic resistance.

FIRST PART
BIBLIOGRAPHY

CHAPTER ONE MEDICINAL PLANTS

1. Introduction

Nature, in all its diversity and color, stands as one of the most profound gifts granted to humanity (Maathai, W., 2010). Within this natural world, the Creator has instilled both aesthetic beauty and countless benefits, as emphasized repeatedly in the Quran. Since the dawn of human existence, people have turned to plants and herbs as essential tools for healing and treatment. In ancient civilizations, herbal remedies were the primary solution for nearly all forms of illness and discomfort.

As societies evolved and scientific knowledge expanded, synthetic pharmaceuticals began to emerge and gradually rival the traditional use of medicinal plants (Ghassan M., 1999). With ongoing technological advancements and the rise of modern medical practices, herbal treatments were increasingly set aside in favor of chemical alternatives.

In recent decades, however, there has been a notable resurgence of interest in herbal medicine. It has reentered public and scientific discourse, sparking debate and discussion among researchers, medical professionals, and patients. While many advocate for its benefits, others remain skeptical of its place in contemporary healthcare (Jeanfils J, 1991).

2. The studied plants:

2.1. *Cotula cinerea* Plant:

2.1.1. *Cotula cinerea* Definition:

Cotula cinerea, commonly referred to as Sheikh, is a plant known for its distinctive scent, which closely resembles that of wormwood. It is a herbaceous annual species characterized by its densely lobed foliage and sturdy, pale bristles. This plant blooms in the springtime, producing yellow flowers that resemble the composite heads typical of the Asteraceae family.

Cotula cinerea is native to arid and desert landscapes, flourishing particularly across Arab regions. It is rich in a variety of bioactive compounds, including flavonoids, terpenes, and essential volatile oils (Bohlmann, F. et al., 1973; Mahran, G.H. et al., 1976).

2.1.2. Botanical Classification of *Cotula cinerea*

- **Scientific name**: *Cotula cinerea* Del.
- **Synonym**: *Brocchia cinerea* (Del.) Vis.
- **Common names**: Sheikh, Rubaita, Sheha al-Bal

Table I-1. Botanical Classification of *Cotula cinerea.*

Reign	*Plants*
Branch	*Angiospermes*
Class	*Dicotyledons*
Order	*Tubiflorales*
Family	*Asteraceae(Composées)*
Generates	*Cotula*
Species	*Cinerea*

2.1.3. Vegetative Characteristics of *Cotula cinerea*

Cotula cinerea is a small, herbaceous plant, typically growing between 10 and 40 centimeters tall. It is easily recognized by its strong, sharp scent (Boning, C., 2010). The plant is covered with fine, white hairs, and its stems are either upright or slightly inclined, cylindrical in shape, and display a yellowish green coloration.

The foliage is pale green and densely coated in woolly bristles. The leaves are thick and trifoliate in form, with the tip often divided into three to five distinct lobes, giving them a segmented appearance.

The flower heads (capitula) are small and flat, ranging from 6 to 10 millimeters in diameter (Naidu, V., 2012). Composed entirely of tubular florets, they are tetramerous and tightly clustered, forming a dense compound inflorescence topped by a central capitulum. The floral buds are initially dark in color and gradually turn bright golden yellow when fully open. The plant produces small, hairless fruits with minimal structure, as shown in Figure (1) (Ahmed, A.A., et al., 1987; Malinskas, G.A.G., et al., 1987).

Figure I-1. *Cotula cinerea* photograph.

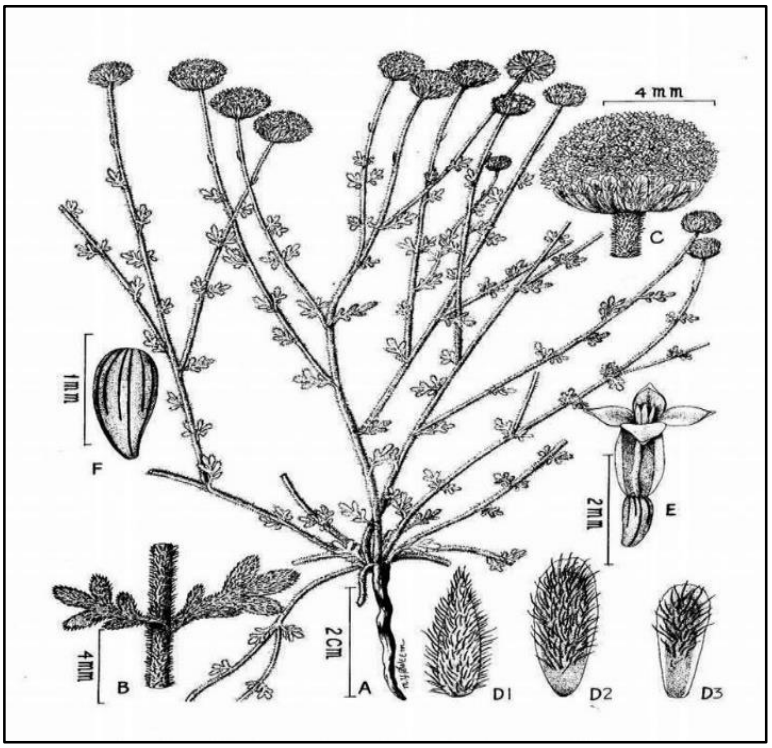

Figure I-2. Diagram form of *Cotula cinerea*

2.1.4 .Geographical Distribution of *Cotula cinerea*

Cotula cinerea is widely distributed throughout the southern hemisphere, with a notable presence in arid regions such as the Sahara Desert, the deserts of India and Iran in Asia, and across the Arabian Peninsula (Rezaei M.B., et al.; G. Fournier'3, H., et al.). In Algeria, this plant is especially prevalent in desert and semi-arid areas, with a higher concentration observed in the southeastern parts of the country. Its geographic range within Algeria is illustrated in Figure 3.

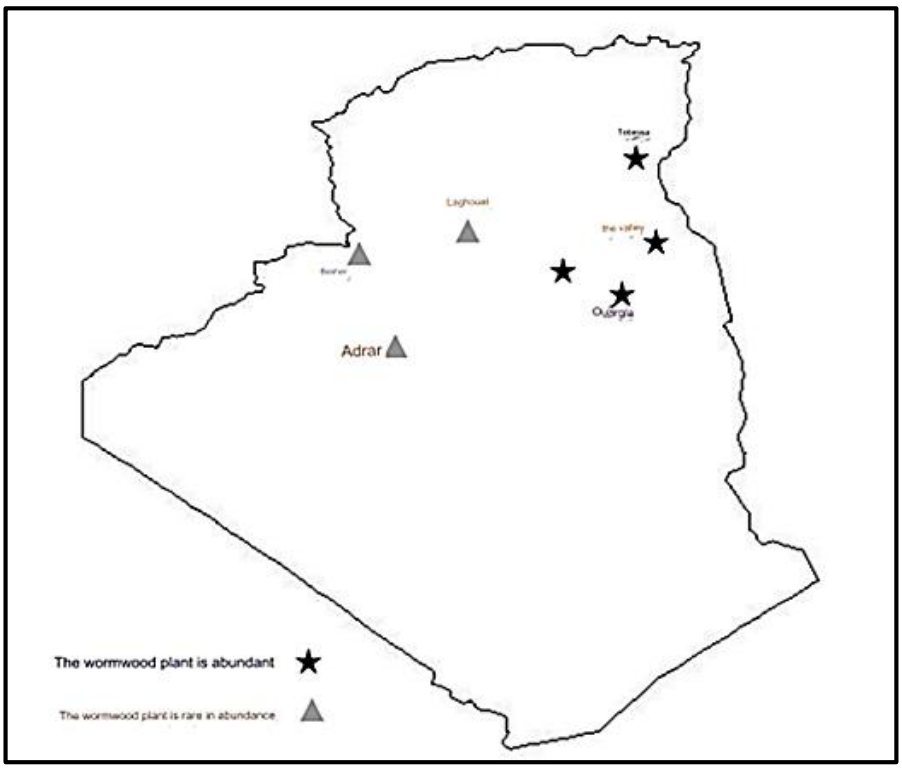

Figure I-3. Distribution of *Cotula cinerea* in Algeria.

2.1.5 .Economic and Medicinal Applications of *Cotula cinerea*

In some cultures, *Cotula cinerea* is used as a flavor enhancer in beverages such as tea and coffee, or as an infusion ingredient. Beyond its culinary applications, the plant plays an important role in traditional medicine. It is commonly used to relieve abdominal discomfort and improve digestion (M. Markouk, H.B. et al.; Boulahbal F., et al., 2002). Its antitussive (cough-suppressant) properties have made it beneficial in treating bronchitis, and extracts of the plant have shown promising antifungal activity (Bryskier A., et al., 1999).

The plant's flavonoid compounds contribute to a range of therapeutic effects, including sedative, anti-inflammatory, and antiseptic actions. In various regions, *Cotula cinerea* continues to be a traditional remedy for treating stomach and abdominal ailments (Larpent J.P., et al., 1989).

2.2. *Origanum Majorana L* Plant

2.2.1. *Origanum Majorana L* Definition:

The name *Origanum* derives from the combination of two Greek words" oros" meaning mountain and " ganos " meaning "joy" or "delight" a reference to its association with the pleasant aroma and beauty of mountainous landscapes where it naturally thrives, particularly throughout the Mediterranean basin (Prena and Neeru Vasudeva, et al., 2015). Botanically,

Origanum Majorana L. is classified as a perennial herb, and it was previously referred to by this full scientific name (Vagi E., Simandi B., et al., 2002).

This plant demonstrates notable morphological and phytochemical variability and includes up to forty-nine distinct taxa found throughout the Mediterranean region. Commonly known as sweet marjoram, it is native to Anatolia (modern-day Turkey) and Cyprus, and is widely cultivated across Mediterranean countries, with Egypt being a significant growing region (Novak J., et al., 2002).

Historically, marjoram was employed by Hippocrates himself as an antiseptic, and it has long served as a traditional household remedy for respiratory ailments, such as coughs, sore throats, and other infections (Bremness L., et al., 1994; Yazdanparast R., et al., 2008).

2.2.2. Botanical Classification of *Origanum Majorana L.*

- **Scientific Name**: *Origanum Majorana L*.
- **Synonym**: Marjolaine
- **Common Name**: Al-Murdagush

Table I-2. Vegetative classification of Origanum Majorana L.

Reign	*Palnts*
Branch	*Mangnoliophyta*
Class	*Mangnoliopsida*
Order	*Lamiales*
Family	*Lamiaceae*
Generates	*Origanum*
Species	*Majorana L*

2.2.3. Vegetative Description of *Origanum Majorana L.*

Origanum Majorana L. is a semi-perennial herb that grows annually and is sensitive to low temperatures. It typically reaches a height between 30 and 60 cm and is known for its aromatic qualities. The plant forms a compact, bushy appearance, with numerous reddish, square-shaped stems that tend to spread outward (Oakman, H., 1995). These stems are upright, slender, and covered with fine hairs. They are generally cylindrical in form, displaying a green color interspersed with red specks (Pimple B.P., et al., 2012).

The leaves are soft and simple, displaying a velvety texture due to dense surface hairs. They are oval to oblong-rectangular in shape, with a grayish-green coloration. The leaf arrangement is opposite, and each leaf typically measures about 1.5 to 0.5 cm in length and width. Leaf margins are entire, with pointed tips and straight, symmetrical bases. Prominent veining is visible on the surface.

During mid-to-late summer, the plant produces clusters of small, tubular flowers that are either white or pale pink. Each flower is less than 0.3 cm long and arranged in elongated spikes reaching up to 13 cm in length. These blossoms are bisexual in nature (A. Blazovics A., et al., 2005).

The fruiting stage yields tiny, oval-shaped seeds that are dark brown and mature between August and September. The seeds are cylindrical and small in size. The root system is composed of long, symmetrical roots aligned longitudinally, often featuring shallow cuts with diameters ranging from 0.2 to 0.6 mm. The outer surface of the roots is dark brown, marked by deep, narrow fissures. These root characteristics are vital for water and nutrient absorption and contribute significantly to the plant's anchorage and overall stability in the soil. The roots also emit a subtle aromatic scent, enhancing both the aesthetic and functional value of the plant (Singla P., et al., 2014).

Figure I-4. *Origanum Majorana L* Photograph

Figure I-5. Diagram for *Origanum Majorana L*

2.2.4. Geographical Distribution of *Origanum Majorana L*.

Origanum Majorana L is predominantly native to Turkey and Cyprus, with its presence extending across several Mediterranean countries such as Lebanon, Iran, and parts of North America. The species also thrives in the Arabian Peninsula and India, particularly in dry climates where it grows well on sunlit slopes, meadows, open fields, and rocky landscapes (Zahran, M., et al., 2010). In Saudi Arabia, it is widely cultivated, especially in the southern regions, where environmental conditions favor its development.

Figure 6 illustrates the distribution of *Origanum Majorana L* in Algeria.

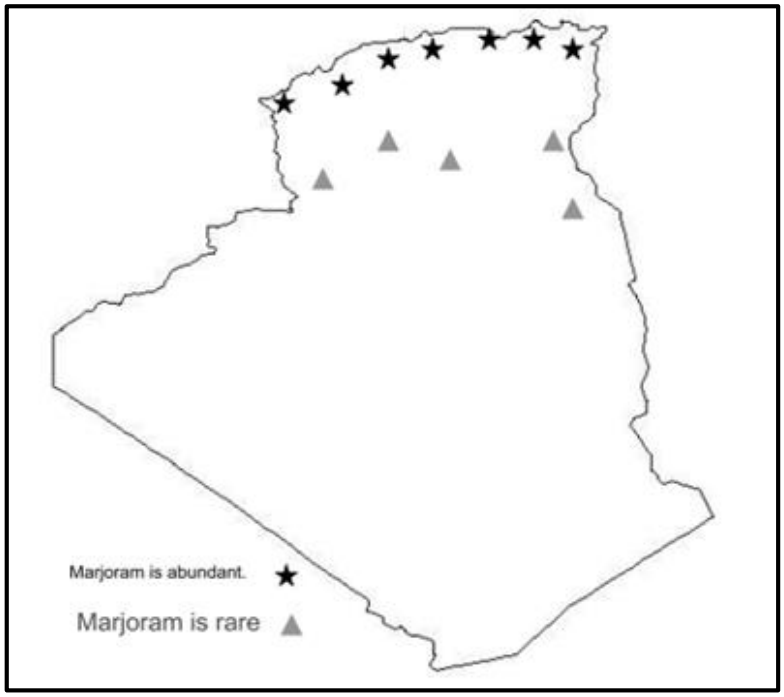

Figure I-6. The spread of *Origanum Majorana L* in Algeria

2.2.5. Economic and Medicinal Applications of *Origanum Majorana L*

Origanum Majorana L is renowned for its numerous medicinal uses, particularly in the treatment of chest infections, coughs, sore throats, rheumatic pain, neurological conditions, and heart disease (Mancak, M., et al., 2023). Many of these remedies can be easily administered at home, providing relief and easing symptoms. Notable treatments include:

1. **Rest and Relaxation**: Adequate rest and sleep are recommended to strengthen the immune system and speed up recovery (Farmawati, C., et al., 2020).

2. **Consumption of Warm Liquids**: Drinking warm liquids, such as herbal teas and soups, can help relieve throat discomfort and reduce congestion (McIntyre, A., 2000).

3. **Steam Inhalation**: Inhaling steam from hot water or using an air humidifier can ease congestion and soothe the respiratory system (Vathanophas, V., et al., 2019).

4. **Honey**: Natural honey, known for its antibiotic properties, can help alleviate sore throats and suppress coughing (Kumar, K. S., et al., 2010).

5. **Omega-3 Rich Foods**: Consuming foods high in omega-3 fatty acids, such as fatty fish and nuts, can help reduce inflammation and support heart health (Simopoulos, A., 2002).

However, individuals suffering from these conditions should consult a healthcare professional before relying on home remedies to ensure they are safe and effective (Sharifi-R., et al., 2021).

Beyond its medicinal uses, *Origanum Majorana L*. is extensively used in the food industry, primarily as a seasoning for meats and vegetables. However, its use during pregnancy is not recommended due to its potential to stimulate uterine contractions.

Traditionally, the leaves of the plant have been used to treat a variety of ailments, including diabetes, insomnia, colds, asthma, and panic attacks (Cano J.H. and Volpato G., et al., 2004). The essential oil extracted from the leaves is also used to impart a unique flavor to culinary dishes. *Origanum Majorana L*. is commonly added to a variety of food products, including soups, gravies, meats, fish, canned goods, liqueurs, and even beers (Farrell K.T. Spices, et al., 1985; Lavrenov V.K., et al., 1999).

3. Previous Studies:

3.1. Previous Research on *Cotula cinerea* Plant

A review of the chemical literature on *Cotula cinerea* reveals extensive studies focused on various bioactive compounds. Key findings include the identification of lactonic sesquiterpenes (Metwally, M., et al., 1986; Jakupovic, J., et al., 1988; Bohlmann, F., et al., 1989), ethereal comarenic sesquiterpenes (Greger, H., et al., 1985), and monocyclic diterpenes, all of which contribute significantly to the plant's chemical profile. Furthermore, triterpenes and distinctive acetylene compounds, particularly the spiroketal enol ethers, have been characterized (Metwally, M., et al., 1986; Bohlmann, F., et al., 1973).

In addition to these chemical analyses, a study by Lotfi et al. examined the active compounds present in *Cotula cinerea*. Their research revealed an absence of alkaloids, contrasting with the presence of flavonoids and glycosides, which were found to be prominent in the plant (Lotfi B., et al., 2011). A summary of the active constituents identified in the *Cotula cinerea* plant is provided in **Table 3** below.

Table I-3. Active Ingredients of *Cotula cinerea* Plant

Glycosides	**turbines and Steroids**	**tannins**	**essential oils**	**Saponics**	**alkaloids**	**Flavonoids**
+	++	++	++	+	-	+++

(+ + +): Highly abundant.

(+ +): Abundant.

(+): Weak.

(-): Absent.

A research team led by Professor M. Markouk and his colleagues from the University of Marrakech, Morocco, conducted a study to examine the anti-pathogenic properties of *Cotula cinerea*. This plant, which thrives in sandy and desert environments, is traditionally used in Moroccan medicine for its anti-inflammatory, sedative, disinfectant, and antibacterial effects, as well as being utilized as an aromatic addition to tea (M. Markouk et al.). A sample of *Cotula cinerea* was collected from the Faculty of Science in Mashba, Marrakech, Morocco, and its extract was used for experimentation.

The study involved 21 white Swiss mice, each weighing between 20 and 22 grams (Mehedi, N., et al., 2013). The mice were kept in plastic cages at a controlled temperature of 22 to 24 degrees Celsius and were fasted for 14 hours before the test (Van de W., et al., 2002). The experiment included the administration of three different extracts from the plant: ethyl acetate, diethyl ether, and ethanol. The results indicated acute toxicity, with some mice succumbing to the treatment and others exhibiting various clinical symptoms (El Kabbaoui, M., et al., 2017). Additionally, acetate and n-butanol extracts were also tested.

Table I-4. presents the toxic effects of the various *Cotula cinerea* plant extracts used in the study.

Oral dose (g/Kg)	Number of Animals Tested	Clinical symptoms decrease of weight ,oedema , hair loss, convulsion /No .tested			Mortality		
Vehicle control (10mL/Kg)		EB	EAc	EE	EB	EAc	EE
1	6	0/6	0/6	0/6	0/6	0/6	0/6
2	6	0/6	0/6	0/6	0/6	0/6	0/6
3	6	0/6	0/6	0/6	0/6	0/6	0/6
4	6	0/6	0/6	0/6	0/6	0/6	0/6
5	6	0/6	0/6	0/6	0/6	0/6	0/6
6	6	0/6	0/6	0/6	0/6	0/6	0/6

EE = Ethyl Ether Extract **EAc** = Ethyl Acetate Extract **EB** = n-Butanol Extract

3.1.1.Toxicity and Antibacterial Evaluation of *Cotula cinerea* Extracts

The results from the toxicity trials, summarized in **Table 4**, show that none of the mice experienced convulsions or deaths after administration of the *Cotula cinerea* extracts—n-butanol (EB), ethyl acetate (EAc), and ethyl ether (EE). Each group of six mice received a vehicle control dose of 10 mL/kg, and throughout the experiment, no abnormal behavior or adverse clinical signs were observed across all trials.

According to the findings, doses up to 6 grams per kilogram of body weight did not produce any lethal effects or behavioral changes in the mice, confirming a high level of tolerance for these concentrations (Mukinda, J., et al., 2007).

In a subsequent phase of the study, the same research group led by Dr. M. Markouk assessed the antibacterial efficacy of *Cotula cinerea* extracts using Minimum Inhibitory Concentration (MIC) testing. After 24 hours of incubation, the inhibitory effects on bacterial growth were recorded. Each test was performed in triplicate to ensure accuracy and reproducibility (Mathur, T., et al., 2006).

Table 5 presents the MIC values of the *Cotula cinerea* extracts, expressed in micrograms per milliliter (µg/mL), indicating their antimicrobl potential.

3.1.2. Antimicrobial and Phytochemical Studies on *Cotula cinerea*

The antimicrobial potential of *Cotula cinerea* was evaluated against various bacterial strains using extracts obtained through different solvents, including ethyl acetate, n-butanol,

and ethyl ether. The Minimum Inhibitory Concentration (MIC) values for each extract, alongside a standard antibiotic (Novobiocin), are presented below:

Table I-5. Toxicity Efficacy of *Cotula* Plant

Bacterial Species	Strain	Ethyl Acetate Extract (µg/mL)	n-Butanol Extract (µg/mL)	Novobiocin (µg/mL)
Pseudomonas fluorescens	456-2	200	12	1
Pseudomonas savastanoi	T12-10	200	100	1
Pseudomonas savastanoi	73-29 88	200	50	1
***Bacillus* sp.**	VP5	200	25	20
Bacillus brevis	VP7	200	25	20
***Bacillus* sp.**	326	200	25	20
Bacillus sphaericus	324	200	200	20
***Bacillus* sp.**	459-1	200	12	20

Key Findings: The ethyl ether extract of *Cotula cinerea* showed no antimicrobial activity, whereas the ethyl acetate extract demonstrated consistent effectiveness across all tested pathogens (Acheuk, F., et al., 2020). Notably, the n-butanol extract exhibited strong antibacterial effects, outperforming other extracts in most cases. A correlation study between extract concentration and antimicrobial activity revealed a significant increase in the inhibition zone as extract concentration increased. This relationship was statistically confirmed through a two-way ANOVA, indicating notable differences in the antimicrobial efficacy of the tested extracts (Atef, C., et al., 2015).

In an investigation conducted by Khallouki et al. (2015), the phytochemical composition of *Cotula cinerea* from southeastern Morocco was analyzed, revealing a high total phenolic content of 2.5 ± 79.23 mg/g of dry material in methanol extracts (Irondi, E., et al., 2018). High-performance liquid chromatography coupled with electrospray ionization mass spectrometry (HPLC-ESI-MS) identified key phenolic compounds including neochlorogenic acid, dicaffeoylquinic acid isomers (3,5; 3,4; 5,4), cryptochlorogenic acid, and chlorogenic acid. Antioxidant potential assessed via FRAP and DPPH assays confirmed strong free-radical

scavenging activity, supporting its traditional use in African medicine for disease prevention—likely attributed to the high flavonoid and phenolic content (Khallouki, F., et al., 2015).

Further research by Santiuste et al. (2008) and Fatiha B., et al., explored the aromatic properties of *Cotula cinerea* essential oil. The study suggested its suitability as a flavoring agent in tea, offering a natural alternative to mint. Additionally, traditional applications of the plant in treating pulmonary and tracheal infections were highlighted.

El-Bouzidi et al. (2011) evaluated the anti-candidiasis properties of *Cotula cinerea* essential oil, demonstrating strong antifungal activity against various *Candida* strains. The MIC ranged from 3.2 to 4.7 mg/mL, with a minimum fungicidal concentration (MFC) of 5.9 mg/mL. GC-MS analysis identified 24 active constituents in the oil, several of which are considered promising candidates for developing antifungal agents targeting resistant strains (Cecchini, C., et al., 2010).

In a related study conducted by Abdenbi Asma et al. (2014), essential oil was extracted via water distillation from aerial parts of the plant in the Bashar region of Morocco. The oil displayed variable antibacterial activity, inhibiting up to seven bacterial strains, with MIC values reaching as low as 2%. The inhibition zone for gut bacteria was reported to be as large as 55 mm, indicating substantial potency.

Lastly, a 2014 review provided an in-depth analysis of the essential oil composition and its antibacterial and antifungal properties. The oil, obtained via hydrodistillation, was analyzed using gas chromatography (GC) and gas chromatography-mass spectrometry (GC/MS). Major components identified included ISO-thujanol-3, Santolina triene, and cavor. These compounds were shown to exhibit antimicrobial effects against four bacterial species and antifungal efficacy against fungal rot (Review, Tutorial, 2014).

3.2. Prior Investigations on *Origanum Majorana L.*

Research into *Origanum Majorana L.* has shed light on its nutritional makeup and potential applications in food preservation and phytochemistry. The chemical composition of its leaves includes a moisture content of 66.3%, alongside 18.7% protein, 8.4% fat, 6.6% ash, and 5.7% carbohydrates, reflecting its considerable nutritional value (Pinela, J., et al., 2017).

An analysis of its mineral profile showed concentrations of various metals in parts per million: barium (0.6 ppm), iron (5.1 ppm), potassium (0.039 ppm), cobalt (0.49 ppm), and sodium (0.01 ppm). Additionally, qualitative evaluations of its aqueous and ethanol-based

extracts confirmed the presence of biologically active compounds such as tannins, flavonoids, phenols, saponins, carbohydrates, and alkaloids (Maryam A., et al., 2017). Studies into its physical and chemical behavior revealed that these extracts dissolve well in non-polar solvents, while showing only partial solubility in polar media.

The preservative properties of *O. Majorana* leaf powder were tested in beef stored at 5°C over a 7 to 10-day period. Applied at concentrations of 0.5% to 1%, the herb reduced peroxide values in meat samples, indicating a slowing of lipid oxidation processes when compared with untreated controls (Sahunie, A., et al., 2024). Moreover, microbial analyses during the same timeframe revealed a decline in the growth of coliforms and Enterobacteriaceae. These results suggest that *O. Majorana* not only enhances the oxidative stability of meat but also contributes to microbial suppression, thereby extending product shelf life (Maryam A., et al., 2017).

CHAPTER TWO
ESSENTIAL OILS

1. Overview of Essential Oils

1.1. Definition

Essential oils, often referred to as volatile or aromatic oils, are defined by their ability to evaporate without undergoing decomposition unlike fixed oils, which are prone to breakdown under heat or exposure to air (L. Mondello, et al., 1995). These oils are volatile, aromatic, and ether-soluble compounds that are primarily colorless to yellowish in hue. Although they are liquids under standard conditions, they are also highly sensitive to oxidation and lack the greasy consistency of fatty oils (E. Guentherin, 1972; S. Rahal, 2004).

They are typically extracted through steam distillation or, in the case of citrus species, via mechanical pressing of peels, followed by physical separation processes. The International Standards Organization defines essential oils as volatile substances isolated from plant materials using such techniques—an internationally accepted definition used in both scientific and industrial applications (D. Lemordant, 1989; K. W. Lee, et al., 2004).

1.2. Storage and Localization in Plants

Essential oils are synthesized and stored by over 2,000 plant species from more than 60 botanical families (Nieto, G., 2017). Their distribution within the plant varies, being found either throughout the organism or concentrated in specific organs such as leaves, flowers, roots, or fruits. These compounds generally accumulate in the cytoplasm of living cells, most often in liquid form. In some instances, they may also be associated with glycosides or resinous matrices, making them solid and non-free (Ogunsina, O., 2020).

Their storage typically occurs within specialized anatomical structures known as secretory tissues. Depending on the species, essential oils can be found in:

- **Leaves** – as seen in mint (*Lamiaceae* family)
- **Flowers** – notably in rose and jasmine
- **Fruits/Peels** – in citrus fruits (*Rutaceae* family), e.g., *Citrus aurantium L.* (Guzmán, E., et al., 2021)
- **Leaves** – in *Eucalyptus* species (*Myrtaceae* family) (Elaissi, A., et al., 2012)
- **Vascular channels** – in *Angelica archangelica* (*Apiaceae* family) (D'Amelio Sr, F., 1998)

- **Aerial parts** – commonly in thyme and mint (*Lamiaceae*) (F. Abdellatif, et al., 2005)

The site and concentration of these oils vary depending on the plant species and organ, contributing to their unique therapeutic and aromatic properties (J. Valnet, 1984; A. Baaliouamer, 1987; K. Bauer, et al., 1997; R. L. Shriner, et al.).

Examples:

Rutaceae: Essential oils are primarily concentrated in the leaves, flowers, and seeds, exemplified by Citrus aurantium L. (Guzmán, E., et al.,2021).

Myrtaceae: Essential oils are concentrated in the leaves, as seen in Eucalyptus species. (Elaissi, A., et al., 2012).

Apiaceae: Essential oils are concentrated within the vascular channels, exemplified by Angelica archangelica. (D'Amelio Sr, F., 1998).

Lamiaceae: Essential oils are predominantly concentrated in the aerial parts of plants, as observed in species like mint and thyme (F. Abdellatif., et al., 2005).

1.3. Physical Characteristics of Essential Oils

Despite the diversity in their chemical profiles, freshly obtained essential oils share several consistent natural features. These physical attributes are outlined below (D. Lemordant, 1989; Anonyme, 2000; D. O. Kennedy et al., 2002; R. J. Grayer et al., 2003):

1. Color

Fresh essential oils are generally colorless, but exposure to air and prolonged storage may lead to oxidation, causing them to darken and eventually turn black (Turek, C. et al., 2013). In some rare cases, such as with chamomile or eucalyptus oils, a greenish-blue tint may appear due to the presence of azulene and chamazulene—compounds known for imparting such hues. Additionally, pale yellow or light-colored oils may result from bleaching effects over time (E. Seguin et al., 2001).

2. Aroma

The majority of essential oils have pleasant and distinctive aromas, rarely emitting strong or offensive odors. Their fragrance is primarily attributed to specific terpenes and major volatile constituents, which are often detectable even before extraction (Sell, C., 2020). For example,

citral lends a lemony scent to certain plants, while menthol, geraniol, and anethol contribute to the aromas of mint, thyme, and aniseed, respectively (B. A. Arthur Riffer et al., 1969).

3. Volatility

One of the defining traits of essential oils is their high volatility at ambient temperatures, a property that sets them apart from non-volatile fixed oils. Unlike fixed oils, which leave a greasy residue, a single drop of essential oil will fully evaporate without trace on a filter paper (B. A. Arthur Riffer et al., 1969).

4. Solubility

Essential oils are only slightly soluble in water, but they dissolve easily in most organic solvents such as diethyl ether and petroleum ether (Aziz, Z. et al., 2018). Alcohol serves as a common solvent for essential oils, with solubility reaching up to 95%, although rose oil may form an emulsion due to certain paraffin-like substances. The solubility of an essential oil in alcohol is often used as a measure of purity—testing at alcohol concentrations ranging from 95% to 35% diluted with water. The presence of fixed oils can interfere with this dissolution (B. A. Arthur Riffer et al., 1969; O. Ekundayo, 1988).

5. Specific Gravity

The specific gravity of essential oils varies depending on their botanical origin, typically ranging from 0.1 to 1.7 (Schmidt, E., 2020). Most essential oils are lighter than water and float, but some—such as clove and cinnamon bark oils—are denser, with values between 1.02 and 1.07, and sink in water. Lower specific gravity values (under 0.9) indicate a higher proportion of aliphatic or tertiary compounds, whereas values above 1 suggest the presence of structurally complex aromatic compounds (B. A. Arthur Riffer et al., 1969).

6. Optical Rotation

Essential oils also exhibit optical activity, which is a critical factor in quality control and purity verification. This optical rotation enables analysts to distinguish between natural oils and synthetic imitations (Sheldon, R., 1993). While most essential oils remain liquid at room temperature, exceptions like rose and elemi oil may solidify. Additionally, essential oils typically have a high refractive index, which further supports their identification and analysis.

1.4. Chemical Constituents of Essential Oils

Essential oils are intricate blends composed of a wide array of chemical compounds. These constituents are generally grouped into two primary categories (Dhifi, W., et al., 2016). The first group includes hydrocarbons—predominantly terpenes—which form the bulk of essential oil composition. The second group consists of oxygenated compounds such as alcohols, esters, ketones, aldehydes, ethers, and organic acids. Additionally, minor elements containing sulfur or nitrogen may also be present. The terpene fraction, in particular, represents a major structural and functional component of these oils (E. Seguin et al., 2001; Dr. Al-Shahat N., 2000).

1. Terpenes

Terpenes are naturally occurring compounds found in various plant organs and play a significant role in secondary metabolism. They are largely responsible for the aromatic properties of essential oils. The term "terpenes" derives from turpentine, a resin-based oil from which these compounds were first isolated (B. A. Arthur Riffer et al., 1969). Most terpenes are volatile and are obtained through processes similar to essential oil extraction (N. Ramarathnam et al., 1986).

In daily life, terpenes serve important biological functions—Vitamin A, for example, is a terpene vital for vision. As early as 1877, German researcher Owllach from the University of Göttingen classified terpenes based on the number of repeating isoprene units. The classification is illustrated in the table below (E. Seguin et al., 2001; Ghassan M., 1999).

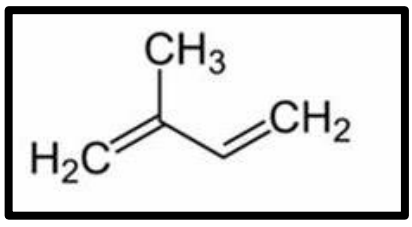

Figure II-1. Isobrin unit

✓ **Types of Terpenes**

1. **Monoterpenes**

These are among the most abundant terpenes in plants (O. Ekundayo, 1988), composed of two isoprene units (10 carbon atoms) and typically possess a monocyclic structure. Common representatives include limonene and α-phellandrene.

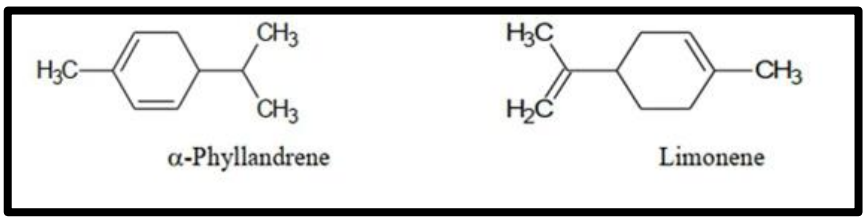

Figure II-2. Mono-ring Monoterbines

Some monoterpenes, like sabinene, α-pinene, and β-pinene, exhibit bicyclic structures (E. Seguin et al., 2001; R. Paris, 1972). These are further classified into structural groups: Thujane, Camphane, Bornane, and Fenchane—found in cedarwood and turpentine, typically extracted from pine bark.

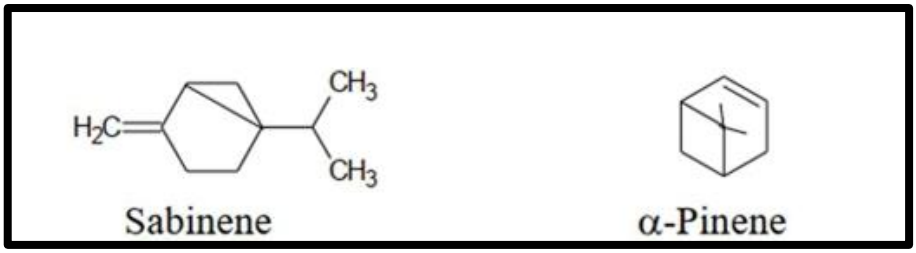

Figure II-3. Bicycle Monoterbines

2. **Sesquiterpenes**

Comprising three isoprene units (15 carbon atoms), sesquiterpenes include over 2,500 known molecules (Ceausescu, E., 2013). They are structurally diverse and categorized accordingly. Notable examples include cadinene and caryophyllene, the latter present in celery oil.

3. **Diterpenes**

Made up of four isoprene units (20 carbon atoms), diterpenes include biologically important compounds such as phytol and Vitamin A1 (Ruzicka, L., et al., 1953).

4. **Triterpenes**

These consist of six isoprene units (30 carbon atoms). A prominent example is esculetin, which serves as a biosynthetic precursor to cholesterol.

5. **Tetraterpenes (Carotenoids)**

Formed by eight isoprene units (40 carbon atoms), this group includes pigment-rich compounds like α-carotene, β-carotene, and δ-carotene, known for their antioxidant properties (Riaz, M., et al., 2021).

6. **Polyterpenes**

Polyterpenes consist of multiple isoprene units—more than eight—and are exemplified by natural rubber. Extracted from the latex of rubber trees, their long-chain structures resemble repeating isoprene-based frameworks (Long, Xiangyu, et al., 2021).

Table II-1. Classification of Terpenes Based on Isoprene Units

Terpene Type	Carbon Atoms	Isoprene Units
Monoterpenes	10	2
Sesquiterpenes	15	3
Diterpenes	20	4
Triterpenes	30	6
Tetraterpenes	40	8
Polyterpenes	>40	>8

1.5. Therapeutic and Practical Uses of Essential Oils

The use of aromatic plant oils dates back thousands of years, with their application traced to ancient civilizations such as the Chinese, Egyptians, as well as to Arab and Islamic traditions. Over time, the role of essential oils has expanded and diversified, becoming a cornerstone in modern cosmetic practices and holistic health treatments aimed at enhancing physical and mental well-being (Wilson, R., 2002).

In nature, essential oils fulfill critical ecological roles. Some attract pollinators, thereby increasing plant fertility and fruit yield, while others act defensively repelling insects or exerting toxic effects to deter herbivores and pests (Regnault-R., 1997). Beyond their ecological functions, these oils are integral to the plant's physiological processes, aiding in the expulsion of metabolic byproducts.

In human health, essential oils are used to support and stimulate bodily systems such as immunity and circulation. For example, lavender oil is known to promote hair growth, improve oxygen uptake, and enhance the synthesis of adenosine triphosphate (ATP), a vital molecule for cellular energy.

Table 7 summarizes the diverse benefits and applications of essential oils across both medicinal and general use contexts:

Table II-2. Common Uses and Benefits of Essential Oils

Medicinal Applications	Other Practical Uses
– Sedative and calming effects	– Improves taste and aroma of medications
– Lowers blood pressure (hypotensive)	– Acts as a flavoring agent in food
– Antiviral properties	– Widely used in perfumes and cosmetics
– Anti-inflammatory effects	– Utilized in the pharmaceutical and soap industry
– Nervous system regulation	– Serves as a repellent for parasites and worms
– Relieves muscle spasms	– Functions as an insect repellent (e.g., mosquitoes)

2. Techniques for Extracting Essential Oils

2.1. Distillation

Distillation is among the oldest and most traditional methods employed in the extraction of essential oils, with roots tracing back more than a century (Schmidt, E., 2020). The process is grounded in the principle of heating plant materials to vaporize their volatile compounds. Upon condensation, the resulting vapors yield a mixture of water and essential oil, which can then be separated based on their differing solubilities (S. Rahal, 2004; F. Abdellatif, 2005). Each distillation session produces a refined portion of high-purity essential oil. This technique encompasses three primary types:

1. **Hydrodistillation**

Hydrodistillation is widely utilized and involves placing plant material in a vessel containing water (Lawrence, B., 1995). The plant matter may either be immersed directly in the water or suspended in a mesh to prevent contact with the container walls. The apparatus—typically made of stainless steel, copper, or glass—is heated by either open flame or electric elements (Das, S., et al., 2013). This technique is especially suitable for extracting oils from dried, heat-tolerant plants, including roots, leaves, fruits, and some flowers with high oil content.

Table II-3. Pros and Cons of Hydrodistillation

Advantages	Disadvantages
- Easy to operate - Cost-effective - Simple equipment setup - No specialized location needed	- Incomplete extraction - Loss of heat-sensitive compounds like oxygenated constituents - Prolonged processing time

2. **Pressurized Microwave-Assisted Extraction**

This method uses microwave radiation in a high-pressure environment to boost extraction efficiency (Jain, T., et al., 2009). Pressure allows deeper microwave penetration into plant tissue, facilitating the release of essential oils.

3. **Atmospheric Pressure Microwave Extraction**

Here, microwaves are applied under standard atmospheric pressure to extract essential oils (Yang, Y., et al., 2014). The method still leverages microwave energy for efficient oil recovery, but operates without added pressure.

4. **Microwave-Assisted Water Distillation under Vacuum**

This approach integrates microwave radiation with water distillation in a vacuum environment (Li, Hong., et al., 2019). By lowering the boiling point of water through vacuum pressure, the process allows efficient oil extraction at reduced temperatures.

5. **Solvent-Assisted Microwave Extraction**

In this variation, a solvent is added to the plant material before microwave exposure to improve oil solubilization and extraction yield (Mandal, V., et al., 2007). The solvent facilitates the release of essential oils during microwave treatment.

Methods (1), (2), and (3) demonstrate improved performance over conventional extraction techniques. Meanwhile, technique (4) is even more efficient in terms of speed. Method (5) allows minimal solvent usage and offers faster extraction compared to traditional processes like Soxhlet extraction. However, techniques (2) through (5) are significantly more expensive. Importantly, all these advanced methods minimize extraction time and protect thermolabile compounds from degradation (Benkaci-A., et al., 2006; M.A. Ferhat, 2006).

2.2. Cold Pressing

Primarily applied to citrus fruits, cold pressing is used because these fruits are particularly sensitive to heat and oxidation. The method uses mechanical or manual pressure under water sprays to extract the oil, which is later separated via centrifugation (M.A. Ferhat, 2006).

2.3. Solvent Extraction

This method involves immersing delicate flowers such as jasmine or rose in an organic solvent at room temperature. The plant material is layered thinly to ensure thorough solvent penetration into oil-bearing cells (El Asbahani, A., et al., 2015). The solvent dissolves the essential oil, forming a mixture that is distilled at low pressure to separate the solvent. The residue, called "concrete," contains waxes and fats. Further treatment with absolute alcohol at low temperatures removes these, yielding "absolute essential oil" (M. Vinatoru, et al., 1997; M. Toma, et al., 2001). Although effective for heat-sensitive components, the technique is limited by high cost and safety/environmental concerns (G.T. Forrest, et al., 2000).

2.4. Supercritical/CO_2 Extraction

This advanced extraction technique employs gases—primarily carbon dioxide—in their supercritical or liquid states to extract essential oils and related compounds like pigments and fragrances (Chakravarty, I., et al., 2021). When CO_2 is brought to its supercritical state (31.4°C and 73 bar), it exhibits fluid-like density and strong solvating properties. Extraction efficiency depends on solute nature, temperature, and pressure (E. Guentherin, 2000; F. Abdellatif, 2005). Due to its low critical temperature, non-flammability, non-toxicity, and easy separation post-extraction, CO_2 is widely used in perfumery and considered a highly sustainable solvent.

2.5. Maceration

Maceration involves soaking plant materials in a solvent long enough to allow for the dissolution of essential oils (Rao, V., et al., 2007). Mechanical stirring helps ensure even solvent exposure. Slight heating may be applied to enhance oil melting, though care is taken to preserve oil integrity. The solvent-oil mixture is then distilled under low temperature and pressure, allowing for solvent recovery and oil isolation (F. Abdellatif, 2005).

CHAPTER THREE ANTIBACTERIAL ACTIVITY

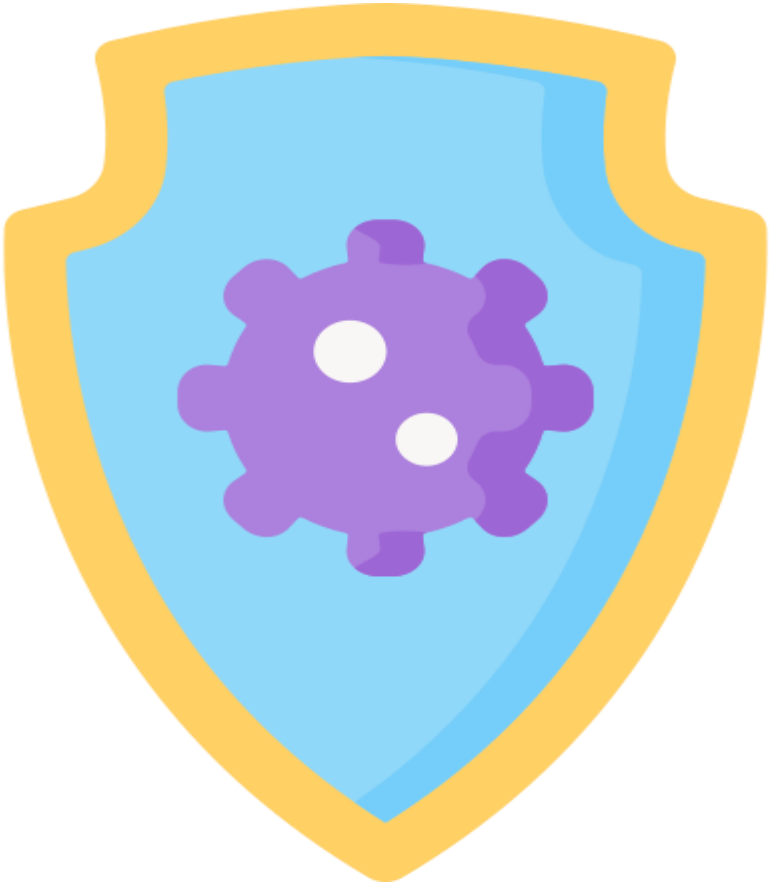

1. Study of antibacterial activity:

1.1. Definition of bacteria:

Bacteria are microscopic living organisms that have only one cell. The word for just one is “bacterium.” Millions (if not billions) of different types of bacteria can be found all over the world, including in your body. They’re on your skin and in your airways and mouth. They’re also in your digestive system, reproductive system, and urinary tract. Scientists estimate you have 10 times more bacterial cells than human cells in your body.

These bacteria make up your microbiome, which keeps your body healthy. Other bacteria can make you sick. Healthcare providers can treat many bacterial infections with antibiotics. (Cleveland Clinic, 2022)

1.2. Structure of a Bacterial Cell

Bacterial cells are enclosed within a rigid cell wall that supports and protects a more delicate inner plasma membrane. Inside, the cytoplasm appears mostly uniform and contains a high concentration of ribosomes, along with occasional storage inclusions. Unlike eukaryotic cells, bacteria do not possess membrane-bound organelles like mitochondria or endoplasmic reticulum. Core components of the bacterial cell include the cell wall, plasma membrane, cytoplasm, and a singular chromosome. Additional structures may also be present, including a capsule (outermost layer), flagella, pili (fimbriae), spores highly resistant dormant forms found in certain species and plasmids, which are small, circular, independently replicating DNA molecules (Prescott, 2003; Hart & Shears, 1997).

1.3. Bacterial Morphologies

While bacteria share certain structural similarities with plants, they are recognized as belonging to a distinct biological kingdom or two separate kingdoms when considering Archaea (also known as Archaebacteria) as a unique lineage within the prokaryotic domain. Morphologically, bacteria may form fine filamentous structures resembling a thallus, composed of uniformly small cells arranged in one, two, or even three-dimensional partitions. However, bacteria are most commonly found as single-celled organisms. In some cases, they may associate with similar cells to form chains or aggregate into visible, gelatinous masses referred to as zoogloeae. In terms of shape, spherical bacteria are classified as *micrococci*. When these round cells separate immediately after division, they are identified using terms such as

Bacterium or *Diplococcus*. If they remain attached in elongated rods, they are termed *bacilli* (Jorda,2004).

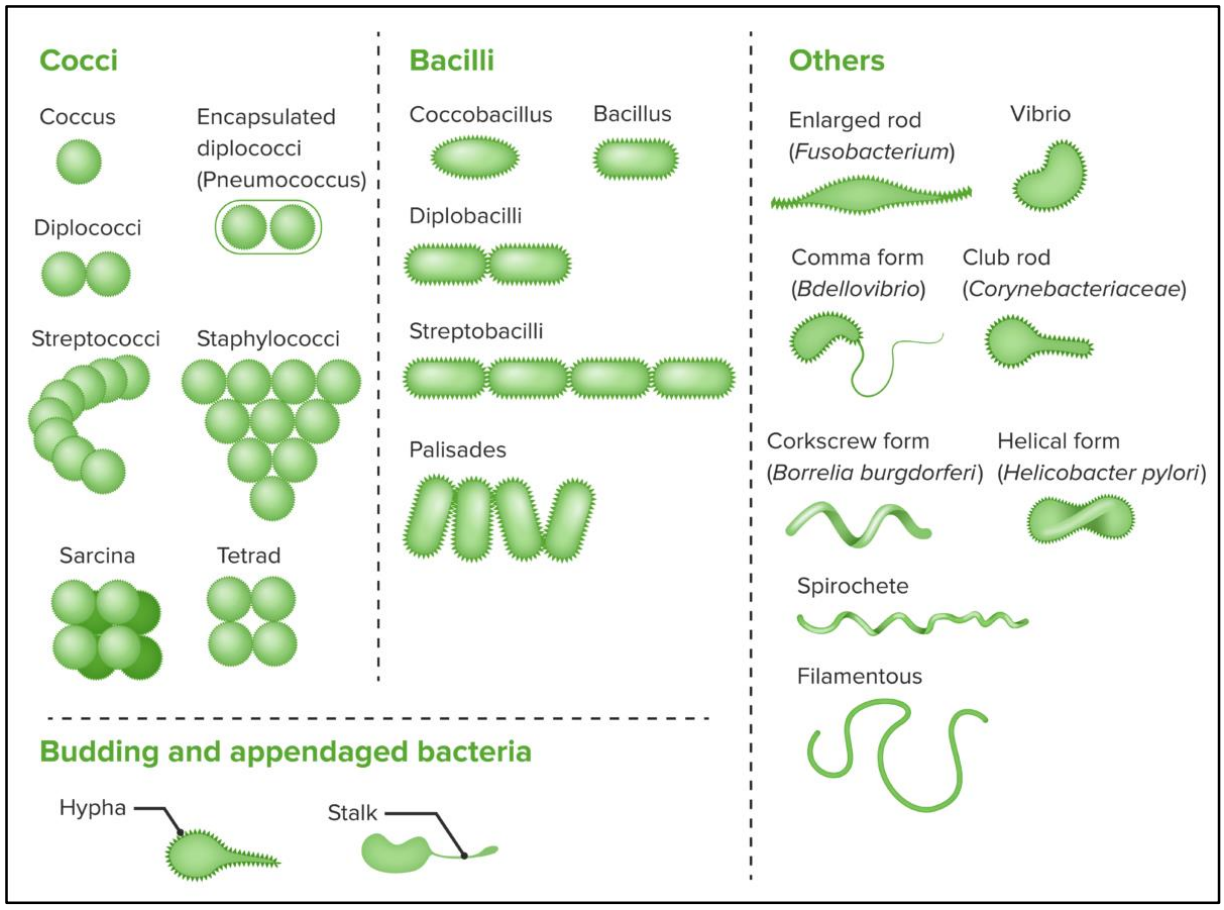

Figure III-1. Morphological Diversity and Cellular Arrangements of Bacteria (Villarreal, 2006)

1.4.Classification of Bacteria :

1.4.1. Classification Criteria

1.4.1.1. Scientific Nomenclature

As with all living organisms, bacteria are systematically classified according to a binomial system that includes both genus and species. The genus groups organisms that share one or more common characteristics, while the species further differentiates them. For example, *Clostridium botulinum* identifies the genus *Clostridium* and the species *botulinum*. Within a species, distinct variants known as *strains* can exist, which differ in their genetic makeup and biochemical properties. The specificity of some drugs and vaccines often makes them effective only against particular strains (Larry & Charles, 2018).

1.4.1.2. Gram Staining

An important and widely used classification method is based on the Gram stain technique, which distinguishes bacteria according to the chemical structure of their cell walls. This differential staining method causes certain bacteria to appear blue or violet—these are classified as Gram-positive—while others appear red or pink, and are classified as Gram-negative (Heart & Shears, 2006). The variation in staining arises from fundamental differences in cell wall composition, which also influence pathogenicity and determine the efficacy of specific antibiotics (Larry & Charles, 2018).

1.4.1.3. Cellular Shapes

Bacteria can also be grouped according to their basic shapes. The primary morphological types include spherical forms (*cocci*), rod-shaped forms (*bacilli*), and spiral or helical forms (*spirochetes*) (Larry & Charles, 2018).

1.4.1.4. Oxygen Requirements

Another classification criterion considers the bacterium's oxygen dependency. Bacteria may be categorized as *aerobic* if they require oxygen to grow, or *anaerobic* if they can thrive in oxygen-deprived environments. When environmental conditions—such as nutrient availability, temperature, pH, and oxygen levels—are favorable, bacteria can proliferate rapidly. Under such conditions, some bacteria may express their pathogenic potential and cause infections ranging from mild to severe (Flandrois, 2000).

1.5. Bacterial Types

In this study, three different bacterial strains will be investigated.

1.5.1. Gram-Negative Bacteria

1.5.1.1. *Escherichia coli :*

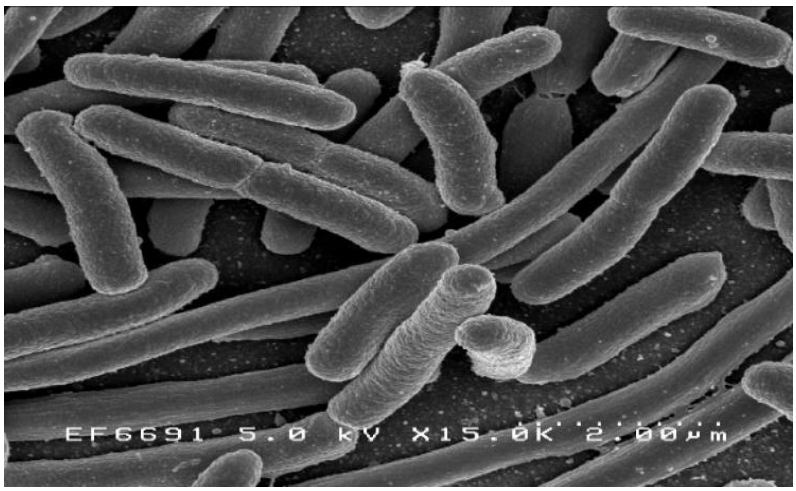

Figure III-2. Micrograph of *Escherichia coli*

Escherichia coli, commonly known as E. coli, is a bacterium found in the human and warm-blooded animal intestines. While most strains of *E. coli* are harmless, some, like Shiga toxin-producing E. coli, can cause severe foodborne illnesses. This bacterium produces toxins called Shiga-like toxins due to their similarity to those produced by Shigella dysenteriae. *E. coli* can multiply at temperatures between 7°C and 50°C, with an optimal temperature of 37°C. It can be transmitted to humans primarily through consuming contaminated foods like raw or undercooked ground meat, raw milk, raw vegetables, and contaminated sprouts. Cooking food thoroughly at a temperature of at least 70°C can destroy Shiga toxin-producing *E. coli* if present[(WHO, 2018)][(pasteur, s.d.)]

1.5.1.1.1. Symptoms and Transmission

Infections caused by Shiga toxin-producing E. coli can lead to symptoms such as abdominal cramps, diarrhea, and in severe cases, bloody diarrhea (hemorrhagic colitis). Fever and vomiting may also occur. The duration of illness from this strain of E. coli is typically around a week in adults but can be longer in children. Preventing infection involves taking measures at all stages of the food chain, including production on farms, to reduce the risk of contamination. The transmission of E. coli primarily occurs through consuming contaminated foods, with the main reservoir being the digestive tract of cattle. Contamination can also arise from fecal matter of ruminants in the environment[(WHO, 2018)][(pasteur, s.d.)].

1.5.1.1.2.Prevention and Treatment

Preventing infections from Shiga toxin-producing E. coli involves hand hygiene practices, thorough cooking of meat, avoiding raw milk and soft cheese made from raw milk, peeling and washing vegetables, and refraining from consuming uncooked flour-based products. Treatment for severe infections caused by this bacterium typically requires hospitalization to manage complications such as anemia and kidney failure. It is important to note that most antibiotics are contraindicated as they can worsen the condition by releasing more toxins into the body[(pasteur, s.d.)]. [(FDA, 2025)]

Escherichia coli, a versatile bacterium with both harmless and pathogenic strains, underscores the importance of food safety and hygiene practices to prevent infections and mitigate the risks associated with this bacterium.

1.5.1.2. *Klebsiella pneumonia*:

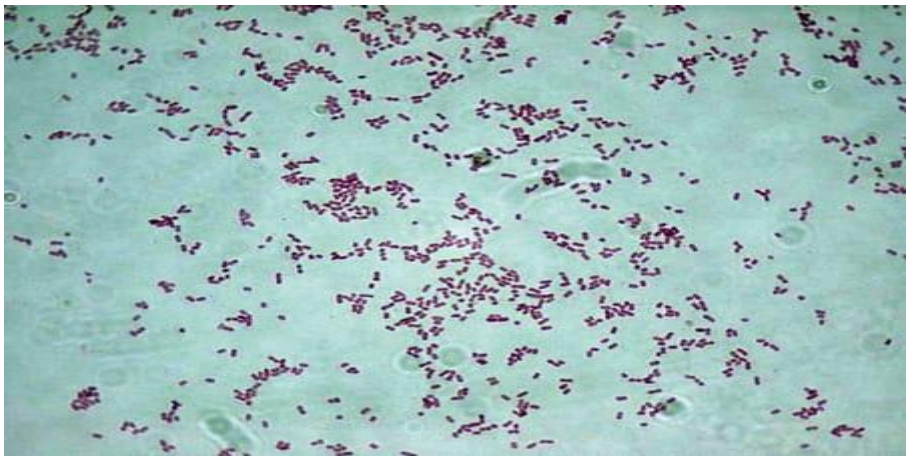

Figure III-3. Micrograph of *Klebsiella pneumonia.*

1.5.1.2.1. Definition of *Klebsiella* :

Klebsiella bacteria is a race of negative bacteria, belonging to the family of intestinal bacteria. These bacteria are characterized by its bacillus shape, its lack of movement, and the presence of a prominent capsule consisting of many sugars. It usually lives in the intestine naturally, but if it spreads to other parts of the body, it may cause a serious infection. *Klebsiella* bacteria are commonly spread in health care environments such as elderly care and intensive care units in hospitals. (PubMed Central, 2016)

- ✓ **Species :**

Klebsiella species are classified based on biochemical reactions and clinical significance:

❖ *Klebsiella pneumoniae*: Causes pneumonia, urinary tract infections, septicemia, and liver abscesses.

❖ *Klebsiella oxytoca*: Found in the nose, mouth, and intestines.

❖ *Klebsiella rhinoscleromatis*: Causes rhinoscleroma.

❖ *Klebsiella ozaenae*: Causes ozena.

Other species include K. planticola, K. terrigena, and K. ornithinolytica (Medscape, 2024) (Ashurst & Dawson, 2023)

1.5.1.2.2. Characteristics :

❖ *Klebsiella* species are encapsulated, which contributes to their virulence.

❖ They are commonly found in the human gastrointestinal tract but can cause serious infections if they spread to other parts of the body.

❖ *Klebsiella* infections are often associated with healthcare settings, such as nursing homes and intensive care units.

❖ *K. pneumoniae* is the most clinically significant species, causing pneumonia, urinary tract infections, septicemia, and liver abscesses.

In summary, *Klebsiella* is an important genus of bacteria that can cause severe infections, particularly in healthcare settings. Understanding its classification and characteristics is crucial for effective prevention and treatment of *Klebsiella* infections. ,(PubMed Central, 2016) (Ashurst & Dawson, 2023)

1.5.2. Gram-Positive Bacteria

1.5.2.1. *Staphylococcus* Bacteria :

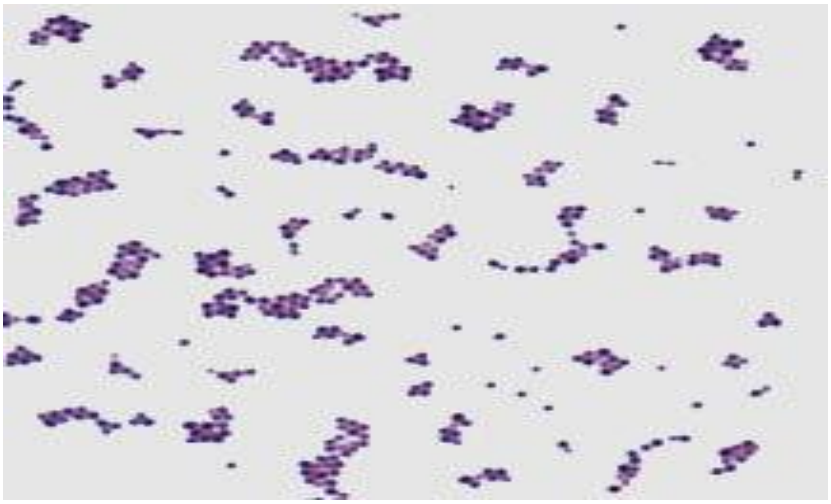

Figure III-4. Micrograph of *Staphylococcus aureus*

1.5.2.1.1. Definition :

Staphylococcus is a genus of Gram-positive bacteria in the family *Staphylococcaceae* from the order *Bacillales*. These bacteria appear spherical (cocci) under the microscope and form grape-like clusters. They are facultative anaerobic organisms, capable of growth both aerobically and anaerobically. The name "*Staphylococcus*" was coined in 1880 by Scottish surgeon and bacteriologist Alexander Ogston, combining the prefix "staphylo-" (from Ancient Greek: σταφυλή, meaning 'bunch of grapes') with the New Latin suffix "coccus" (from Ancient Greek: κόκκος, meaning 'spherical bacterium'). (CDC, 2013)

1.5.2.1.2. Species and Characteristics:

❖ *Staphylococcus* includes at least 44 species, with some having subspecies. Many of these species reside normally on the skin and mucous membranes of humans and animals, while some can cause infections.

❖ These bacteria have been found to be nectar-inhabiting microbes and are a small component of the soil microbiome.

❖ *Staphylococcus* species have been implicated in human infections, with strains like S. lugdunensis, S. schleiferi, and S. caprae being notable.

❖ Antibiotic resistance is a significant concern with *Staphylococcus*, and many strains have become resistant to antibiotics, posing challenges in treatment. (Ghebremedhin et al., 2008)

1.5.2.1.3. Taxonomy and Genomics:

❖ The taxonomy of *Staphylococcus* is based on 16S rRNA sequences, and most species fall into distinct clusters.

❖ Genomic data, including sequences of various genes like gap, 16S rRNA, hsp60, rpoB, sodA, and tuff, have been used to classify and distinguish *Staphylococcus* species. (NCBI, n.d.)

❖ Whole genome technologies have provided valuable insights into the diversity of *Staphylococcus* strains, aiding in understanding their pathogenic behavior and evolution.

In conclusion, Staphylococcus bacteria are diverse, with some species causing infections and exhibiting antibiotic resistance. Understanding their taxonomy, characteristics, and genomic features is crucial for effective management and control of infections caused by these bacteria. (ScienceDirect, n.d.)

1.6. Mechanisms of Antibacterial Resistance

1.6.1. Enzymatic Inactivation

One of the primary mechanisms by which bacteria resist antibiotics is through enzymatic degradation or modification of the drug:

- **Beta-lactamase production**: This is a key resistance strategy wherein beta-lactamase enzymes hydrolyze the amide bond of the beta-lactam ring, effectively neutralizing beta-lactam antibiotics. The *bla* genes responsible for encoding these enzymes may be located on chromosomes, plasmids, or mobile genetic elements like transposons (Alioua & Bouamoucha, n.d.).

- **Penicillinase synthesis**: Some bacterial species exhibit intrinsic resistance via chromosomal penicillinase enzymes. Additionally, resistance can be acquired through plasmid-mediated penicillinase expression.

- **Chromosomal beta-lactamases (Cephalosporinases)**: Naturally produced by certain bacteria—such as *Enterobacter cloacae*, *Pseudomonas aeruginosa*, and *Acinetobacter* species—these enzymes target and degrade cephalosporins.

- **Aminoglycoside-inactivating enzymes**: Bacteria can produce three main types of modifying enzymes—acetyltransferases, nucleotidyltransferases, and phosphotransferases—that deactivate aminoglycosides. The genes for these enzymes are frequently plasmid-borne.

- **Chloramphenicol inactivation**: Resistance to chloramphenicol often involves a plasmid-encoded chloramphenicol acetyltransferase, which prevents the drug from binding its ribosomal target by enzymatically modifying the antibiotic (via acetylation).

1.6.2. Alteration of Antibiotic Targets

Bacteria may also evade antibiotics by modifying the molecular targets to which these drugs normally bind:

- **Penicillin-Binding Protein (PBP) modification**: Mutations in chromosomal genes or the acquisition of genes encoding altered PBPs can reduce the binding affinity of beta-lactam antibiotics, thereby diminishing their effectiveness (Alioua & Bouamoucha, n.d.).

- **Ribosomal site alteration**: Intracellular modification of ribosomal subunits can reduce the efficacy of antibiotics such as macrolides, aminoglycosides, and chloramphenicol. Once binding is impeded, these drugs can no longer inhibit protein synthesis or halt bacterial growth.

- **Peptidoglycan precursor modification**: In enterococci, resistance to glycopeptide antibiotics emerges when the terminal D-alanine in the peptidoglycan precursor is replaced with a lactate group, disrupting the antibiotic's target site.

- **DNA gyrase and topoisomerase IV mutations**: Quinolone antibiotics target DNA gyrase, an enzyme essential for bacterial DNA replication. Resistance can occur through point mutations that alter specific amino acids in DNA gyrase or topoisomerase IV, impairing drug binding.

- **Alterations in target enzymes**: Resistance to sulfonamides arises when mutations occur in dihydropteroate synthase or dihydrofolate reductase, the enzymes targeted by these drugs. The altered enzymes display reduced affinity for the antibiotics.

1.6.3. Reduced Membrane Permeability

Another resistance mechanism involves limiting antibiotic entry into the bacterial cell. Modifications in the permeability of bacterial membranes—particularly changes in porin channels in Gram-negative bacteria—can restrict or prevent the drug from accessing its intracellular target (Alioua & Bouamoucha, n.d.).

1.6.4. Efflux Pumps

Efflux pumps represent a vital mechanism of resistance by actively expelling antibiotics from the bacterial cell. These transport proteins utilize energy to remove a wide range of antibacterial agents, thereby reducing their intracellular concentration and effectiveness. The presence of multiple efflux systems contributes significantly to the innate resistance observed in many bacterial specie.

SECOND PART
EXPERIMENTAL

CHAPTER ONE MATERIALS AND METHODS

1. Introduction:

This study was conducted collaboratively between two specialized laboratories: the Valorisation and Technology of the Saharian Resources Laboratory (VTRS) at the Faculty of Exact Sciences, Department of Chemistry, University of El Oued, and the Centre de Recherche Scientifique et Technique en Analyses Physico-Chimique (CRAPC) in Ouargla, Algeria. The VTRS lab facilitated essential oil extraction, conducted *in vitro* and *in-silico*. Meanwhile, CRAPC handled the precise GC/MS analysis of the extracted oils. This collaborative effort ensured thorough and accurate experimentation, combining expertise and resources from both institutions.

2. Plant Material:

2.1. *Cotula cinerea*

The *Cotula cinerea* plant was harvested at various time intervals ranging from December 2023 to January 2024 in a desert forest area in southeastern Algeria, specifically in Hassi Khalifa region in El Oued province. This region is characterized by the following specifications:

- Geographic Coordinates: Longitude 48°10' East, Latitude 23°09' North.
- Elevation above Sea Level: 44 meters.
- Distance from Sea Level: 290 kilometres.
- Bioclimatic Characterization: Desert.

2.2. *Origanum Majorana L:*

The *Origanum Majorana L* plant was harvested at different time intervals extending from March 2023 to April 2023 in a desert forest area in southeastern Algeria, specifically in Akfadou region in El Oued province. This region is characterized by the following specifications:

- Geographic Coordinates: Longitude 67°6' East, Latitude 33° North.
- Elevation above Sea Level: 58 meters.
- Distance from Sea Level: 300 kilometres.
- Bioclimatic Characterization: Desert.

3. Chemicals and reagents:

Microorganisms Used:

All microorganisms used in these studies were provided by the pedagogical laboratory of the faculty of biology.

- *Escherichia coli (ATCC 25922):* Belongs to the Enterobacteriaceae family. It is non-spore forming, facultative anaerobic, and typically motile due to flagella. Its length ranges from 2 to 6 µm and its width from 1.1 to 1.5 µm.
- *Klebsiella pneumoniae (ATCC 13883)*: A Gram-negative, rod-shaped bacterium with a length typically ranging from 1.0 to 2.0 µm and a width from 0.5 to 0.8 µm. It is encapsulated, non-motile, and commonly associated with nosocomial infections.
- *Staphylococcus aureus (ATCC 25923)*: Is a Gram-positive spherical bacterium with a diameter ranging from 0.5 to 1.5 µm, belonging to the genus Staphylococcus.

4. Materials and Methods:

4.1. Essential Oils Extraction:

4.1.1. Apparatus:

The essential oil extraction process required the use of specialized equipment to ensure accuracy and efficiency. In this study, the following apparatus was utilized:

- ✓ Adventurer – Pro AV53 sensitive balance
- ✓ Heating flask
- ✓ Refrigerant
- ✓ Clevenger apparatus
- ✓ Separating funnel
- ✓ Rotary evaporator

The Clevenger apparatus, a key component in the extraction process, is depicted in Figure1

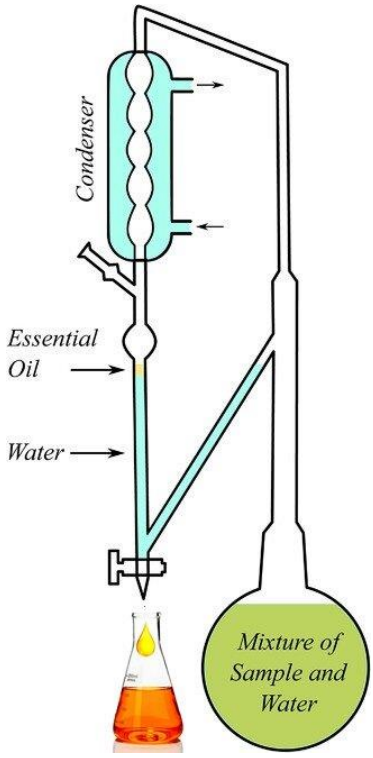

Figure I-1. Schematic representation of the Clevenger apparatus used in the essential oil extraction process (Biswa et al., 2023)

4.1.2. Procedure:

The procedure for essential oil extraction involved a series of meticulous steps to ensure optimal results. The extraction process was conducted as follows:

- ✓ Cleaning of the plant sample to remove any impurities.
- ✓ Weighing the plant sample to a quantity of 100 g using a sensitive balance.
- ✓ Washing the plant sample with water to prevent burning, followed by placement in a heating flask.
- ✓ Addition of small pieces of boiling regulator to the flask.
- ✓ Direct heating of the mixture at a temperature of 100 degrees Celsius for three and a half hours.
- ✓ Conducting the steam distillation process and subsequent separation of oil and water phases using liquid-liquid separation with diethyl ether.
- ✓ Drying of the organic oily phase with anhydrous sodium sulphate.
- ✓ Filtration of the dried oil phase through filter paper to remove diethyl ether particles.
- ✓ Evaporation of the filtered oil phase using a rotary evaporator to remove any remaining organic solvent.

✓ Storage of the obtained essential oil in small brown bottles and refrigeration at a temperature of 5°C.

4.2. Yield of Essential Oil Extraction:

Two distinct methodologies are commonly employed to ascertain the yield of essential oil extraction, each offering unique perspectives on the efficiency of the process.

4.2.1. Volumetric Yield - Mass-based: (Naima et al., 2019)

This method entails an assessment of the mass of the utilized plant material intended for essential oil extraction, juxtaposed against the volume of the resultant oil. The yield is then computed utilizing the following Equation 1:

$$R_{EO} = \frac{V_{EO}(ml)}{m_0(g)} \times 100 \quad (1)$$

Where: R_{EO}: Essential oil yield, m_0: Mass of the utilized plant sample, V_{EO}: Volume of the extracted essential oil

4.2.2. Mass-based Yield - Mass-based: (Larbi et al., 2018)

Alternatively, the essential oil extraction yield is defined as the quotient of the mass of the extracted essential oil and the mass of the plant material utilized. This yield is calculated using Equation 2:

$$R_{EO} = \frac{m_{EO}(g)}{m_0(g)} \times 100 \quad (2)$$

Where: R_{EO}: Essential oil yield, m_0: Mass of the utilized plant sample, m_{EO}: Mass of the extracted essential oil

These methodologies have been systematically applied to derive essential oil yields for all examined plant specimens.

4.3. Characterization of Essential Oils:

The characterization of essential oils comprises two fundamental components: physicochemical properties and Gas Chromatography-Mass Spectrometry (GC/MS) analysis.

4.3.1. Physicochemical Properties:

Here, we delve into the fundamental traits of essential oils, including their relative density, acidity, ester content, and refractive index. These properties offer valuable insights into

the composition and behavior of essential oils, helping us understand their chemical makeup and how they interact with their environment (Atti-Santos et al., 2005).

Relative Density (AFNOR NF T75-111 Standard):

At 20°C, 1 mL of the essential oil is measured using a pipette, and its mass is then determined. The procedure is repeated for distilled water, and density is calculated using the following Equation 3 (Valarezo et al., 2015):

$$d = \frac{m_{EO}}{m_{H_2O}} \quad (3)$$

Where: m_{EO}: Mass of the extracted essential oil, m_{H_2O}: Mass of the distilled water

Acidity Index (AFNOR NF T75-111 Standard):

To determine the acid value, representing the concentration of free acids in 1 g of the essential oil, a titration method with potassium hydroxide (KOH) solution is employed (Sahoo et al., 2007).

Initially, a small aliquot (0.5 mL) of the essential oil is mixed with 2 to 3 drops of phenolphthalein indicator in a small vessel. Subsequently, titration is performed with 0.5 N KOH solution until the appearance of a faint pink colour, indicating complete neutralization of the acids. The acid value is then calculated using the following Equation 4.

$$I_a = \frac{56.11 \times V \times C}{m} \quad (4)$$

Where: V: the volume of the KOH solution, C: Concentration of KOH, m: the mass of the essential oil

Ester Index (AFNOR NF T75-111 Standard):

The determination of free acids resulting from ester hydrolysis within the essential oil involves a titration process utilizing 0.5 N potassium hydroxide (KOH) solution (Alajtal et al., 2018).

- Begin by placing 0.5 mL of the essential oil into a small vessel.
- Add 1 mL of 0.5 N potassium hydroxide (KOH) solution to the vessel to initiate the titration process.

- Place the mixture in a gas-evacuated water bath for a specified duration to facilitate reaction.
- After cooling, introduce 0.5 mL of distilled water and add 3 drops of phenolphthalein indicator to the mixture.
- Titrate the excess potassium hydroxide (KOH) using 0.5 N hydrochloric acid (HCl) until a colour change is observed, indicating neutralization.
- Quantify the volume of hydrochloric acid (HCl) required to neutralize the excess potassium hydroxide (KOH).
- Calculate the ester content using the following Equation 5:

$$I_e = \frac{2805}{m}\left(V_0 - V_1\right) - I_a \quad (5)$$

Where: V_0 (ml): Volume of hydrochloric acid (HCl) without essential oil, V_1 (ml): Volume of hydrochloric acid (HCl) in the presence of essential oil, I_a: Acid value, I_e: Ester value and m: Mass of the essential oil sample.

Refractive Index (AFNOR NF T75-111 Standard):

The refractive index of an essential oil is defined as the ratio between the sine of the angle of incidence and the sine of the angle of refraction of a light ray, with a specific wavelength, transitioning from air into the essential oil, while the latter is maintained at a constant temperature (Singh, 2002)

The refractive index of the essential oil is directly measured using a refractometer at a reference temperature 20°C.

4.3.2. Gas Chromatography-Mass Spectrometry (GC/MS) analysis:

The coupling (GC/MS) technique stands as the most frequently employed method within the field of essential oils, facilitating the concurrent separation, identification, and quantitative measurement of the various constituents present in extracted oils.

Principle:

The principle is founded on the varying affinities of compounds within the mixture towards two phases: a stationary phase and a mobile phase. This technique relies on the distribution of constituents between a stationary phase and a gas phase. The stationary phase comprises a silicone-based liquid that permeates an inert and granular solid material, housed within a typically coiled steel or glass column measuring 1 to 3 meters in length and 2 to 4

millimetres in diameter. The mobile phase consists of an inert carrier gas such as nitrogen, helium, or argon.

The column is maintained at a high temperature via a furnace. Under the influence of temperature, constituents vaporize and become separable. The basis of separation lies in the discrepancy of partition coefficients of volatile compounds between the stationery and gas phases. A detection system generates a signal at the exit of each molecule from the column, manifesting as the recording of peaks corresponding to each constituent.

Gas chromatography is coupled with a mass spectrometer (MS); this coupling relies on computerized comparison of the spectrum of an unknown peak with one or more reference libraries, enabling its identification.

Apparatus:

The identification of the chemical constituents of our essential oils was performed using a gas chromatographic system (HP 5890-SERIE II) equipped with an HP5 MS capillary column (30 meters in length, 0.25 mm internal diameter, and 0.25 µm film thickness) coupled with a mass spectrometer (HP-MSD 5972).

N_2 was employed as the carrier gas for the analysis of the two essential oils. Spectra were recorded at an emission energy of 70 eV, and spectral analysis of the compounds was conducted by comparison with their counterparts using the WILEY275 (Chiu et al., 1982; Guinaudeau et al., 1975; Kiryakov, 1968; Shamma, 1972) spectral libraries.

Procedure:

The carrier gas (N_2) is introduced at a flow rate of 1 mL/min, with the injected volume of the essential oil being 1 µL in split injection. The injector and detector temperatures are set at 250°C and 320°C, respectively. The oven temperature is programmed to initially reach 60°C and held for 8 minutes, then gradually increased to 250°C at a rate of 2°C/min, maintained isothermally at 250°C for 15 minutes, and finally elevated to 300°C at a rate of 10°C/min.

4.4. *In Vitro* Assessment of the Antibacterial Activity:

Procedure:

Antimicrobial tests were conducted to evaluate the biological activity of the studied essential oils against *Escherichia coli, Klebsiella pneumoniae* and *Staphylococcus aureus*. The

antimicrobial activity was assessed using the disc diffusion method as described in the literature (Klančnik et al., 2010):

- *Preparation of test products:* Dissolve EOs in DMSO to prepare solutions of different concentrations ranging from 1 to 10 mg/ml.
- *Preparation of precultures:* Cultivate the microbial strains to be tested on Petri dishes containing nutrient agar and incubate for 24 hours at 37°C to obtain a young culture of bacteria and isolated colonies.
- *Preparation of discs:* Prepare discs using 6mm diameter Whatman filter paper, followed by sterilization for 30 minutes at 120°C in the autoclave.
- *Preparation of bacterial suspensions:* Take a few well-isolated and identical colonies using a Pasteur pipette and suspend them in 10 ml of sterile physiological saline solution (0.9% NaCl). Standardize the bacterial suspension using a densitometer for seeding into the MH milieu.
- *Preparation of culture milieu:* Utilize various culture milieu including nutrient broth for isolation and maintenance of bacterial strains, nutrient agar for reactivation of the bacterial strain, and Mueller-Hinton agar for studying bacterial sensitivity to different concentrations of EO.
- *Testing antibacterial activity:* Spread the bacterial suspension over the entire surface of Mueller Hinton agar (MHA) three times using a sterile swab, then leave on the bench for 30 minutes. Assess antibacterial activity by measuring the diameter of the inhibition zone using a ruler and comparing it with that of DMSO as a negative control and antibiotics as positive controls (Amoxicillin 25 µg/disc). Measure absorbance using UV-vis spectroscopy.

The inhibitory activity of bacteria was calculated as a percentage of inhibition using the following Equation 6 (Klančnik et al., 2010):

$$\%Inhibition = \left(1 - \frac{Abs_{Essential\ oil}}{Abs_{Controle}}\right) \times 100 \quad (6)$$

4.5. *In-Silico* analysis:

4.5.1. Software

Computational simulations, including Induced Fit Docking, molecular dynamics studies, and MM-GBSA calculations, were conducted employing the Glide module, Induced Fit Docking module, Prime module, and the Desmond module within the Maestro version 11.7 user interface of the Schrödinger suite (Small-Molecule Drug Discovery Suite 2021-4,

Schrödinger, LLC, New York, NY, 2021) (Schrödinger, 2015). The simulations were executed on a DELL Intel(R) Core (TM) i9-13900HX CPU @ 2.20 GHz processor, equipped with 32.0 GB RAM, and operated on a 64-bit Linux Ubuntu 18,04.1 LTS operating system.

4.5.2. ADMET and drug-likeness evaluation:

Drug candidates should possess favourable ADMET properties and ideally non-toxic. Therefore, the major identified compounds from the essential oils extract were evaluated of their ADME profile, including physicochemical, lipophilicity, water solubility, pharmacokinetics, drug-like nature, medicinal chemistry, and several other parameters using SwissADME (Daina et al., 2017; Riyadi et al., 2021) module provided in SIB (Swiss Institute of Bioinformatics) webserver (https://www.sib.swiss). Furthermore, the toxicity aspect of designed compound was also predicted using ProTox (Banerjee et al., 2018) webserver (https://comptox.charite.de/protox3/).

4.5.3. Docking setup:

Ligands preparation:

The three-dimensional configurations of the major compounds isolated from *Cotula cinerea* and *Origanum Majorana L e*ssential oils were obtained from the National Library of Medicine (NCBI) database (Kim et al., 2016), accessible through the NCBI website (https://pubchem.ncbi.nlm.nih.gov/).

Ligand preparation involved an energy optimization process to derive the most energetically favourable conformations for each compound. Utilizing LigPrep module within the Schrödinger suite (Schrödinger, 2024), this optimization procedure ensured the attainment of the lowest energy state for the studied drugs, including Montbretin A (a co-crystallized ligand). The ionization states were established at a pH of 7.0 ± 2.00, as computed by the Epik classic module, while maintaining specified chirality and generating relevant tautomeric forms. Furthermore, partial atomic charges were computed using Optimized Potentials for Liquid Simulations OPLS4 force field (Lu et al., 2021).

Receptor Preparation:

The 3D structures of specifically selected receptors have been scrutinized, including the *Escherichia coli* (PDB ID: 6F86) (Narramore et al., 2019), *Klebsiella pneumoniae* (PDB ID: 4EY2) (King et al., 2012), and *Staphylococcus aureus* (PDB ID: 6LKI) (M. Wang et al., 2020). Details pertaining to these receptors, encompassing their designations and corresponding PDB IDs, are delineated within Table 1.

Processing of the proteins and DNA structures was executed through the “protein preparation Workflow” module within the Schrödinger suite (Madhavi Sastry et al., 2013), involving consecutive stages of import and processing, review and modification, and refinement.

In the initial stage, the Prime tool was employed to address missing residues and side chains, maintaining the pH of PROPKA at 7.0 ± 2.00. Subsequent steps included the optimization and assignment of hydrogen bonds, along with the removal of water molecules beyond 8 Å. Restrain minimization utilizing the Optimized Potentials for Liquid Simulations (OPLS4) force field was performed to achieve a low-energy state for the protein (Lu et al., 2021). This phase of protein preparation signifies an energy optimization methodology, presenting the protein in its energetically favourable state for subsequent *in-silico* studies.

The "Receptor grid generation" panel facilitated the creation of a grid encompassing the active site of the protein, delimited by the co-crystallized ligand Montbretin A. Default parameters were maintained, and the grid centre was generated at the coordinates X = -6.65; Y = 6.99; Z = -20.65.

Table I-1. Target receptors information chosen for docking studies

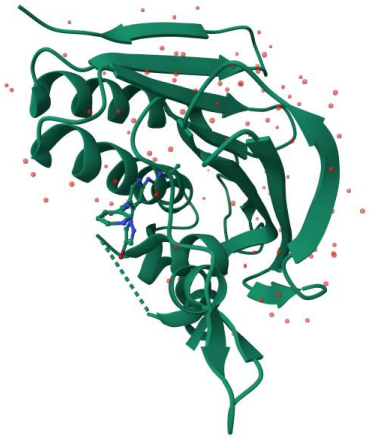	***Crystal Structure of E. coli GyraseB 24kDa***	
	PDB ID	6F86
	Mutation	No
	Resolution (Å)	1.90
	R-Value Observed	0.204
	Organism	*Escherichia coli*
	Space Groupe	P 3_2 2 1
	Sequence Length	206
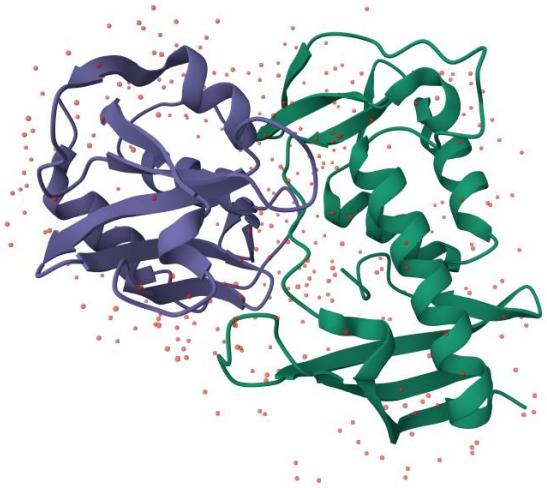	***Crystal structure of NDM-1 bound to hydrolyzed methicillin***	
	PDB ID	4EY2
	Mutation	No
	Resolution (Å)	1.17
	R-Value Observed	0.131
	Organism	*Klebsiella pneumoniae*
	Space Groupe	P 2_1 2_1 2_1
	Sequence Length	270
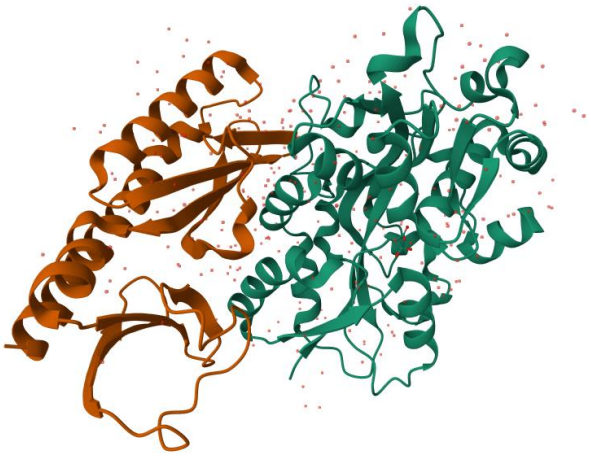	***Two-component system protein mediate signal transduction***	
	PDB ID	6LKI
	Mutation	No
	Resolution (Å)	1.78
	R-Value Observed	0.210
	Organism	*Staphylococcus aureus*
	Space Groupe	C 2 2 2_1
	Sequence Length	471

Molecular Docking:

Computational simulations, including Induced Fit Docking, molecular dynamics studies, and MM-GBSA calculations, were conducted employing the Glide module, Induced Fit Docking module, Prime module, and the Desmond module with in the Maestro version 11.7 user interface of the Schrödinger suite (Small-Molecule Drug Discovery Suite 2021-4, Schrödinger, LLC, New York, NY, 2021) (Schrödinger, 2015). The simulations were executed

on a DELL Intel(R) Core(TM) i9-13900HX CPU @ 2.20 GHz processor, equipped with 32.0 GB RAM, and operated on a 64-bit Linux Ubuntu 18,04.1 LTS operating system.

The molecular docking tool employed for all docking studies was Glide (Grid-based Ligand docking with Energetics), a module within the Schrödinger suite (Yang et al., 2021). The prepared ligands underwent docking onto the specified protein site utilizing the Glide module, in Standard Precision (SP) modes (Friesner et al., 2006).

Induced Fit Docking (IFD):

The Induced Fit docking (IFD) module of the Maestro molecular modelling suite has been noted as a reliable and effective docking approach to consider flexibility in both ligands and the binding pocket residues in the binding pocket of target receptors (Khelil et al., 2020). During the IFD process, Glide/SP (Standard Precision) was performed for each ligand, the Prime refinement step specifically addressed the side chains of residues within a 5 Å radius of the ligand. Noteworthy is the retention of a maximum of 20 poses for each ligand.

Molecular Dynamics Simulation (MDS):

The best compound in each plant exhibiting the highest IFD docking score was chosen for Molecular Dynamics Simulation (MDS). Recognizing the limitations of ligand docking in representing the biological system under aqueous conditions (Korb et al., 2012), a 100 ns simulation time for MDS was executed using the Desmond module within the Schrödinger suite (Bowers et al., 2006).

The MDS protocol comprised three essential steps: system builder, minimization, and MDS. In the system builder phase, the protein and ligand complex were selected and immersed in a biological environment. The transferable intermolecular potential with 3 points (TIP3P) solvent model, with the boundary condition maintained in an orthorhombic box form throughout the process with dimensions of 10 x 10 x 10 Å (Akbar et al., 2022). The OPLS-3e force field was consistently applied (Roos et al., 2019). The neutralization of model was conducted by addition of counter ions when needed and 0.15 M of NaCl salt was included to mimic the physiological state.

Subsequently, the NPT ensemble was utilized for energy minimization, maintaining pressure and temperature at 1.0132 bar and 300 K, respectively. Finally, MDS was conducted for the minimized protein-ligand complex (Halder et al., 2023).

Free Energy (MM-GBSA) Calculation:

Upon completion of the dynamic simulation, an assessment of the free binding energy between the protein and the ligand was systematically undertaken utilizing the Prime MM-GBSA module within the Maestro molecular modelling suite (E. Wang et al., 2021). The calculation of ligand binding affinities was accomplished through the Molecular Mechanics/Generalized Born Surface Area ΔG (MM-GBSA ΔG) metric applied to the optimized Receptor-Ligand Complex. This computation, facilitated by the VSGB solvation model and the OPLS4 force field, stands as a methodologically rigorous approach for the comprehensive evaluation of molecular interactions and binding strengths (Gorla et al., 2021).

CHAPTER TWO RESULTS AND DISCUSSION

1. Introduction:

This chapter delves into the findings regarding the extraction yield, characterization, and comprehensive exploration of the antibacterial properties inherent in two essential oils derived from the aerial constituents of *Cotula cinerea* and *Origanum Majorana L*. The overarching aim of this investigation was to assess the potential antibacterial efficacy exhibited by essential oils as significant agents in the domain of novel pharmaceutical development.

The elucidations provided herein furnish intricate insights into the chemical constitution of the essential oils, thereby enabling their utilization in the *in-silico* study. This involved the application of advanced computational techniques such as Induced Fit Docking (IFD) and Molecular Dynamics Simulation (MDS) for each compound, capabilities not feasible in traditional *in vitro* studies.

2. Extraction Yield:

Figure 2 illustrates the yields of essential oils obtained through hydrodistillation of the aerial parts of *Cotula cinerea* and *Origanum Majorana L*. variety of El Oued.

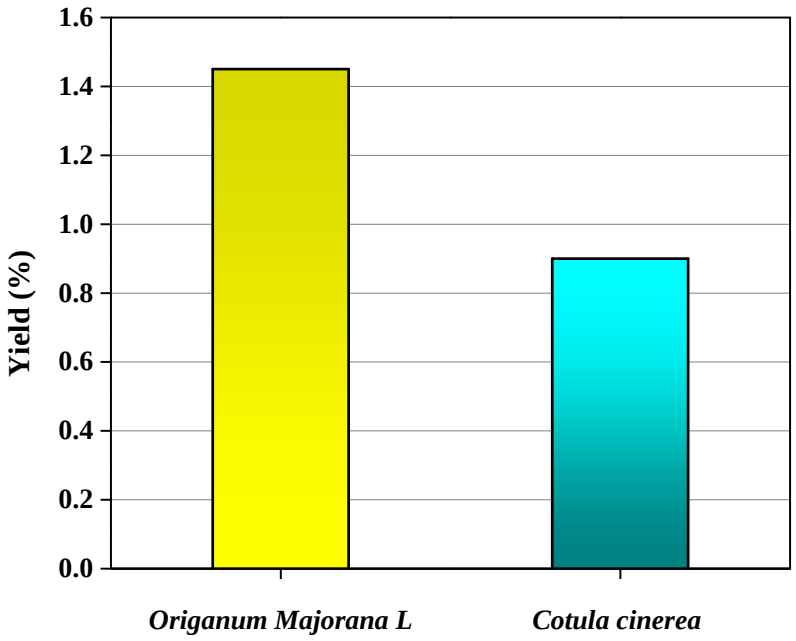

Figure II-1. The yields of extracted essential oils

We observe that *Origanum Majorana L* exhibits a higher essential oil yield than *Cotula cinerea* (1.45% and 0.90% respectively). However, the difference between the two yields is non-significant.

Nevertheless, findings reported by (Alimi et al., 2022) indicate lower yields of essential oils extracted by hydrodistillation from *Origanum Majorana L* and *Cotula cinerea* at ambient temperature.

Similar results to ours were, however, obtained by (Naima et al., 2019) for the essential oil extracted from the same variety using the same method.

Furthermore, significantly higher yields were achieved by (Vera & Chane-Ming, 1999) during the hydrodistillation of *Origanum Majorana L*, Indian variety.

These variations in results can be explained by the fact that essential oil yields are influenced by several factors during extraction: either factors related to the plant (species, variety, chemical composition, etc.) or factors associated with experimental conditions (extraction process, extraction duration, etc).

3. Chemical composition of essential oils:

3.1. Organoleptic characteristics:

Through the conducted work, it has been revealed that the essential oil extracted from the studied plants exhibits the following (Table 2) organoleptic properties:

Table II-1. The organoleptic characteristics of essential oils

Plant	Smell	Aspect	Colour
Cotula cinerea	A distinctive aroma	liquid at room temperature	Dark-yellow
Origanum Majorana L	A pleasant fragrance	liquid at room temperature	Light-yellow

3.2. Physicochemical Properties:

The physicochemical properties were meticulously determined according to the standards of the French Association for Standardization (AFNOR) using established methodologies to measure relative density, refractive index, acidity index, and ester index, as depicted in the following Table 3.

Table II-2. The physicochemical properties of essential oils

Plant	Relative Density	Refractive Index	Acidity Index	Ester Index
Cotula cinerea	0.958	1.4720	5.01	43.72
Origanum Majorana L	0.908	1.4512	4.39	41.23

By comparing these results to those obtained by (Naima et al., 2019) (density 0.953, refractive index 1.474, acidity index 4.93 and ester index 45.96) and (Alimi et al., 2022) (density: 0.834 ± 0.02, 0.835 ± 0.02, refractive index, at 25°C 1.4596 ± 0.03, 1.4622 ± 0.04), and considering that the refractive index was measured at a temperature of 23°C, we can conclude that these values are in accordance with the standards described by AFNOR (Afnor, 1982).

3.3. Gas Chromatography-Mass Spectrometry (GC/MS) analysis:

The analysis focused on the essential oil constituents extracted from two specific plant species using gas chromatography-mass spectrometry (GC/MS). Mass spectra corresponding to each chromatographic peak were juxtaposed with spectra from relevant scientific literature and the Weily electronic database for mass spectra (Horai et al., 2010). Retention indices were employed to ascertain compound identities. Moreover, utilizing the identical non-polar HP5 stationary phase in the gas chromatography column facilitated the preservation of consistent peak numbers and elution sequences for the compounds under investigation.

Figure 3 and Figure 4 depict the chromatograms illustrating the essential oil compositions of *Cotula cinerea* and *Origanum Majorana L*, respectively, as obtained through gas chromatography-mass spectrometry (GC/MS) analysis:

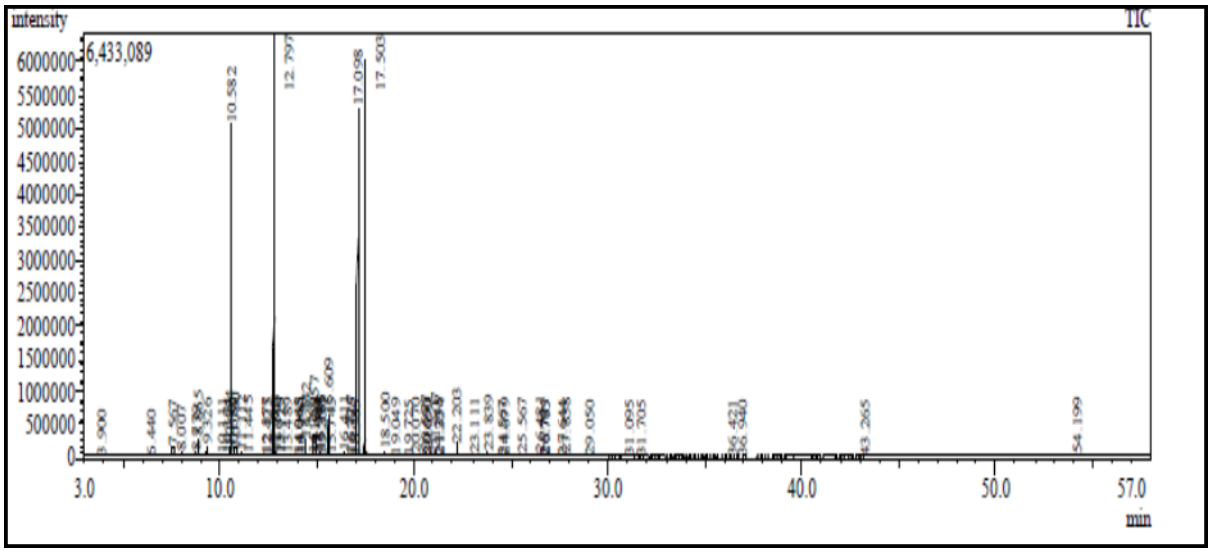

Figure II-2. Chromatogram of the essential oil of *Cotula cinerea* plant obtained by GC/MS

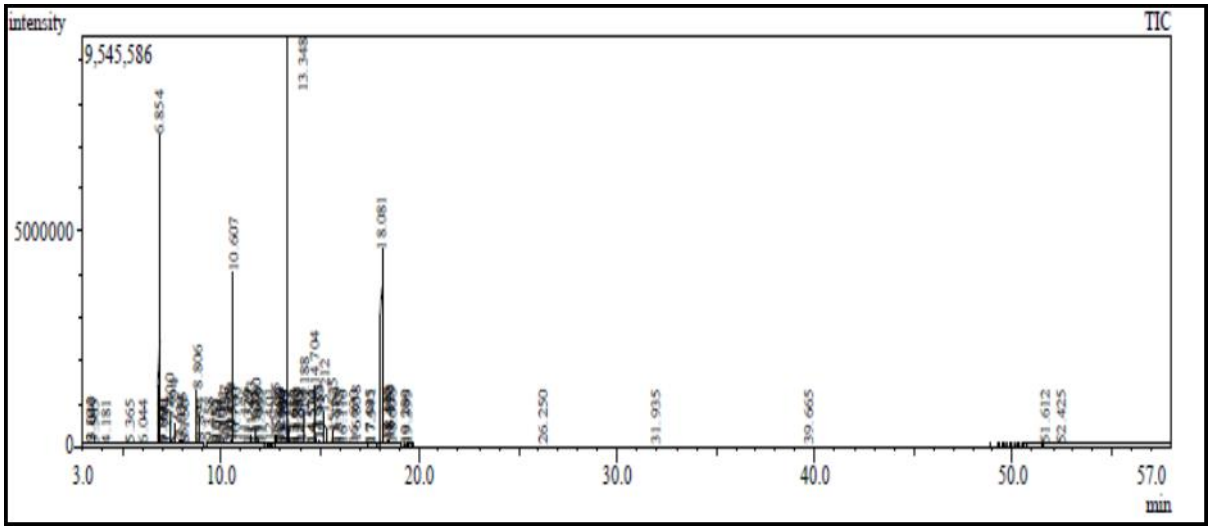

Figure II-3. Chromatogram of the essential oil of *Origanum Majorana L* plant obtained by GC/MS

Upon scrutinizing the two chromatograms, notable resemblances are evident, with discernible bands interspersed with overlapping ones. Generally, distinct regions can be identified, delineating three segments:

1. The initial segment, delimited within the time frame of (4 min to 12.4 min), hosts several bands denoting the presence of hydrocarbon monoterpenes.

2. The succeeding segment, spanning from (12.4 min to 24 min), encompasses the predominant bands, indicative of oxygenated monoterpenes prevalent in the plant's essential oil.

3. The final segment, spanning (24 min to 32.5 min), exhibits minimal banding, suggesting a negligible presence of hydrocarbon sesquiterpenes in the plant's essential oil.

The pertinent compounds in each essential oil, extracted from *Cotula cinerea* and *Origanum Majorana L*, have been identified and collated as follows

3.3.1. *Cotula cinerea*:

The hydrodistillation extraction of *Cotula cinerea* yielded a dark yellow oil with a yield of 0.91%. Gas chromatography-mass spectrometry (GC/MS) analysis identified 31 compounds, collectively constituting 95.64% of the oil's composition (as presented in Table 4). Predominantly, oxygenated monoterpenes accounted for 68.16%, followed by hydrocarbon monoterpenes at 23.27%, while the percentage of oxygenated sesquiterpenes was minimal at 0.15%. The remaining 4.06% comprised various other compounds.

Table II-3. Essential oil constituents of *Cotula cinerea* identified by GC/MS

No	Compounds	IR_{Exp}	IR_{Ref}	(%)
01	**Santolina triene**	**908**	**914**	**10.6**
02	Alpha-thujene	931	935	0.88
03	**Alpha-pinene**	**939**	**943**	**2.02**
04	Camphene	953	956	0.85
05	**Sabinene**	**976**	**976**	**6.17**
06	Beta- pinene	980	981	0.58
07	Dehydro-1.8-cineole	991	988	0.64
08	Myrcene	991	993	0.07
09	Meta mentha-1(7)-8dien	999	997	0.06
10	Alpha-terpinene	1018	1017	0.83
11	Ortho cymene	1022	1020	0.43
12	Para cymene	1026	1029	0.6
13	**1.8-cineole**	**1033**	**1033**	**5.34**
14	**Delta-terpinene**	**1062**	**1057**	**1.57**
15	Cis sabinene hydrate	1068	1069	0.46
16	Terpinolene	1088	1088	0.36
17	Cis thujone	1102	1100	0.52
18	**Trans thujone**	**1114**	**1117**	**51.86**
19	**Camphor**	**1143**	**1140**	**2.63**
20	**Beta-terpineol**	**1163**	**1160**	**1.39**
21	**Terpin-4-ol**	**1177**	**1178**	**1.73**
22	Alpha-terpineol	1189	1190	0.58
23	Myrtenol	1194	1195	0.13
24	Neo iso dihydro carveol	1226	1224	0.53
25	Carvotanacetone	1246	1247	0.9
26	**Cis verbenyl acetate**	**1262**	**1264**	**5.07**
27	Iso pulegol acetate	1273	1274	0.06
28	Para cymen-7-ol	1287	1285	0.08
29	Neryl acetate	1365	1367	--
30	Cis jasmone	1394	1390	0.15
31	Germacrene D	1480	1481	0.06
	Total		**95.64**	

Our analysis unveiled ten compounds with concentrations surpassing 1% (Table 4), with trans-thujone emerging as the predominant compound at 51.86%, followed by santolina triene at 10.69%, and sabinene at 6.17%. Additionally, 1,8-cineole constituted 5.34%, while four compounds α-pinene, terpin-4-ol, β-terpineol, and camphor appeared in lesser proportions at 2.02%, 1.73%, 1.39%, and 2.63%, respectively.

Comparison with other studies revealed some congruence, particularly with the percentage of santolina triene in Ekhlil et al.'s (Ekhlil et al., 2016) investigation (11.67%). However, disparities arose in the primary compound, with iso-thujanol predominating at 47.38% in their study. Conversely, El bouzidi et al.'s (Bouzidi et al., 2011) findings aligned closely with ours, particularly regarding trans-thujone (41.4%), 1,8-cineole (8.2%), and santolina triene (7.2%), while reporting camphor at 5.5%. Notably, Fournier et al.'s (Fournier et al., 1989) study diverged, identifying camphor as the principal compound at 50%.

For a visual representation of the top major compounds (more than 1%) and their structures, refer to Figure 5, which depicts the chemical structures and IUPAC names of the predominant constituents identified in the essential oil of *Cotula cinerea*.

3.3.2. *Origanum Majorana L*:

The hydrodistillation extraction method was employed to obtain the essential oil from *Origanum Majorana L.*, yielding a noteworthy 1.5% output. Analysis revealed the identification of 98.84% of the constituents, comprising a total of 42 compounds (as presented in Table 5). Oxygenated monoterpenes dominated the composition, constituting over 57%, followed by hydrocarbon monoterpenes at 25.14%.

Of particular interest is the prominent presence of trans-Thujone, constituting 33.3% of the essential oil, a compound conspicuously absents in the majority of prior studies. For instance, J. Chane et al.'s (Vera & Chane-Ming, 1999) investigation reported Terpinen-4-ol as the primary compound at 38.4%, a constituent entirely absents in our study. Similarly, Santolina triene emerged as the second major compound in our analysis at 16.40%, a finding not corroborated in extant literature.

Despite these disparities, concordance exists with previous studies regarding the occurrence of Sabinene, which manifested at 3.12% in our study, compared to 15% in J. Chane et al.'s (Vera & Chane-Ming, 1999) study and 17% in K.H.C Baser et al.'s study (Baser et al., 1993). Additionally, Sellami et al (Sellami et al., 2009) documented Sabinene at 2.14%.

Supplementary compounds identified include α-Thujene (1.44%), α-Pinene (1.19%), and β-Pinene oxide (4.42%).

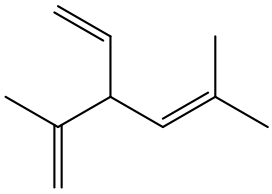

2,5-dimethyl-3-vinylhexa-1,4-diene
(Santolina triene)

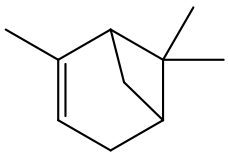

2,6,6-trimethylbicyclo[3.1.1]hept-2-ene
(Alpha-pinene)

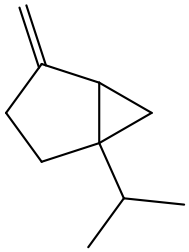

1-isopropyl-4-methylenebicyclo[3.1.0]hexane
(Sabinene)

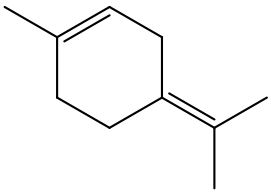

1-methyl-4-(propan-2-ylidene)cyclohex-1-ene
(Delta-terpinene)

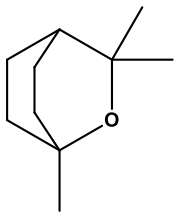

1,3,3-trimethyl-2-oxabicyclo[2.2.2]octane
(1.8-cineole)

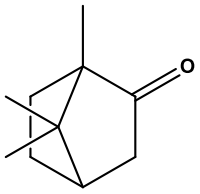

1,7,7-trimethylbicyclo[2.2.1]heptan-2-one
(Camphor)

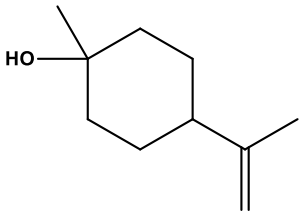

1-methyl-4-(prop-1-en-2-yl)cyclohexanol
(Beta-terpineol)

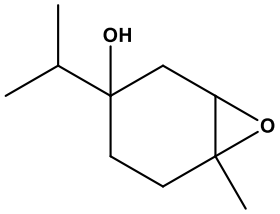

3-isopropyl-6-methyl-7-oxabicyclo[4.1.0]heptan-3-ol
(Terpin-4-ol)

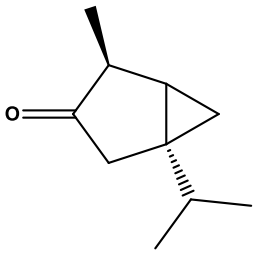

(1*S*,4*S*)-1-isopropyl-4-methylbicyclo[3.1.0]hexan-3-one
(Trans thujone)

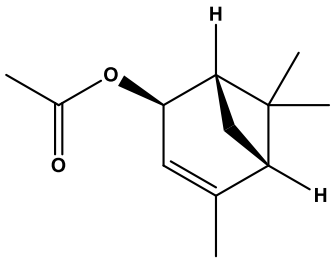

(1*S*,2*R*,5*S*)-4,6,6-trimethylbicyclo[3.1.1]hept-3-en-2-yl acetate
(Cis verbenyl acetate)

Figure II-4. Chemical structures and IUPAC names of the top major compounds identified in the essential oil of *Cotula cinerea*

In summary, the essential oil derived from *Origanum Majorana L.* exhibits distinctive chemical compositions in Eloued region compared to oils from other geographical locales,

characterized notably by the prevalence of trans-Thujone and Santolina triene as major constituents. This variance likely stems from multifactorial influences such as soil quality, climatic conditions, and harvest timing. For an illustrative overview of the major compounds identified, Figure 6, displaying the structures and IUPAC nomenclature of these constituents.

Table II-4. Essential oil constituents of *Origanum Majorana L* identified by GC/MS

No	Compounds	IR_{Exp}	IR_{Ref}	(%)
01	Pentanol	759	762	0.12
02	Cis-2-Penten-1-ol	762	765	0.03
03	Hexanal	801	801	0.02
04	(Z)-Salvene	844	847	0.02
05	Isopentyl acetate	869	869	0.02
06	**Santolina triene**	**898**	**906**	**16.42**
07	Tricyclene	912	921	0.02
08	**Alpha-Thujene**	**918**	**924**	**1.44**
09	**Alpha-Pinene**	**925**	**932**	**1.19**
10	Camphene	941	946	0.43
11	**Sabinene**	**969**	**969**	**3.12**
12	Beta-Pinene	972	974	0.22
13	Beta-Myrcene	989	988	0.14
14	Alpha-Phellandrene	1003	1002	0.03
15	Propanoic acid, 2-methyl-, 3-methylbutyl ester	1012	1007	0.02
16	Alpha-Terpinene	1016	1014	0.36
17	Para cymene	1024	1020	0.20
18	Ortho Cymene	1026	1022	0.45
19	Sylvestrene	1028	1025	0.20
20	**1,8-Cineole**	**1031**	**1026**	**10.71**
21	Trans-decahydroNaphthalene	1054	1053	0.03
22	Terpinene	1059	1054	0.76
23	Cis Sabinene hydrate	1068	1065	0.89
24	Para-Mentha-2'4(8)-diene	1088	1085	0.11
25	Trans-Sabinene hydrate	1100	1198	0.86
26	Isopentyl-2-methylbutanoate	1104	1100	0.14

27	cis-Thujone	1107	1101	0.24
28	**trans-Thujone**	**1119**	**1112**	**33.30**
29	iso-3-Thujanol	1136	1134	0.04
30	**Camphor**	**1146**	**1141**	**2.85**
31	**Beta pinene oxide**	**1163**	**1154**	**4.42**
32	3-Thujanol	1168	1164	0.48
33	Alpha Terpineol	1192	1186	0.88
34	Dihydrocarveol	1197	1192	0.06
35	Safranal	1203	1197	0.01
36	Cis-3-Hexenyl 2-methyl butanoate	1233	1229	0.25
37	trans-Myrtanol	1257	1258	0.04
38	2-(1E)-propenyl Phenol	1258	1264	0.09
39	**cis Verbenyl acetate**	**1277**	**1280**	**15.05**
40	neoiso-3Thujanol acetate	1287	1281	0.09
41	Isobornyl acetate	1290	1283	0.21
42	Lavandulyl acetate	1293	1288	0.32
Total		**95.64**		

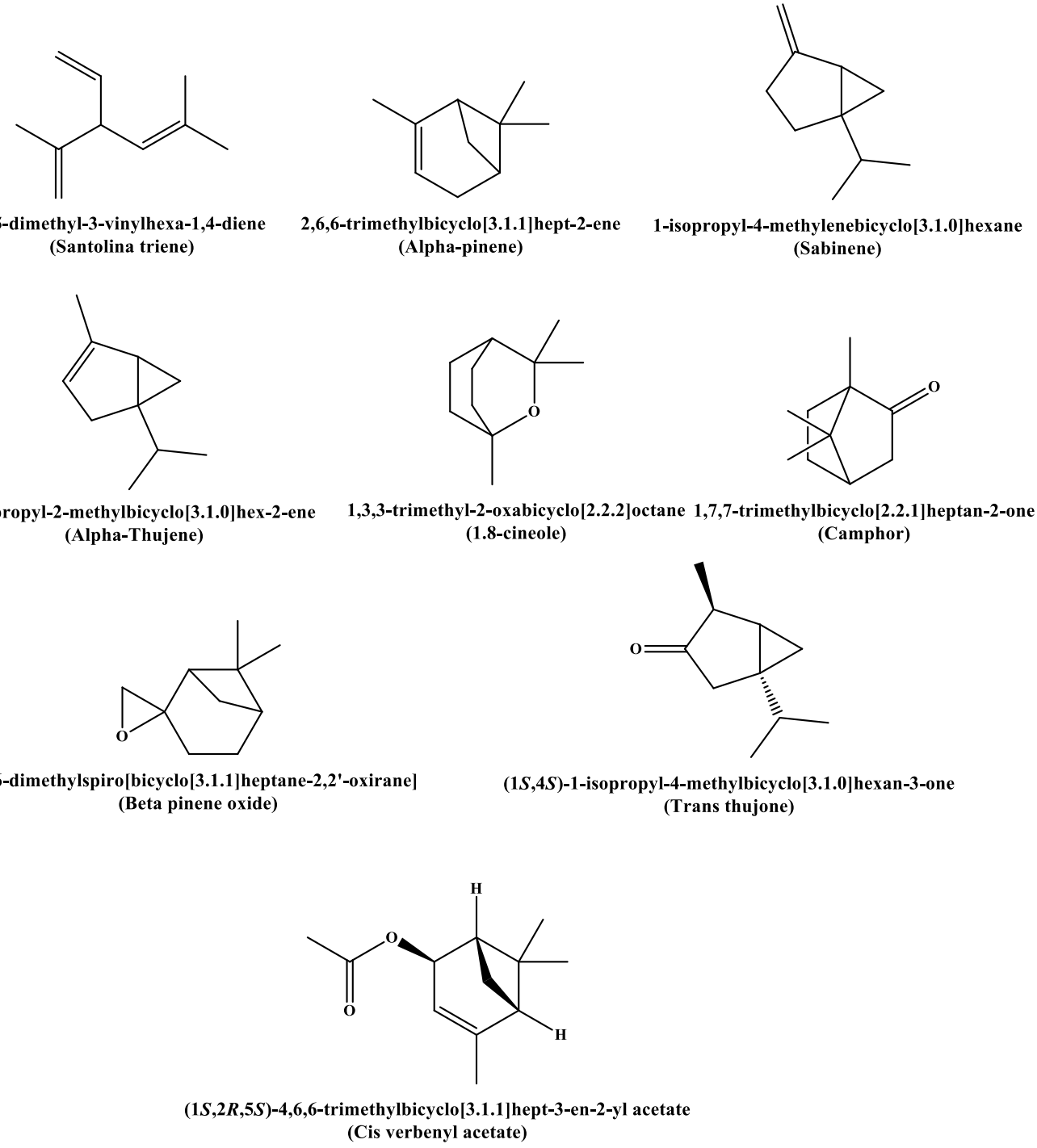

Figure II-5. Chemical structures and IUPAC names of the top major compounds identified in the essential oil of *Origanum Majorana L*

4. Assessment of Antibacterial Activity:

The *in vitro* assessment of the antimicrobial efficacy of *Cotula cinerea* and *Origanum Majorana* essential oils was conducted utilizing the disk diffusion technique against two prevalent bacterial strains associated with infections, *Escherichia coli* (*E. coli*), *Klebsiella*

pneumoniae (*K. pneumoniae*) and *Staphylococcus aureus* (*S. aureus*). Two distinct methodologies were employed to gauge the antibacterial activity: quantifying the zone of inhibition surrounding the EOs-impregnated disk and measuring the optical density of the bacterial suspension subsequent to treatment with varying concentrations of EOs. Comparative analysis was performed with amoxicillin, a widely utilized antibiotic. This study presents the findings derived from the diverse methodologies employed to evaluate the antibacterial efficacy of the studied essential oils and juxtaposes these outcomes with those obtained with amoxicillin.

4.1. Determination of the Diameter of the Inhibition Zone:

Following a 24-hour incubation period at 37°C, the zones of inhibition surrounding the disks impregnated with *Cotula cinerea* and *Origanum Majorana* essential oils and amoxicillin were measured. The diameters of the inhibition zones obtained with EOs and amoxicillin against *E. coli, K. pneumoniae* and *S. aureus* are summarized below (Table 6). The inhibition zones are identified by clear areas devoid of bacterial growth surrounding the disks.

Table II-5. Diameters of the inhibition zones of the studied essential oils and amoxicillin against *E. coli, K. pneumoniae* and *S. aureus*

Antibiotics	Bacteria	Diameter of the inhibition zone (mm)
Cotula cinerea	*E. coli*	10.9
	K. pneumoniae	20.2
	S. aureus	21.6
Origanum Majorana L	*E. coli*	13.8
	K. pneumoniae	22.3
	S. aureus	25.6
Amoxicillin	*E. coli*	24.6
	K. pneumoniae	18.5
	S. aureus	20.1

The table provides a systematic examination of the antimicrobial efficacy of natural compounds, specifically *Cotula cinerea* and *Origanum Majorana L* essential oils, alongside the conventional antibiotic Amoxicillin, against three bacterial strains: *Escherichia coli (E. coli), Klebsiella pneumoniae (K. pneumoniae), and Staphylococcus aureus (S. aureus)*. The diameter of the inhibition zones, measured in millimetres, serves as a quantitative indicator of antimicrobial activity (Cooper, 1963).

Analysis of the data reveals discernible trends in antimicrobial effectiveness across the tested antibiotics and bacterial strains. *Origanum Majorana L* and Amoxicillin consistently demonstrate larger inhibition zones compared to *Cotula cinerea*, indicating superior antimicrobial potency. Furthermore, *K. pneumoniae* exhibits the largest inhibition zones among the bacterial strains tested, suggesting varying susceptibility to the antibiotics among different bacterial species.

These findings underscore the importance of considering both the antimicrobial spectrum and potency of antibiotics when selecting appropriate treatment options for bacterial infections (Giurazza et al., 2021). Moreover, the observed efficacy of natural compounds like *Origanum Majorana L* highlights their potential as viable alternatives or adjuncts to conventional antibiotics.

4.2. Electronic Spectroscopy Interaction Study:

4.2.1. Bacterial inhibitory activities (IC_{50}):

The antibacterial activity of *Cotula cinerea* and *Origanum Majorana L* was assessed using the absorbance measurement method to determine the IC_{50}. This methodology entails measuring bacterial growth in wells containing varying concentrations of EOs. The resulting data facilitated the determination of the minimum concentration of EOs required to inhibit bacterial growth by 50%.

To this end, cultures of *E. coli*, *K. pneumoniae* and *S. aureus* were incubated with different concentrations of EOs and amoxicillin, ranging from 1 to 10 mg/ml, for 24 hours at 37°C. Subsequently, the optical density of each sample was measured at 620 nm using a spectrophotometer. The findings obtained are summarized in the following Table 7.

Table II-6. Absorbance values sorted from the antibacterial assays.

C (mg/ml)	*Cotula cinerea*			*Origanum Majorana L*			Amoxicillin		
	E. coli	*K. pneumoniae*	*S. aureus*	*E. coli*	*K. pneumoniae*	*S. aureus*	*E. coli*	*K. pneumoniae*	*S. aureus*
0	2.571	2.571	2.571	2.571	2.571	2.571	2.117	2.209	1.954
1	1.587	1.21	1.752	1.461	1.089	1.576	1.718	2.191	1.816
2	1.438	1.207	1.634	1.309	0.965	1.42	1.658	2.183	1.626
3	1.196	1.12	1.481	0.944	0.822	1.2	1.103	2.176	1.389
4	1.081	0.845	1.232	0.905	0.788	0.97	0.828	2.169	1.344
5	0.689	0.779	1.099	0.718	0.673	0.843	0.677	2.153	0.868

6	0.547	0.572	0.94	0.704	0.55	0.652	0.638	2.144	0.71
7	0.478	0.514	0.732	0.478	0.5	0.526	0.395	2.133	0.697
8	0.468	0.421	0.53	0.389	0.398	0.419	0.198	2.103	0.587
9	0.294	0.352	0.418	0.353	0.317	0.317	0.127	2.098	0.477
10	0.246	0.313	0.406	0.172	0.222	0.268	2.117	2.209	1.954

This table presents the outcomes of the investigation into the antibacterial efficacy of *Cotula cinerea* and *Origanum Majorana L* essential oils and amoxicillin against *E. coli*, *K. pneumoniae* and *S. aureus*, employing the absorbance measurement technique. The results depict a gradual decline in optical densities alongside escalating concentrations of EOs or amoxicillin, indicative of diminished bacterial proliferation. Subsequently, IC_{50} values, delineating the concentration of EOs or amoxicillin necessary to impede 50% of bacterial growth, were derived from these observations by plotting the inhibition percentage against the compound concentrations (refer to Figure 7). The resultant of IC_{50} values is meticulously documented in Table 8.

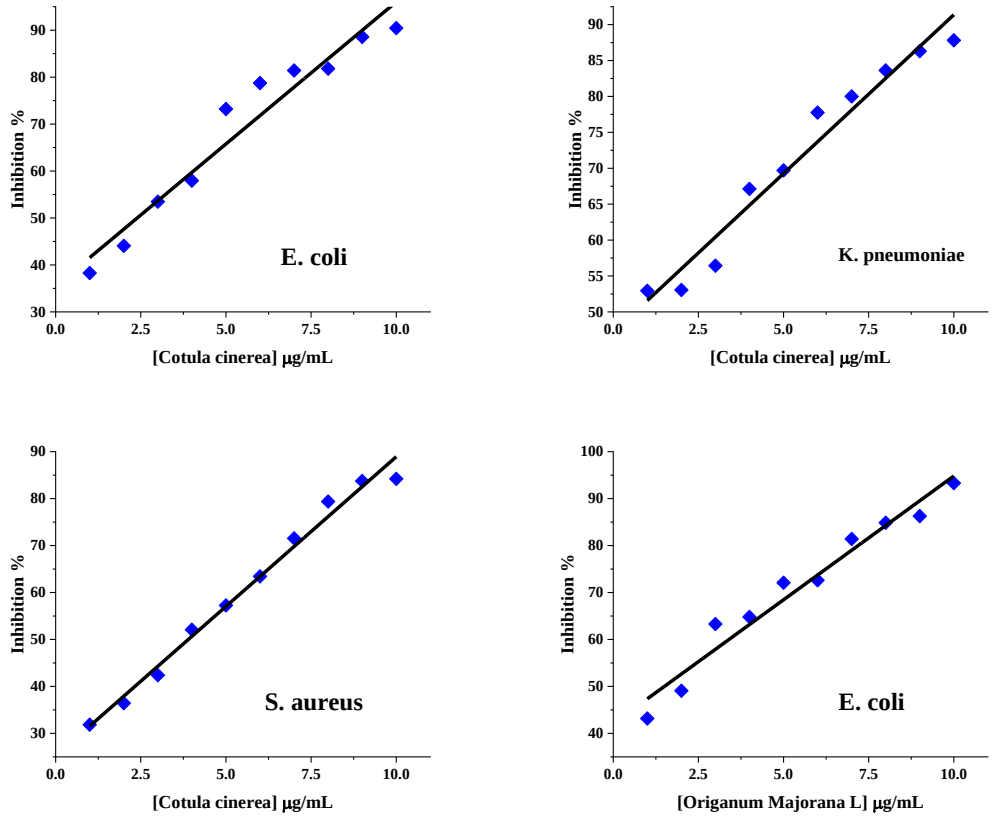

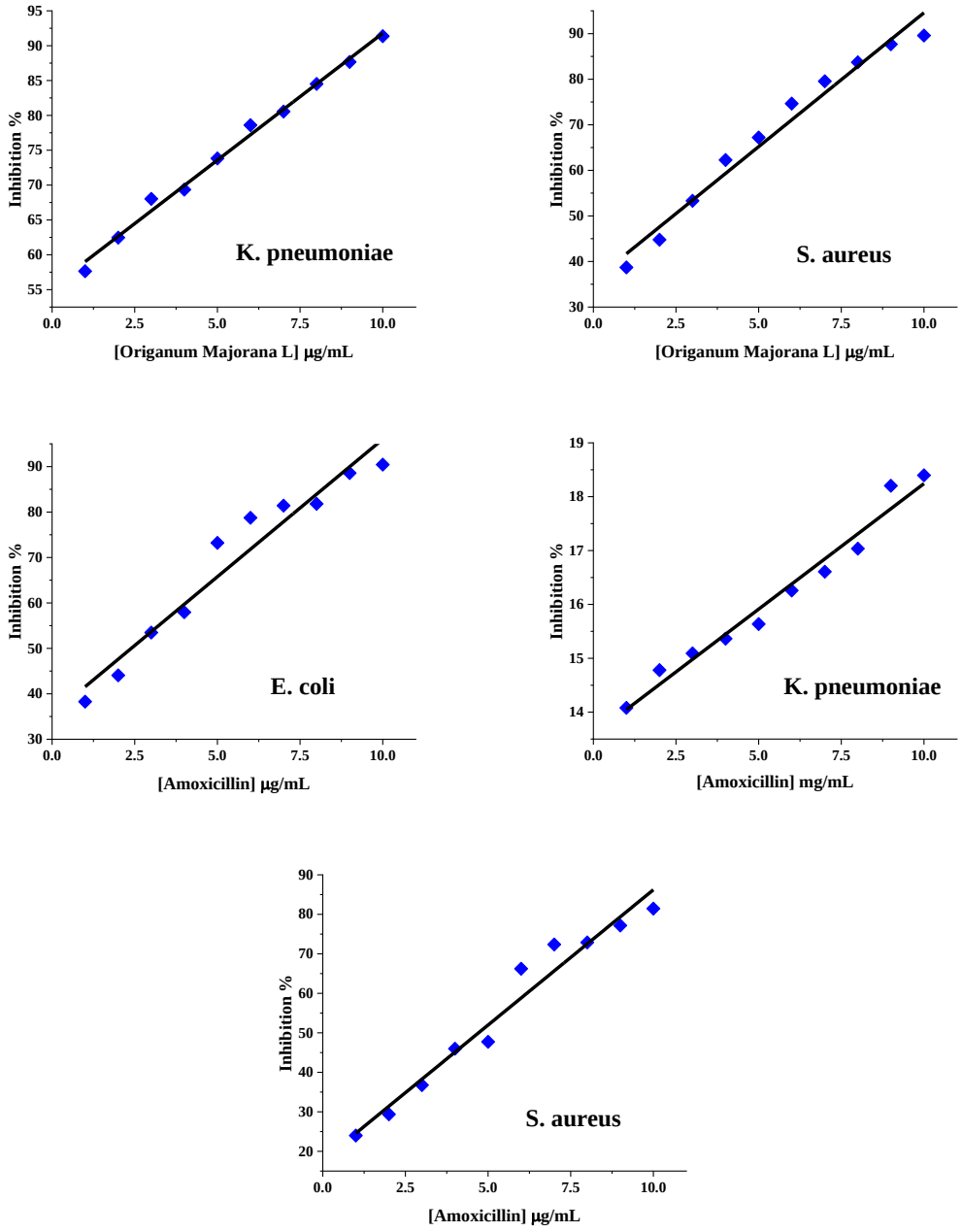

Figure II-6. The linear regression curves depicting the percentage inhibition of bacteria versus the concentration of *Cotula cinerea* and *Origanum Majorana L* essential oils and Amoxicillin

Table II-7. The antibacterial activity of *Cotula cinerea* and *Origanum Majorana L* essential oils and amoxicillin through the inhibition test against *E. coli, K. pneumoniae* and *S. aureus*.

Cotula cinerea			***Origanum Majorana***			**Amoxicillin**		
E. coli	*K. pneumoniae*	*S. aureus*	*E. coli*	*K. pneumoniae*	*S. aureus*	*E. coli*	*K. pneumoniae*	*S. aureus*
38.273	52.937	31.855	43.174	57.643	38.701	17.658	14.080	23.998
44.068	53.053	36.445	49.086	62.466	44.769	33.178	14.780	29.366
53.481	56.437	42.396	63.283	68.028	53.326	35.511	15.091	36.756
57.954	67.133	52.081	64.800	69.350	62.271	57.098	15.364	45.974
73.201	69.701	57.254	72.073	73.823	67.211	67.795	15.636	47.725
78.724	77.752	63.438	72.618	78.608	74.640	73.668	16.258	66.239
81.408	80.008	71.529	81.408	80.552	79.541	75.185	16.608	72.384
81.797	83.625	79.385	84.870	84.520	83.703	84.636	17.036	72.890
88.565	86.309	83.742	86.270	87.670	87.670	92.299	18.203	77.168
90.432	87.826	84.208	93.310	91.365	89.576	95.060	18.398	81.447
IC_{50} = 2.935 mg/ml	IC_{50} = 0.641 mg/ml	IC_{50} = 3.895 mg/ml	IC_{50} = 1.500 mg/ml	IC_{50} = 1.477 mg/ml	IC_{50} = 2.412 mg/ml	IC_{50} = 3.961 mg/ml	IC_{50} = 8.154 mg/ml	IC_{50} = 4.712 mg/ml

The findings reveal the growth inhibitions of *E. coli, K. pneumoniae*, and *S. aureus* bacteria in the presence of *Cotula cinerea* and *Origanum Majorana L* essential oils, alongside amoxicillin. The results demonstrate a notably potent efficacy of *Cotula cinerea* and *Origanum Majorana L* compared to amoxicillin, with IC_{50} values of 3.961 mg/ml, 8.154 mg/ml, and 4.712 mg/ml, respectively.

Concerning *Cotula cinerea*, the outcomes indicate bacterial growth inhibition of up to 90% for *E. coli*, 87% for *K. pneumoniae*, and 84% for *S. aureus* at the highest tested concentration (10 mg/ml). This suggests that *Cotula cinerea* may possess antimicrobial activity, albeit at relatively elevated concentrations.

In contrast, *Origanum Majorana L* results in bacterial growth inhibition of up to 93% for E. coli, 81% for K. pneumoniae, and 89% for S. aureus at the highest tested concentration (10 mg/ml). This underscores the superior efficacy of this essential oil as an antibiotic against bacterial infections.

In conclusion, the findings of this study highlight the notable antibacterial effects exhibited by the two essential oils under investigation, *Cotula cinerea* and *Origanum Majorana*

L, surpassing those of amoxicillin. This suggests their potential as promising alternatives or adjuncts in combating bacterial infections.

4.2.2. Binding constants:

The spectrophotometric absorption method was employed to assess the binding constant (K_b) of *Cotula cinerea* and *Origanum Majorana L* essential oils with the three types of bacteria under investigation. This constant was expressed in M^{-1}. Decreasing concentrations of EOs and amoxicillin resulted in a gradual decrease in the absorption of the solution containing the bacteria. By plotting $A_0/(A-A_0)$ against 1/C (Figure 8) (Tyagi et al., 2015), the slope was calculated as $\varepsilon/(\varepsilon_0-\varepsilon).Kb$, where ε represents the absorbance of the solution containing the compound, and ε_0 denotes the absorbance of the control solution. The "y" intercept was also calculated as $\varepsilon/(\varepsilon_0-\varepsilon)$. Subsequently, the binding constant was determined by dividing the slope by the intercept (K_b = slope/intercept).

4.2.3. Binding free energy:

Utilizing Equation 10, the variation in binding free energy was calculated. Negative values of ΔG signify the spontaneity of the interaction between the specified bacteria and the studied compounds, with their magnitude indicative of a robust binding affinity between the protein and the ligands. The binding constants alongside their corresponding binding free energies are succinctly presented in Table 13.

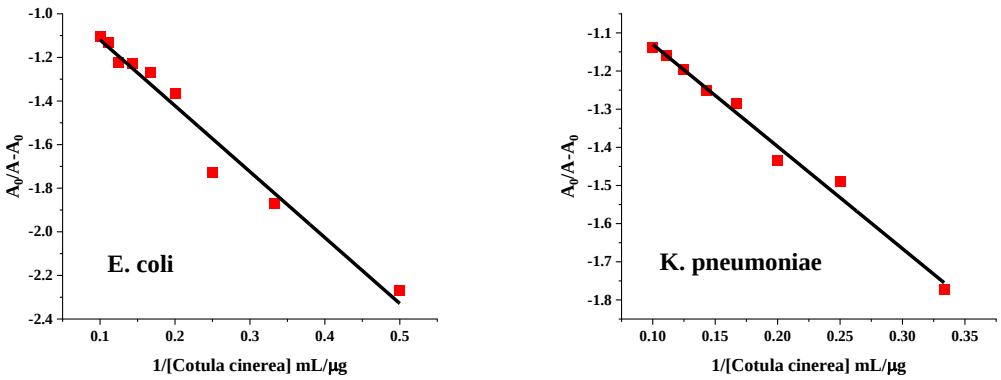

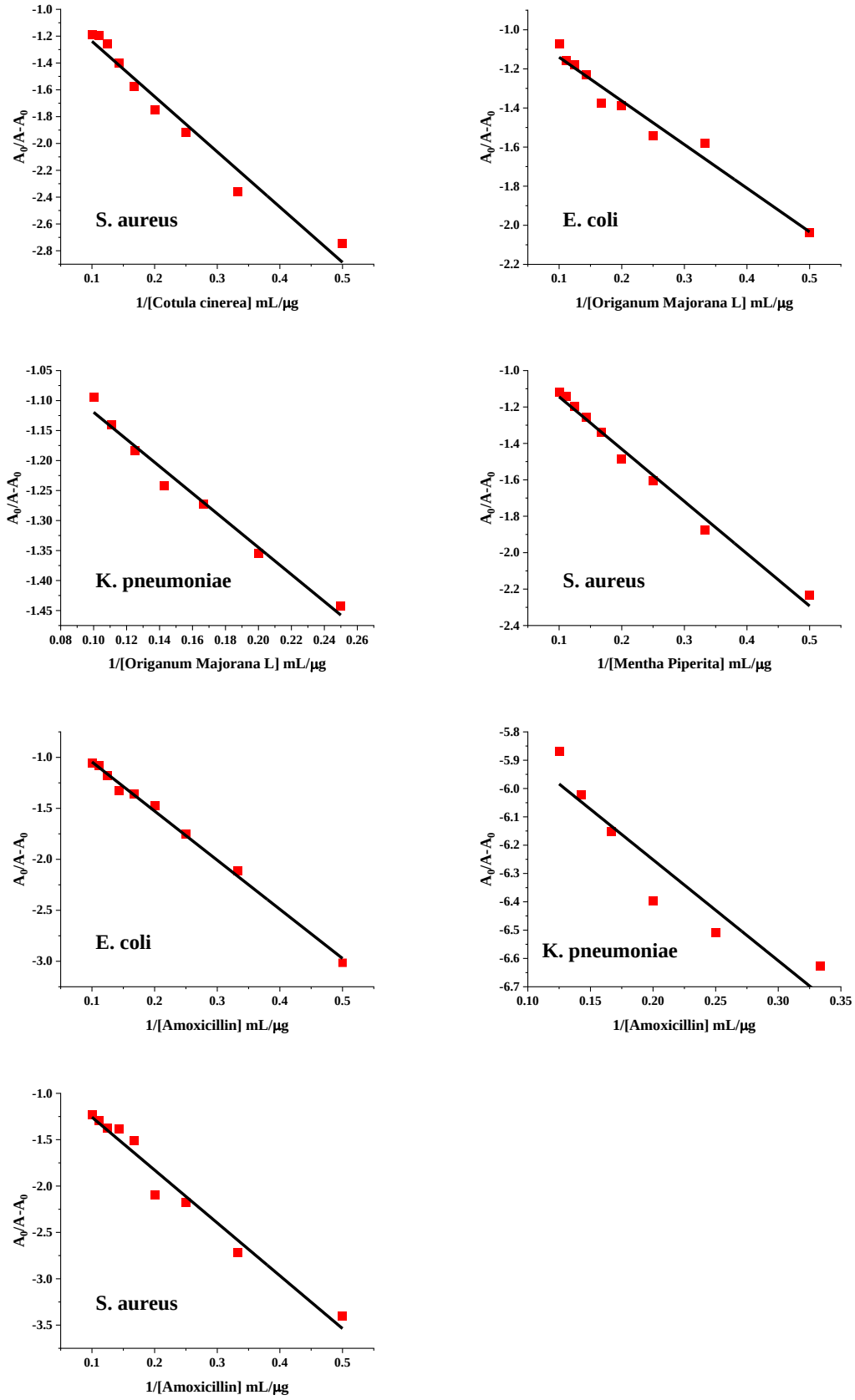

Figure II-7. Plots of $A_0/(A - A_0)$ against 1/[*Cotula cinerea*], 1/[*Origanum Majorana L*] and 1/[Amoxicillin] were constructed to calculate the binding constants

Table II-8. Binding constants and binding free energies of the studied compounds with bacterial strains.

Compounds	Bacteria's	Equations	R^2	K (M^{-1})	-ΔG ($KJ.mol^{-1}$)
Cotula cinerea	*E. coli*	y = -3.024x – 0.817	0.968	2.70×10^5	31.01
	K. pneumoniae	y = -2.677x – 0.862	0.985	3.22×10^5	31.45
	S. aureus	y = -4.118x – 0.827	0.962	2.00×10^5	30.27
Origanum Majorana L	*E. coli*	y = -2.232x – 0.917	0.960	4.11×10^5	32.05
	K. pneumoniae	y = -2.254x – 0.894	0.977	3.97×10^5	31.96
	S. aureus	y = -2.871x – 0.857	0.986	2.98×10^5	31.26
Amoxicillin	*E. coli*	y = -4.817x – 0.563	0.995	1.17×10^5	28.93
	K. pneumoniae	y = -3.566x – 5.538	0.853	1.55×10^5	35.35
	S. aureus	y = -5.697x – 0.688	0.964	1.21×10^5	29.01

The table provides a comprehensive overview of the binding interactions between various compounds, including *Cotula cinerea*, *Origanum Majorana L*, and amoxicillin, with different bacterial strains, namely *E. coli*, *K. pneumoniae,* and *S. aureus*. Each entry includes the equation of the linear regression line obtained from the plots of $A/(A_0 - A)$ against 1/[EOs], the coefficient of determination (R^2) indicating the goodness of fit of the regression model, the binding constant (K) expressed in M^{-1}, and the corresponding negative change in Gibbs free energy (-ΔG) in kJ/mol (Ozer, 1985).

The high values of R^2 across all entries indicate a strong correlation between the experimental data and the fitted regression lines, suggesting the reliability of the models in describing the binding behavior (Plonsky & Ghanbar, 2018). Additionally, the binding constants (K) provide quantitative measures of the strength of interaction between the compounds and the bacterial strains, with higher values indicating stronger binding affinities (Lanez et al., 2018).

The negative values of ΔG underscore the spontaneity of the binding interactions, with larger magnitudes indicating more favourable and energetically stable associations between the compounds and the bacteria (Kedadra et al., 2022). Notably, Amoxicillin exhibits relatively lower binding constants and ΔG values compared to the essential oils, suggesting potentially weaker interactions with the bacterial strains studied.

In the context of this study, higher values of K indicate stronger binding affinities between the compounds and the bacterial strains (Adaika et al., 2019). *Cotula cinerea* and *Origanum Majorana L* essential oils exhibit notably higher K values compared to amoxicillin across all

bacterial strains tested. This suggests that the essential oils have a greater propensity to bind to the bacterial receptors, potentially leading to enhanced antimicrobial efficacy. Conversely, amoxicillin demonstrates relatively lower K values, indicating comparatively weaker binding interactions with the bacterial strains. This observation aligns with the known mechanism of action of amoxicillin, which primarily targets specific bacterial cell wall components rather than interacting directly with bacterial receptors.

4.3. Molecular Docking Interaction Study:

In order to validate the experimentally measured antibacterial activity against E. coli, K. pneumoniae, and S. aureus, an *in silico* molecular docking study was conducted on the proteins of the respective bacteria. The objective of this study was to predict the molecular interactions between the compound of interest and the studied bacteria, and to assess their antibacterial potential using Maestro version 11.7 user interface of the Schrödinger suite (Small-Molecule Drug Discovery Suite 2021-4, Schrödinger, LLC, New York, NY, 2021) (Schrödinger, 2015). Additionally, a comparison of the results obtained with amoxicillin, a commonly used antibiotic, was performed. The results obtained after the docking assays are presented in the Table 14.

Table II-9. Rigid and induced fit docking scores of the studied compounds against *E. coli*, *K. pneumoniae*, and *S. aureus*

Compound	**E. coli**		**K. pneumoniae**		**S. aureus**	
	Rigid Docking Score (Kcal/mol)	IFD scores (Kcal/mol)	Rigid Docking Score (Kcal/mol)	IFD scores (Kcal/mol)	Rigid Docking Score (Kcal/mol)	IFD scores (Kcal/mol)
trans thujone	-9.505	-10.120	-8.480	-9.095	-7.168	-8.767
alpha-Terpineol	-9.464	-10.079	-11.748	-12.363	-7.127	-8.726
beta-Terpineol	-8.480	-9.095	-11.032	-11.647	-6.143	-7.742
cis Verbenyl acetate	-11.748	-12.363	-10.540	-11.155	-9.411	-11.010
Camphor	-11.032	-11.647	-9.916	-10.531	-8.695	-10.294
Sabinene	-10.540	-11.155	-9.269	-9.884	-8.203	-9.802
gamma terpinene	-9.916	-10.531	-9.916	-10.531	-7.579	-9.178
alpha-Pinene	-9.269	-9.884	-6.932	-8.531	-6.932	-8.531
1,8-Cineole	-8.603	-9.218	-6.266	-7.865	-6.266	-7.865
Santolina triene	-8.261	-8.876	-5.924	-7.523	-5.924	-7.523

alpha-Thujene	-8.138	-8.753	-5.555	-7.424	-5.555	-7.394
Beta Pinene oxide	-8.119	-8.734	-5.549	-7.407	-5.547	-7.391

The table presents the results of rigid docking scores and induced fit docking (IFD) scores for various compounds against three bacterial strains: Escherichia coli, K. pneumoniae, and Staphylococcus aureus. These scores provide insights into the potential antibacterial activity of each compound by indicating the strength of interaction with the target proteins or receptors within the bacteria.

Observing the rigid docking scores, it is evident that compounds such as trans thujone and cis Verbenyl acetate exhibit the most favourable scores across all three bacterial strains, suggesting strong binding affinities towards their respective targets. Conversely, Camphor Sabinene demonstrate comparatively weaker rigid docking scores, indicating potentially weaker interactions with the bacterial proteins.

The induced fit docking (IFD) scores further validate the binding affinities of the compounds by considering the flexibility of both the ligands and the target proteins during the docking process. Notably, compounds like trans thujone and cis Verbenyl acetate maintain their favourable IFD scores, affirming their potential as promising antibacterial agents.

Comparing the results obtained for each compound across the three bacterial strains, variations in docking scores are observed, suggesting potential differences in the binding interactions with the specific target proteins or receptors present in each strain. This highlights the importance of considering the target specificity of antibacterial agents in rational drug design.

The photographs depicting the interaction of the best compound in each essential oil with the studied bacteria are presented in Figures below:

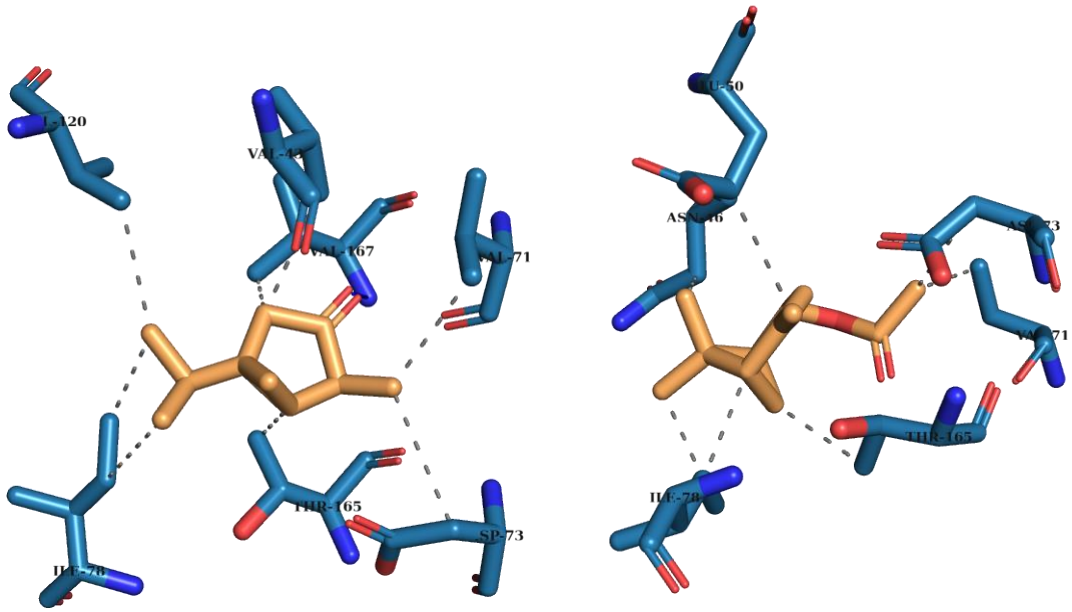

Docking complex and interaction plot for compound trans thujone and cis Verbenyl acetate with E. coli

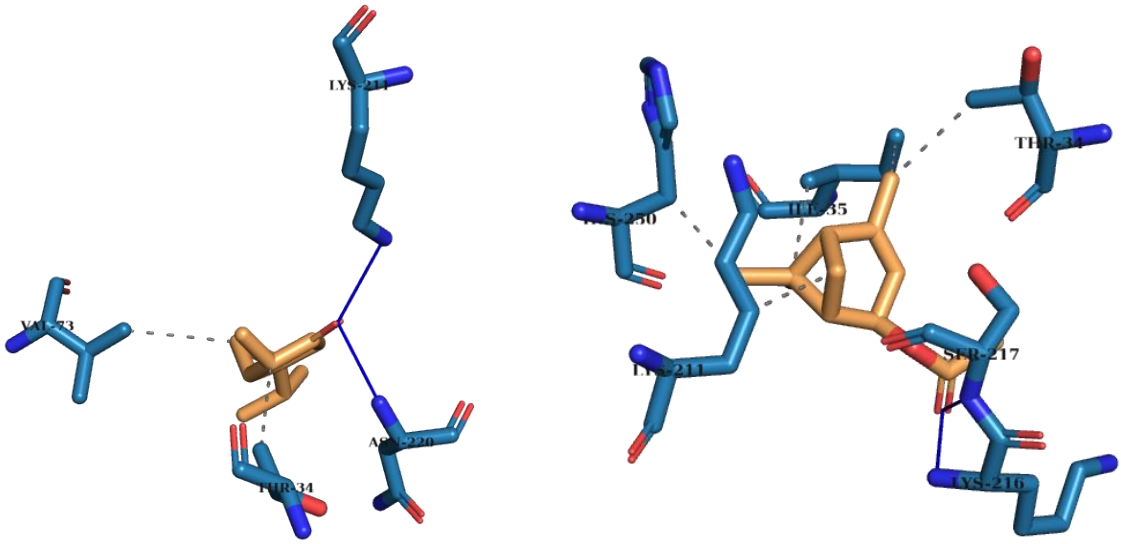

Docking complex and interaction plot for compound trans thujone and cis Verbenyl acetate with K. pneumoniae

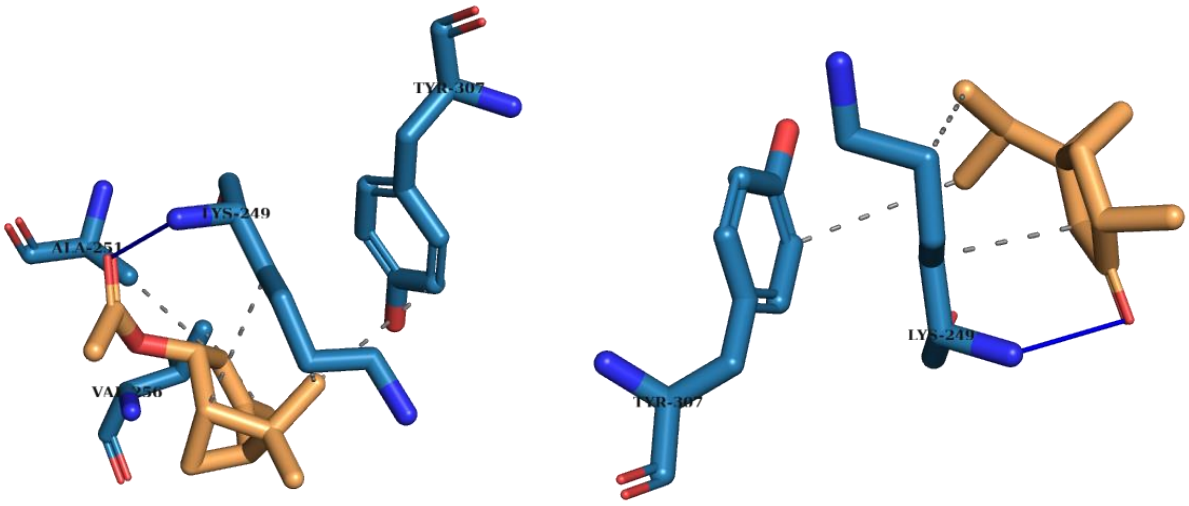

Docking complex and interaction plot for compound trans thujone and cis Verbenyl acetate with S. aureus

5. ADMET and drug-likeness prediction:

Modern drug discovery involves assessment of competence of the dynamic molecules and their strength to reach target site in bioactive form, which involves cellular, animal and human clinical trials which are highly priced and encumbered with risks (Ranjith & Ravikumar, 2019; Ranjith D & Viswanath S, 2019). Presently computer aided drug development encouraged the estimate of absorption, distribution, metabolism and excretion of drugs (ADME), they postulate anticipatory and dependable data very quickly and compliment for experimental approaches (Ranjith & Ravikumar, 2019; Sliwoski et al., 2014). It has been determined that the initial appraisal of ADME properties in the discovery period diminishes remarkably the fraction of pharmacokinetics related failures in the clinical phase (Hay et al., 2014; Ranjith & Ravikumar, 2019).

In the present study we evaluated the ADME properties of the major compounds (more than 10%) present in both essential oils using SwissADME web tool. A total of 4 potent phytoconstituents were analysed to study general characteristics (Table 11), Physicochemical properties (Table 12), lipophilicity and water solubility characteristics (Table 13 & 14), pharmacokinetic parameters (Table 15), drug likeness rule and bioavailability score (Table 16) and medicinal chemistry properties (Table 17), respectively. General characteristics of the studied compounds revealed all the compounds having molecular weight less than 500 Da, which is a good prime property to be called as drug likeness of the small molecules.

Table II-10. General characteristics of the phytoconstituents of essential oils

SI. No	Compounds	Molecular formula	Canonical SMILES	Molecular weight (g/mol)
1	**Santolina triene**	$C_{10}H_{16}$	CC(=CC(C=C)C(=C)C)C	136.23
2	**trans-Thujone**	$C_{10}H_{16}O$	CC1C2CC2(CC1=O)C(C)C	152.53
3	**1,8-Cineole**	$C_{10}H_{18}O$	CC1(C2CCC(O1)(CC2)C)C	154.25
4	**cis-Verbenyl acetate**	$C_{12}H_{18}O_2$	CC1=CC(C2CC1C2(C)C)OC(=O)C	194.27

Table II-11. Physicochemical properties of the phytoconstituents of essential oils

Properties	Santolina triene	trans-Thujone	1,8-Cineole	cis-Verbenyl acetate
Num. heavy atoms	10	11	11	14
Num. arom. heavy atoms	0	0	0	0
Fraction Csp3	0.40	0.90	1.00	0.75
Num. rotatable bonds	3	1	0	2
Num. H-bond acceptors	0	1	1	2
Num. H-bond donors	0	0	0	0
Molar refractivity	48.76	45.90	47.12	56.12
TPSA (Å²)	0.00	17.07	9.23	26.30

Table II-12. Lipophilicity characteristics of the phytoconstituents of essential oils

Properties	Santolina triene	trans-Thujone	1,8-Cineole	cis-Verbenyl acetate
iLOGP	2.90	2.27	2.58	2.53
XLOGP3	4.22	2.27	2.74	3.73
WLOGP	3.33	2.26	2.74	2.54
MLOGP	3.56	2.30	2.45	2.65
SILICOS-IT	2.88	2.63	2.86	2.26
Consensus Log Po/w	3.38	2.35	2.67	2.74

Table II-13. Water Solubility characteristics of the phytoconstituents of essential oils

Small molecules	ESOL				Ali				SILICOS-IT			
	Log S (ESOL)	Solubility		Class	Log S (Ali)	Solubility		Class	Log S (SILICOS-IT)	Solubility		Class
		mg/ml	mol/L			mg/ml	mol/L			mg/ml	mol/L	
Santolina triene	-3.15	9.75e-2	7.16e-4	S	-3.93	1.60e-2	1.17e-4	S	-2.04	1.24e-0	9.10e-3	S
trans-Thujone	-2.15	1.08e-0	7.11e-3	S	-2.27	8.27e-1	5.43e-3	S	-2.15	1.08e-0	7.10e-3	S
1,8-Cineole	-2.52	4.63e-1	3.00e-3	S	-2.59	3.98e-1	2.58e-3	S	-2.45	5.45e-1	3.53e-3	S
cis-Verbenyl acetate	-3.26	1.06e-1	5.47e-4	S	-3.97	2.06e-2	1.06e-4	S	-2.11	1.51e-0	7.78e-3	S

Table II-14. Pharmacokinetics parameters of the phytoconstituents of essential oils

Proprieties	Santolina triene	trans-Thujone	1,8-Cineole	cis-Verbenyl acetate
GI absorption	Low	High	High	Low
BBB permeant	Yes	Yes	Yes	Yes
P-gp substrate	No	No	No	No
CYP1A2 inhibitor	No	No	No	No
CYP2C19 inhibitor	No	No	No	No
CYP2C9 inhibitor	No	No	No	Yes
CYP2D6 inhibitor	No	No	No	No
CYP3A4 inhibitor	No	No	No	No
Log Kp (Skin Permeation) (cm/s)	-4.13	-5.62	-5.30	-4.84

Table II-15. Druglikeness rule and bioavailability score of the phytoconstituents of essential oils

Proprieties	Santolina triene	trans-Thujone	1,8-Cineole	cis-Verbenyl acetate
Lipinski	Yes; 0 violations	Yes; 0 violations	Yes; 0 violations	Yes; 0 violations
Ghose	No; 1 violation: MW<160	No; 1 violation: MW<160	No; 1 violation: MW<160	Yes
Veber	Yes	Yes	Yes	Yes
Egan	Yes	Yes	Yes	Yes
Muegge	No; 2 violations: MW<200, XLOGP3>3.5	No; 2 violations: MW<200, Heteroatoms<2	No; 2 violations: MW<200, Heteroatoms<2	No; 1 violation: MW<200,
Bioavailability score	0.55	0.55	0.55	0.55

Table II-16. Medicinal Chemistry properties of the Phytoconstituents of essential oils

Proprieties	Santolina triene	trans-Thujone	1,8-Cineole	cis-Verbenyl acetate
PAINS	0 alert	0 alert	0 alert	0 alert
Brenk	1 alert: isolated_alkene	0 alert	0 alert	1 alert: isolated_alkene
Leadlikeness	No; 2 violations: MW<250, XLOGP3>3.5	No; 1 violation: MW<250	No; 1 violation: MW<250	No; 2 violations: MW<250, XLOGP3>3.5
Synthetic accessibility	3.22	2.79	3.65	4.50

Lipophilicity property of the compounds portrays an important role for molecular discovery activities in multifarious domains. The quantitative descriptor of the lipophilicity is the partition coefficient P of a given molecule between *n*-octanol and water system (Daina et al., 2014). Because of its amphiphilic nature, *n*-octanol is considered a good mimic of phospholipid membrane characteristics (Liu et al., 2011). Multifarious algorithms are accessible to compute log Po/w, which rely on factual methodologies. The classic log P predictors branched in to two division, first ones split molecular structures into molecular fragments includes fragmental approach e.g. KLOGP (Klopman et al., 1993), KOWWNIN (Meylan & Howard, 2000) or atomic approach e.g. ALOGP (Ghose et al., 1998; R. Wang et al., 1997), XLOGP (Cheng et al., 2007; Moriguchi et al., 1994). The second division gathers the topological methods in which, the molecules description is related to its topology being as count or flags for specific atoms, groups or structural properties e.g. MLOGP (Brenk et al., 2008; Moriguchi et al., 1992), the prediction attained by manifold linear regression trained on large molecular data sets. The SILICOS-IT is a hybrid technique which combines both molecular fragments and topological parameters, which confide on 27 fragments and 7 topological descriptors, it was disciplined on 23,455 molecules with experimental *n*-octanol/water partition values (Daina et al., 2014). The version three of the XLOGP atomic model is established on a system of 87 fragments and two corrective factors. If the input structures are similar to a reference compound, the fragments differentiating them are treated and the corresponding log P contributions added to the reference structure log P value (Cheng et al., 2007). Lipophilicity estimated as consensus Log P, which is the average value of all Log P evaluated with various lipophilicity criteria, determined trans-Thujone as most lipophilic whereas santolina triene as least lipophilic and water solubility of the small molecules ranged from highly water soluble to water soluble.

The SwissADME model returns “Yes” or “No” if the compound under examination has greater probability to be a substrate or non-substrate of P-gp or inhibitor or non-inhibitor of Cytochrome P450 isoenzymes (CYP1A2, CYP2C9, CYP2C19, CYP2D6 and CYP3A4).

The pharmacokinetics and drug likeness performed using SwissADME showed a low level of GI absorption and BBB permeant with santolina triene and cis-Verbenyl acetate while a high absorption detected with trans-Thujone and 1,8-Cineole. All the compounds present in the essential oils are not the substrates for P-gp except contrarily to the trans-Thujone (Table 12), so they are not susceptible to the efflux mechanism performed by this transporter which is used by many tumours cell lines as a drug-resistance mechanism (Ranjith & Ravikumar, 2019)

All of the small molecules returned as non-inhibitors for inactivation for CYP isoenzymes. The skin permeability coefficient (Log Kp), a multiple linear regression, the more negative the log Kp (with Kp in cm/s), the less skin permeant is the molecule. Among the phytoconstituents, trans-Thujone (-5.62) is the least permeant and santolina triene (-4.13) is highly permeant respectively. This SwissADME section gives access to five different rule-based filters, with diverse ranges of properties inside of which the molecule is defined as drug-like. The Lipinski (Pfizer) filter is the pioneer rule-of-five implemented and with the Ghose (Amgen), Veber (GSK), Egan (Pharmacia) and Muegge (Bayer) methods. Multiple estimations allow consensus views or selection of methods best fitting the end-user's specific needs in terms of chemical space or project-related demands. Any violation of any rule described here appears explicitly in the output panel. All the four compounds followed the filtered rule invoked in the SwissADME; the violation shown by the molecules are minimal.

SwissADME interpretation posts 0 PAINS alert of the 4 studied compounds. Brenk considered compounds that are smaller and less hydrophobic and not those defined by "Lipinski's rule of 5" to widen opportunities for lead optimization. This was after exclusion of compounds with potentially mutagenic, reactive and unfavourable groups such as nitro groups, sulphates, phosphates, 2-halopyridines and thiols (Brenk et al., 2008). All the compounds examined flouted Brenk's rule with only one alert, all the compounds failed Lead-likeness criteria due to their molar weight.

In silico toxicity study aims to help in optimizing compounds regarding their toxicity proprieties. The study could offer an important improvement to the awareness of the full perspective of virtual screening for the identification of target compounds with negligible or no toxicity, which may open a path for the selection of novel nontoxic phytoconstituents present in *Cotula cinerea* and *Origanum Majorana L* essential oils with high antidiabetic activity. In silico toxicity study of the chosen compounds was performed using the ProTox-II web server (Drwal et al., 2014). It aims to predict hepatotoxicity (Dili), carcinogenicity (Carcino), immunotoxicity (Immuno), mutagenicity (Mutagen), cytotoxicity (Cyto), median lethal dose (LD50), and toxicity class (TC).

According to in silico toxicity profiles presented in Table 19, the toxicity class of all the phytoconstituents was detected to be equal to 5 except the trans-Thujone which predicted to be 4. Santolina triene, trans-Thujone**,** 1,8-Cineole and cis-Verbenyl acetate were predicted to be nontoxic except in immunotoxicity for the last wrote compound.

Table II-17. In silico toxicity profiles of the studied compounds

Molecule	Dili	Carcino	Immuno	Mutagen	Cyto	LD_{50} (mg.Kg^{-1})	TC
Santolina triene	Inactive	Active	Inactive	Inactive	Inactive	2610	5
trans-Thujone	Inactive	Inactive	Inactive	Inactive	Inactive	500	4
1,8-Cineole	Inactive	Inactive	Inactive	Inactive	Inactive	2480	5
cis-Verbenyl acetate	Inactive	Inactive	Active	Inactive	Inactive	2600	5

6. Molecular Dynamics Simulation:

Molecular Dynamics Simulation (MDS) investigations were conducted for the premier compound show the best IFD score, trans thujone, in complex with E. coli. The principal objective of these MDS endeavours was to subject the ligand-receptor complex to physiological conditions, a feat unattainable through the confines of molecular docking (Dumitrică & James, 2007). Throughout the MDS protocol, a trajectory frame was generated at intervals of 100 picoseconds (Tu et al., 2008), accumulating a total of 1000 frames over the course of a 100-nanosecond simulation. Analysis encompassed metrics such as 'Root Mean Square Deviation (RMSD), and 'Root Mean Square Fluctuation (RMSF). Specifically, RMSD values were computed by aligning the frames of the protein and ligand-protein complex with the reference frame, respectively. These analytical approaches provide a detailed understanding of the structural stability and dynamic fluctuations exhibited by the trans thujone _E. coli complex throughout the simulation period (Schreiner et al., 2012).

The Root Mean Square Deviation (RMSD) values for the complex consistently fall within the acceptable range of 0 – 2 Å. Examination of the analysed complex revealed no significant conformational alterations; however, an initial minor deviation was discerned in the vicinity of 8 – 20 nanoseconds, and a subtle drift was observed approximately between 45 – 55 nanoseconds. Beyond these periods, the complex demonstrated marked stability throughout the entirety of the simulation process, with no notable occurrence of major conformational changes. (Figure 9).

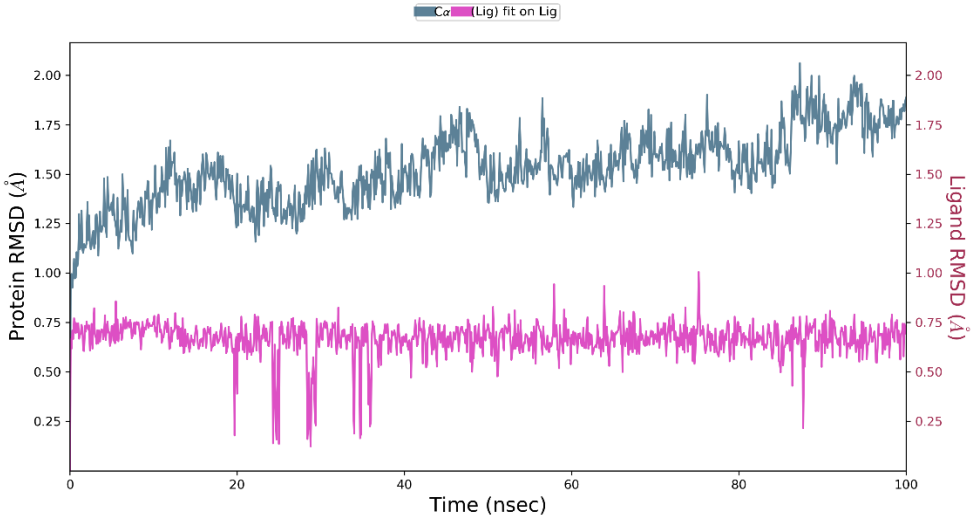

Figure II-8. RMSD plot of trans thujone and *E. coli* complex

The Root Mean Square Fluctuation (RMSF) analysis provides insights into local variations along the protein chain, facilitating the identification of residues contributing to structural fluctuations within the complex (Dey et al., 2021). In the examined complex, the observed fluctuation variation remained below 3 Å. Major fluctuations (2.20-2.63 and 1.81-2.96Å) were observed in the C-terminal and loop regions (223-225 and 363-366), respectively, which are positioned away from the binding pocket of alpha amylase. Except for the loop regions, the RMSF values of most residues are less than 1.5 Å, indicating that the residue conformation is relatively stable during the simulation. A graphical representation of the RMSF plot depicting the specific ligand interactions with amino acid residues in the protein is presented in Figure 10.

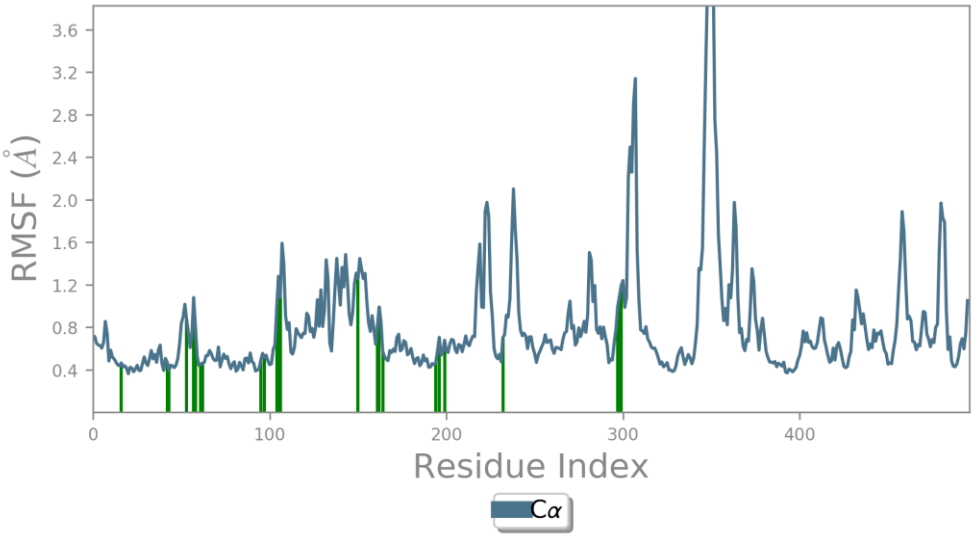

Figure II-9. RMSF plot of trans thujone and *E. coli* complex

Within the investigated complex, notable hydrogen bond interactions were observed involving HIS299, ASP197, and TRP58. Additionally, water-mediated hydrogen bond interactions were formed, encompassing the same residues, as visually depicted in Figure 11.

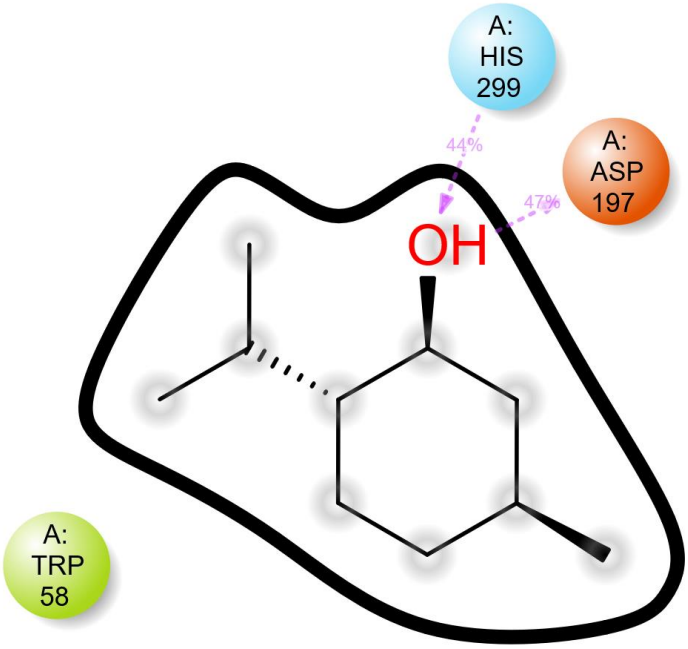

Figure II-10. Interaction diagram of protein-ligand after MDS

The analysis of Protein-ligand contact serves to elucidate the temporal continuity of interactions between the ligand and protein amino acids throughout the simulation. A numerical representation is employed, where a value of 0.5 denotes that a specific interaction was sustained for 50% of the simulation duration. Conversely, a value exceeding 1 suggests that protein amino acids may establish multiple contacts of the same subtype with the ligand (Hatmal & Taha, 2017).

In the context of the investigated complex, the interaction values for the residues GLU240, HIS201, ASP197, GLN63, GLU233, and THR163 are recorded as 1.25, 1, 1.75, 1, 0.60, and 1.5, respectively. These values signify varying degrees of sustained interactions between the ligand and corresponding amino acid residues. The graphical representation of the protein-ligand contact histograms for the complex is depicted in Figure 12 for visual elucidation.

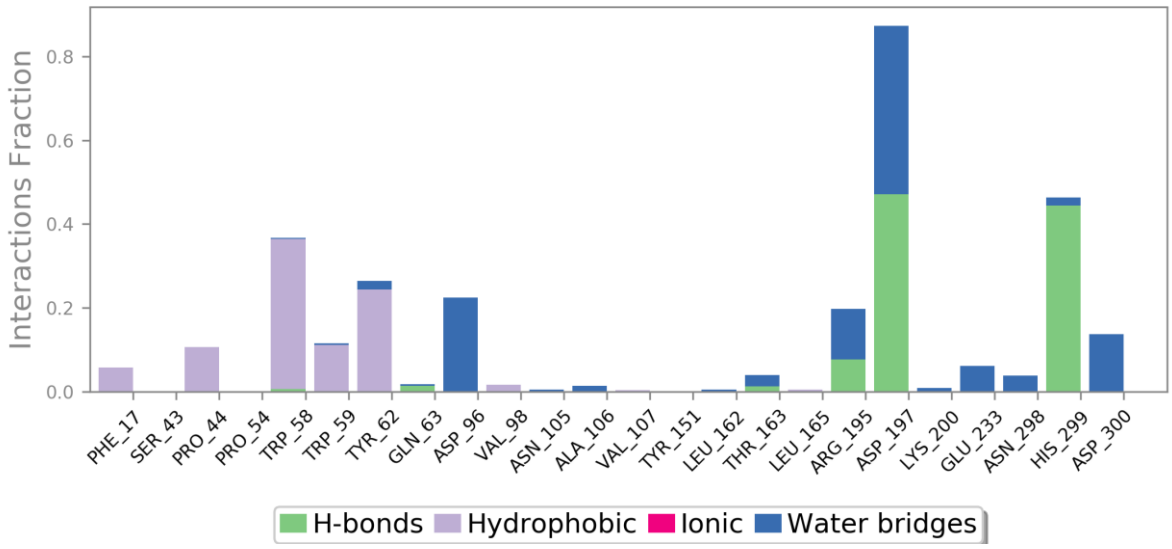

Figure II-11. Histogram of protein-ligand complex

To comprehensively investigate the interactions between the ligand and alpha-amylase receptor, two supplementary panels were introduced by Schrödinger post Molecular Dynamics Simulation (MDS), as depicted in Figure 13. The upper panel provides insights into the total number of specific contacts established by the protein with the ligand throughout the trajectory. Conversely, the lower panel delineates the residues engaged in interactions with the ligand in each trajectory frame.

Notably, certain residues exhibit multiple specific contacts with the ligand, visualized through varying shades of orange on the plot, in accordance with the scale positioned to the right of the diagram. This nuanced representation captures the dynamic nature of the interactions, offering a detailed portrayal of the residues that consistently contribute to the ligand-receptor interface. The incorporation of these supplementary panels enhances the granularity of our understanding of the molecular dynamics and specific contacts governing the ligand-receptor interaction over the course of the simulation.

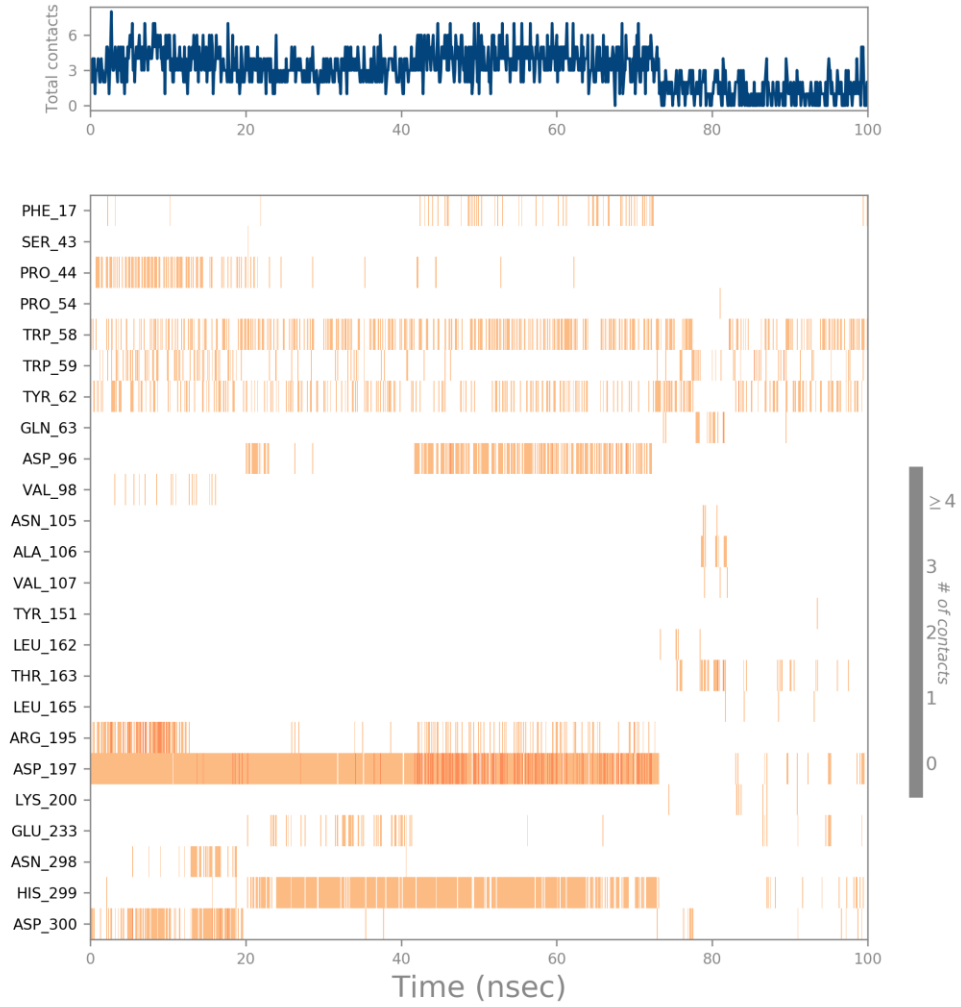

Figure II-12. Details of the protein ligand contact

6.1. Free Energy (MM-GBSA) Calculation:

To evaluate the binding efficacy of the preeminent compound, trans thujone, with the E. coli protein, the Prime-MM-GBSA method was applied to compute the binding free energies. The establishment of stable complexes is evidenced by favourable binding interactions between the compound and the protein. The determination of binding free energy entails the consideration of various energy components, encompassing van der Waals (vdW), lipophilic (lipo), Generalized Born electrostatic solvation (Solv GB), Coulomb, and hydrogen-bonding (hbond) energies. The discrete contributions of these energy components to the overall binding free energy of the Pulegone and E. coli complex are delineated in Table 19.

Table II-18. Energy components of the studied complex

Component	Energy (kcal/mol)
ΔG Bind	-61.14
ΔG Bind Coulomb	-30.03
ΔG Bind Solv GB	48.10
ΔG Bind vdW	-54.91
ΔG Bind lipo	-20.51
ΔG Bind hbond	-3.79

Notably, ΔG Bind is calculated at -61.14 kcal/mol, indicating a robust favourable binding interaction. Individual positive contributions include Coulombic energy at -30.03 kcal/mol, van der Waals interactions at -54.91 kcal/mol, lipophilic energy at -20.51 kcal/mol, and hydrogen-bonding energy at -3.79 kcal/mol. However, solvation energy through Generalized Born model contributed negatively at 48.10 kcal/mol. This collective interplay of energy components underscores the strong binding affinity observed in the complex.

Conclusion

Conclusion

This study highlights the significant potential of *Cotula cinerea* and *Origanum Majorana L.* essential oils as natural antibacterial agents, supported by their unique chemical compositions and strong bioactivity. The high content of bioactive compounds such as trans-thujone and santolina triene contributed to their remarkable effectiveness against pathogenic bacteria, surpassing conventional antibiotics in some cases. Computational studies further confirmed the molecular basis of their antibacterial activity, while ADMET predictions indicated a favorable pharmacological safety profile.

These findings validate the traditional medicinal use of these plants and open promising avenues for their application in the development of natural antimicrobial agents. However, further in vivo and clinical studies are necessary to fully confirm their therapeutic potential and ensure their safety for medical use.

Future Perspectives:

Based on the promising results of this study, several important research directions can be pursued, including:

• Conducting additional biological studies to verify the efficacy of the essential oils in vivo and to expand the range of targeted microorganisms, including fungi and viruses.

• Performing clinical trials to determine optimal dosages, evaluate potential toxicity, and assess possible side effects to ensure safe human application.

• Developing new pharmaceutical formulations based on these oils, such as antibacterial creams or sprays.

• Carrying out molecular studies aimed at enhancing the therapeutic properties of the active compounds and improving their efficacy, particularly against antibiotic-resistant bacterial strains.

These future perspectives underline the importance of continued exploration of medicinal plants as a source of innovative and effective solutions to address emerging health challenges.

References

References

❖ **References in English:**

1. Adefegha, S. A., Olasehinde, T. A., & Oboh, G. (2017). Essential oil composition, antioxidant, antidiabetic and antihypertensive properties of two Afromomum species. Journal of Oleo Science, 66(1), 51–63.

2. Adaika, A., Lanez, T., & Lanez, E. (2019). In vitro and in silico evaluation of anticancer activity of N,N-dimethylaminomethylferrocene. Journal of Fundamental and Applied Sciences, 11(2), 748–768. https://jfas.info/index.php/JFAS/article/view/289

3. Afnor, Ø. (1982). Recueil de normes françaises des produits dérivés des fruits et légumes jus de fruits. AFNOR, 325.

4. Akbar, S., Das, S., Iqubal, A., & Ahmed, B. (2022). Synthesis, biological evaluation and molecular dynamics studies of oxadiazine derivatives as potential anti-hepatotoxic agents. Journal of Biomolecular Structure and Dynamics, 40(20), 9974–9991. https://doi.org/10.1080/07391102.2021.1938233

5. Alajtal, A. I., Sherami, F. E., & Elbagermi, M. A. (2018). Acid, peroxide, ester and saponification values for some vegetable oils before and after frying. AASCIT Journal of Materials, 4(2), 43–47.

6. Alimi, D., Hajri, A., Jallouli, S., & Sebai, H. (2022). Valorization of volatile oils and some crude extracts from the Tunisian plants Juniperus communis and Origanum majorana for the control of Hyalomma scupense (Acari: Ixodidae). Waste and Biomass Valorization, 13(10), 4165–4177.

7. Atti-Santos, A. C., Rossato, M., Pauletti, G. F., Rota, L. D., Rech, J. C., Pansera, M. R., Agostini, F., Serafini, L. A., & Moyna, P. (2005). Physico-chemical evaluation of Rosmarinus officinalis L. essential oils. Brazilian Archives of Biology and Technology, 48, 1035–1039.

8. Auzat, I., Chapuy-Regaud, S., Le Bras, G., Dos Santos, D., Ogunniyi, A. D., Le Thomas, I., Garel, J. R., Paton, J. C., & Trombe, M. C. (1999). The NADH oxidase of Streptococcus pneumoniae: Its involvement in competence and virulence. Molecular Microbiology, 34(5), 1018–1028.

9. Banerjee, P., Eckert, A. O., Schrey, A. K., & Preissner, R. (2018). ProTox-II: A webserver for the prediction of toxicity of chemicals. Nucleic Acids Research, 46(W1), W257–W263. https://doi.org/10.1093/nar/gky318

10. Baser, K. H. C., Kirimer, N., & Tümen, G. (1993). Composition of the essential oil of Origanum Majorana L. from Turkey. Journal of Essential Oil Research, 5(5), 577–579.

11. Biswa, M. S., Varsha, T., Abhishek, T., & Bimal, K. B. (2023). Green chemistry using essential oils as synthons. Journal of Indian Chemical Society, Mar2023, 1–24. https://doi.org/10.5281/zenodo.7841465

12. Bohlmann, F., Burkhardt, T., & Zdero, C. (1973). Naturally occurring acetylenes. Academic Press.

13. Bowers, K. J., Chow, E., Xu, H., Dror, R. O., Eastwood, M. P., Gregersen, B. A., Klepeis, J. L., Kolossvary, I., Moraes, M. A., & Sacerdoti, F. D. (2006). Scalable algorithms for molecular dynamics simulations on commodity clusters. Proceedings of the 2006 ACM/IEEE Conference on Supercomputing, 84-es.

14. Brenk, R., Schipani, A., James, D., Krasowski, A., Gilbert, I. H., Frearson, J., & Wyatt, P. G. (2008). Lessons learnt from assembling screening libraries for drug discovery for neglected diseases. ChemMedChem, 3(3), 435–444. https://doi.org/10.1002/cmdc.200700139

15. Cheng, T., Zhao, Y., Li, X., Lin, F., Xu, Y., Zhang, X., Li, Y., Wang, R., & Lai, L. (2007). Computation of octanol-water partition coefficients by guiding an additive model with knowledge. Journal of Chemical Information and Modeling, 47(6), 2140–2148. https://doi.org/10.1021/ci700257y

16. Chiu, S. Y. C., Dobberstein, R. H., Fong, H. H. S., & Farnsworth, N. R. (1982). Oxoaporphine alkaloids from Siparuna gilgiana. Journal of Natural Products, 45(2), 229–230.

17. Cooper, K. E. (1963). The theory of antibiotic inhibition zones. In Analytical microbiology (pp. 1–86). Elsevier.

18. Daina, A., Michielin, O., & Zoete, V. (2014). ILOGP: A simple, robust, and efficient description of n-octanol/water partition coefficient for drug design using the GB/SA approach. Journal of Chemical Information and Modeling, 54(12), 3284–3301. https://doi.org/10.1021/ci500467k

19. Daina, A., Michielin, O., & Zoete, V. (2017). SwissADME: A free web tool to evaluate pharmacokinetics, drug-likeness and medicinal chemistry friendliness of small molecules. Scientific Reports, 7(1), 1–13. https://doi.org/10.1038/srep42717

20. Dey, D., Paul, P. K., Azad, S. Al, Mazid, M. F. Al, Khan, A. M., Sharif, M. A., & Rahman, M. H. (2021). Molecular optimization, docking, and dynamic simulation profiling of selective aromatic phytochemical ligands in blocking the SARS-CoV-2 S protein attachment to ACE2 receptor: An in silico approach of targeted drug designing. Journal of Advanced Veterinary and Animal Research, 8(1), 24–35. https://doi.org/10.5455/javar.2021.h481

21. Drwal, M. N., Banerjee, P., Dunkel, M., Wettig, M. R., & Preissner, R. (2014). ProTox: A web server for the in silico prediction of rodent oral toxicity. Nucleic Acids Research, 42(W1), W53–W58. https://doi.org/10.1093/nar/gku401

22. Dumitrică, T., & James, R. D. (2007). Objective molecular dynamics. Journal of the Mechanics and Physics of Solids, 55(10), 2206–2236. https://doi.org/10.1016/j.jmps.2007.03.001

23. Friesner, R. A., Murphy, R. B., Repasky, M. P., Frye, L. L., Greenwood, J. R., Halgren, T. A., Sanschagrin, P. C., & Mainz, D. T. (2006). Extra precision glide: Docking and scoring incorporating a model of hydrophobic enclosure for protein−ligand complexes. Journal of Medicinal Chemistry, 49(21), 6177–6196.

24. Ghose, A. K., Viswanadhan, V. N., & Wendoloski, J. J. (1998). Prediction of hydrophobic (lipophilic) properties of small organic molecules using fragmental methods: An analysis of ALOGP and CLOGP methods. Journal of Physical Chemistry A, 102(21), 3762–3772. https://doi.org/10.1021/jp980230o

25. Giurazza, R., Mazza, M. C., Andini, R., Sansone, P., Pace, M. C., & Durante-Mangoni, E. (2021). Emerging treatment options for multi-drug-resistant bacterial infections. Life, 11(6), 519.

26. Gorla, U. S., Gsn, K. R., Kulandaivelu, U., Alavala, R. R., Das, S., & Joseph, A. (2021). Bioflavonoids as potential target inhibitors in COVID-19: An in silico analysis. Journal of Research in Pharmacy, 25(6), 982–997. https://doi.org/10.29228/jrp.94

27. Guinaudeau, H., Leboeuf, M., & Cave, A. (1975). Aporphine alkaloids.

28. Halder, D., Das, S., Joseph, A., & Jeyaprakash, R. S. (2023). Molecular docking and dynamics approach to in silico drug repurposing for inflammatory bowel disease by targeting TNF alpha. Journal of Biomolecular Structure and Dynamics, 41(8), 3462–3475. https://doi.org/10.1080/07391102.2022.2050948

29. Hatmal, M. M., & Taha, M. O. (2017). Simulated annealing molecular dynamics and ligand-receptor contacts analysis for pharmacophore modeling. Future Medicinal Chemistry, 9(11), 1141–1159. https://doi.org/10.4155/fmc-2017-0061

30. Hay, M., Thomas, D. W., Craighead, J. L., Economides, C., & Rosenthal, J. (2014). Clinical development success rates for investigational drugs. Nature Biotechnology, 32(1), 40–51. https://doi.org/10.1038/nbt.2786

31. Horai, H., Arita, M., Kanaya, S., Nihei, Y., Ikeda, T., Suwa, K., Ojima, Y., Tanaka, K., Tanaka, S., & Aoshima, K. (2010). MassBank: A public repository for sharing mass spectral data for life sciences. Journal of Mass Spectrometry, 45(7), 703–714.

32. Kedadra, A., Lanez, T., Lanez, E., Hemmami, H., & Henni, M. (2022). Synthesis and antioxidant activity of six novel N-ferrocenylmethyl-N-(nitrophenyl) and -N-(cyanophenyl)-acetamides: Cyclic voltammetry and molecular docking studies. Journal of Electrochemical Science and Engineering, 12(2), 293–304. https://doi.org/10.5599/jese.1162

33. Kim, S., Thiessen, P. A., Bolton, E. E., Chen, J., Fu, G., Gindulyte, A., Han, L., He, J., He, S., Shoemaker, B. A., Wang, J., Yu, B., Zhang, J., & Bryant, S. H. (2016). PubChem substance and compound databases. Nucleic Acids Research, 44(D1), D1202–D1213. https://doi.org/10.1093/nar/gkv951

34. King, D. T., Worrall, L. J., Gruninger, R., & Strynadka, N. C. J. (2012). New Delhi Metallo-β-Lactamase: Structural insights into β-Lactam recognition and inhibition. Journal of the American Chemical Society, 134(28), 11362–11365. https://doi.org/10.1021/ja303579d

35. Kiryakov, H. G. (1968). Structure of dehydroglaucine: A new aporphine alkaloid.

36. Klančnik, A., Piskernik, S., Jeršek, B., & Možina, S. S. (2010). Evaluation of diffusion and dilution methods to determine the antibacterial activity of plant extracts. Journal of Microbiological Methods, 81(2), 121–126. https://doi.org/10.1016/j.mimet.2010.02.004

37. Klopman, G., Li, J. Y., Wang, S., & Dimayuga, M. (1993). Computer automated log P calculations based on an extended group contribution approach. Journal of Chemical Information and Computer Sciences, 33(4), 752–781.

38. Korb, O., Olsson, T. S. G., Bowden, S. J., Hall, R. J., Verdonk, M. L., Liebeschuetz, J. W., & Cole, J. C. (2012). Potential and limitations of ensemble docking. Journal of Chemical Information and Modeling, 52(5), 1262–1274.

39. Lanez, T., Benaicha, H., Lanez, E., & Saidi, M. (2018). Electrochemical, spectroscopic and molecular docking studies of 4-methyl-5-((phenylimino)methyl)-3H- and 5-(4-fluorophenyl)-3H-1,2-dithiole-3-thione interacting with DNA. Journal of Sulfur Chemistry, 39(1), 76–88. https://doi.org/10.1080/17415993.2017.1391811

40. Liu, X., Testa, B., & Fahr, A. (2011). Lipophilicity and its relationship with passive drug permeation. Pharmaceutical Research, 28(5), 962–977. https://doi.org/10.1007/s11095-010-0303-7

41. Lu, C., Wu, C., Ghoreishi, D., Chen, W., Wang, L., Damm, W., Ross, G. A., Dahlgren, M. K., Russell, E., & Von Bargen, C. D. (2021). OPLS4: Improving force field accuracy on challenging regimes of chemical space. Journal of Chemical Theory and Computation, 17(7), 4291–4300.

42. Madhavi Sastry, G., Adzhigirey, M., Day, T., Annabhimoju, R., & Sherman, W. (2013). Protein and ligand preparation: Parameters, protocols, and influence on virtual screening enrichments. Journal of Computer-Aided Molecular Design, 27, 221–234.

43. Meylan, W. M., & Howard, P. H. (2000). Estimating log P with atom/fragments and water solubility with log P. Perspectives in Drug Discovery and Design, 19(1), 67–84. https://doi.org/10.1023/A:1008715521862

44. Moriguchi, I., Hirano, H., & Nakagome, I. (1994). Comparison of reliability of log P values for drugs calculated by several methods. Chemical and Pharmaceutical Bulletin, 42(4), 976–978. https://doi.org/10.1248/cpb.42.976

45. Moriguchi, I., Hirono, S., Liu, Q., Nakagome, I., & Matsushita, Y. (1992). Simple method of calculating octanol/water partition coefficient. Chemical and Pharmaceutical Bulletin, 40(1), 127–130. https://doi.org/10.1248/cpb.40.127

46. Narramore, S., Stevenson, C. E. M., Maxwell, A., Lawson, D. M., & Fishwick, C. W. G. (2019). New insights into the binding mode of pyridine-3-carboxamide inhibitors of E. coli DNA gyrase. Bioorganic and Medicinal Chemistry, 27(16), 3546–3550. https://doi.org/10.1016/j.bmc.2019.06.015

47. Ozer, D. J. (1985). Correlation and the coefficient of determination. Psychological Bulletin, 97(2), 307.

48. Plonsky, L., & Ghanbar, H. (2018). Multiple regression in L2 research: A methodological synthesis and guide to interpreting R2 values. The Modern Language Journal, 102(4), 713–731.

49. Roos, K., Wu, C., Damm, W., Reboul, M., Stevenson, J. M., Lu, C., Dahlgren, M. K., Mondal, S., Chen, W., Wang, L., Abel, R., Friesner, R. A., & Harder, E. D. (2019). OPLS3e: Extending force field coverage for drug-like small molecules. Journal of Chemical Theory and Computation, 15(3), 1863–1874. https://doi.org/10.1021/acs.jctc.8b01026

50. Sahoo, P. K., Das, L. M., Babu, M. K. G., & Naik, S. N. (2007). Biodiesel development from high acid value polanga seed oil and performance evaluation in a CI engine. Fuel, 86(3), 448–454.

51. Schreiner, W., Karch, R., Knapp, B., & Ilieva, N. (2012). Relaxation estimation of RMSD in molecular dynamics immunosimulations. Computational and Mathematical Methods in Medicine, 2012. https://doi.org/10.1155/2012/173521

52. Schrödinger. (2015). Small-Molecule Drug Discovery Suite 2015-3: Schrödinger Suite 2015-3 Induced Fit Docking protocol; Glide version 6.8; Prime version 4.1. Glide Version, 6.

53. Schrödinger. (2024). Schrödinger Release 2024-1: LigPrep. Schrödinger, LLC.

54. Sellami, I. H., Maamouri, E., Chahed, T., Wannes, W. A., Kchouk, M. E., & Marzouk, B. (2009). Effect of growth stage on the content and composition of the essential oil and phenolic fraction of sweet marjoram (Origanum Majorana L.). Industrial Crops and Products, 30(3), 395–402.

55. Shamma, M. (1972). The isoquinoline alkaloids. Academic Press.

56. Singh, S. (2002). Refractive index measurement and its applications. Physica Scripta, 65(2), 167.

57. Sliwoski, G., Kothiwale, S., Meiler, J., & Lowe, E. W. (2014). Computational methods in drug discovery. Pharmacological Reviews, 66(1), 334–395.

58. Tu, T., Rendleman, C. A., Borhani, D. W., Dror, R. O., Gullingsrud, J., Jensen, M. O., Klepeis, J. L., Maragakis, P., Miller, P., Stafford, K. A., & Shaw, D. E. (2008). A scalable parallel framework for analyzing terascale molecular dynamics simulation trajectories. 2008 SC - International Conference for High Performance Computing, Networking, Storage and Analysis, SC 2008, 1–12. https://doi.org/10.1109/SC.2008.5214715

59. Tyagi, P., Singh, M., Kumari, H., Kumari, A., & Mukhopadhyay, K. (2015). Bactericidal activity of curcumin I is associated with damaging of bacterial membrane. PLOS ONE, 10(3), 1–15. https://doi.org/10.1371/journal.pone.0121313

60. Valarezo, E., Rosales, J., Morocho, V., Cartuche, L., Guaya, D., Ojeda-Riascos, S., Armijos, C., & González, S. (2015). Chemical composition and biological activity of the essential oil of Baccharis obtusifolia Kunth from Loja, Ecuador. Journal of Essential Oil Research, 27(3), 212–216.

61. Vera, R. R., & Chane-Ming, J. (1999). Chemical composition of the essential oil of marjoram (Origanum Majorana L.) from Reunion Island. Food Chemistry, 66(2), 143–145.

62. Wang, E., Fu, W., Jiang, D., Sun, H., Wang, J., Zhang, X., Weng, G., Liu, H., Tao, P., & Hou, T. (2021). VAD-MM/GBSA: A variable atomic dielectric MM/GBSA model for improved accuracy in protein–ligand binding free energy calculations. Journal of Chemical Information and Modeling, 61(6), 2844–2856.

63. Wang, M., Guo, Q., Zhu, K., Fang, B., Yang, Y., Teng, M., Li, X., & Tao, Y. (2020). Interface switch mediates signal transmission in a two-component system. Proceedings of the National Academy of Sciences of the United States of America, 117(48), 30433–30440. https://doi.org/10.1073/pnas.1912080117

64. Wang, R., Fu, Y., & Lai, L. (1997). A new atom-additive method for calculating partition coefficients. Journal of Chemical Information and Computer Sciences, 37(3), 615–621.

65. Yang, Y., Yao, K., Repasky, M. P., Leswing, K., Abel, R., Shoichet, B. K., & Jerome, S. V. (2021). Efficient exploration of chemical space with docking and deep learning. Journal of Chemical Theory and Computation, 17(11), 7106–7119.

❖ **References in French:**

1. Alioua, R., & Bouamoucha, I. (n.d.). Etude de l'activité antibactérienne de l'extrait méthanolique du fruit de Zaarour rouge (Crataegus monogyna) vis-à-vis des bactéries résistantes aux antibiotiques.

2. Atef, Chouikh, Mayache Boualem, Maazi Cherif, Hadef Youcef, & Chefrour Azzedine. (2015). Chemical composition and antimicrobial activity of essential oils in xerophytic plant Cotula cinerea Del (Asteraceae) during two stages of development: Flowering and fruiting. Journal of Applied Pharmaceutical Science, 5(03), 029–034. https://doi.org/10.7324/JAPS.2015.50306

3. Bryskier, A. (1999). Antibiotiques agents anti-bactériens et antifongiques. Ellipses.

4. Denbi, A., Abdelwahed, D. E., Bouaaza, M., & Touati, B. (2014). Screening phytochimique et activité antibactérienne de l'huile essentielle de Cotula cinerea (Gartoufa) dans la région de Bechar. IMPACT: International Journal of Research in Engineering & Technology, 2(2), 49–54.

5. El-Bouzidi, L., Abbad, A., Fattarsi, K., Hassani, L., Leach, D., Markouk, M., Legendre, L., & Bekkouche, K. (2011). Chemical composition and anticandidal properties of the essential oil isolated from aerial parts of Cotula cinerea: A rare and threatened medicinal plant in Morocco. Natural Product Communications, 6(10), 1491–1494.

6. Flandrois, J. P. (2000). Bactériologie Médicale. Coll Azay. Puf.

7. Hennekinne, J. A. (2009). Nouvelles approches pour la caractérisation des toxi-infections alimentaires à staphylocoques à coagulase positive [Doctoral thesis]. Université Agro Paris Tech.

8. Jodra, S. (2004–2014). Les bactéries. Imago Mundi.

9. Larpent, J. P., & Sanglier, J. J. (1989). Biotechnologie des antibiotiques. Masson.

10. Leclerc, H., Gaillard, J. L., & Simonet, M. (1995). Microbiologie générale, la bactérie et le monde bactérien. Doin Éditeurs.

11. Merabet, S. A., & Sekhsoukh, M. N. (2020). Synthèse et évaluation in vitro du potentiel antioxydant et antimicrobien d'une série de composés 1,5 benzodiazépines. 32–37.

12. Ryan, K. J., & Ray, C. G. (Eds.). (2004). Medical Microbiology (4th ed.). McGraw-Hill.

13. Singleton, P. (1999). Bactériologie (4th ed.). Dunod.

Annexes

Figure 1: Plant Essential Oil Extraction by Clevenger

Figure 2: autoclave

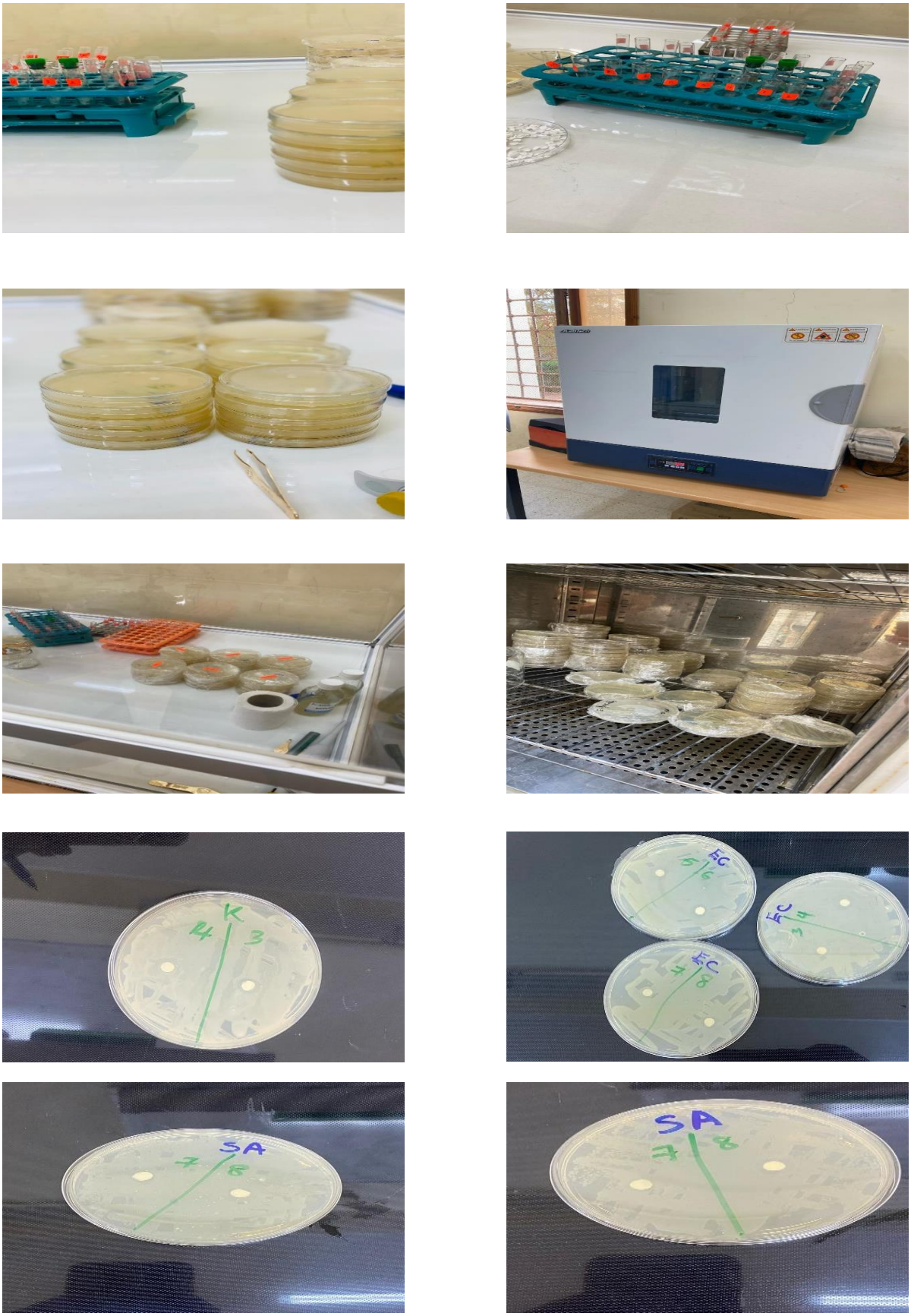

Figure 3: In vitro

Figure 4: Transmission spectrophotometry